NTNU – Trondheim
Norwegian University of
Science and Technology

Ultimate Strength and Post-Ultimate Behavior of Hybrid Platform Deck Girders

Chunqi Zhou

Marine Technology
Submission date: June 2014
Supervisor: Jørgen Amdahl, IMT

Norwegian University of Science and Technology
Department of Marine Technology

NTNU – Trondheim
Norwegian University of
Science and Technology

ULTIAMTE STRENGTH AND POST-ULTIMATE BEHAVIOR OF HYBRID PLATFORM DECK GIRDERS

Author:

Chunqi Zhou

Supervisor:

Prof. Jørgen Amdahl

MASTER THESIS

DEPARTMENT OF MARINE TECHNOLOGY

NORWEGIAN UNIVERSITY OF SCIENCE AND TECHNOLOGY

TRONDHEIM, JUNE 2014

Preface

This report aims to present the result of the master thesis for Stud. Chunqi Zhou at the Department of Marine Technology at Norwegian University of Science and Technology (NTNU), during the spring semester of 2014.

Throughout the semester, more time than participated is devoted to establishing the finite element model in Msc Patran and Abaqus. Linear eigenvalue analysis and nonlinear ultimate analysis in Abaqus are carried out with various load inputs and boundary conditions. USFOS is also applied to check the ultimate strength from the nonlinear ultimate analysis.

The work has been a highly educational experience, where I have had the opportunity to put theoretical knowledge from different fields of marine structure into practice for problems of high relevance in today's maritime industry. I have also had the chance to gain experience using different software packages that are widely adopted in the engineering industry.

At last, I wish to extend my gratitude towards thesis advisor Professor Jørgen Amdahl for his helpful guidance and discussions. In addition, Martin Storheim at the Department of Marine Technology deserves recognition for his help regarding finite element modelling. Finally, I will also show my thanks to Md. Mosfiqur Rahman, Yao Ma and Ørjan Fredriksen for the inspiration from the layout of their papers.

Trondheim, 2014-06-08

Chunqi Zhou

Scope of work

MASTER THESIS SPRING 2014

for

Stud. Techn. Chunqi Zhou

Ultimate strength and post-ultimate behavior of hybrid platform deck girders

Sammenbruddstyrke og etterkritisk oppførsel av hybride bærekonstruksjoner i platformdekk

Topside load-carrying structures in floating offshore platforms may be constructed in many ways. One option is to use a truss-work structure in combination with plate girders, where the latter constitute the top flange of the girder. The plate girder carries both local, lateral loads as we´ll as axial stresses form the global bending moment.

The deck girder may be designed according to conventional rules based on ultimate limit state principles. These design formulations may be conservative; it may notably be considered that the stressed skin concept may be utilized. and if it can be documented that the ultimate strength is significantly larger, this effect may be taken into account in conjunction with reassessment of the platform, e.g. if more equipment on the deck is desired. The behaviour in the post-ultimate region will also have to be considered; if the load from failing members may be shed to other intact members, the structure will be robust.

The purpose of the present work is to contribute to a better understanding of the ultimate strength and post-ultimate behaviour of such deck girder by performing nonlinear analysis with the computer programme USFOS.

The project work should comprise the following tasks:

1) Perform modelling of a stiffened plate girder in the deck area exposed to axial compression,

bending and shear. Introduce appropriate boundary conditions to the girder. The analysis shall be carried out with ABAQUS. Perform eigenvalue analysis and introduce one or more eigenmodes as imperfections to the girder. Perform nonlinear analysis with proportional loading. The load combinations to be agreed with the supervisor. Identify the ultimate resistance of the girder. Compare numerical results with strength formulations given in DNV-RP-C201 and NS-EN 1993-1-5.

2) Perform nonlinear analysis of the plate girder with stronger secondary stiffeners on the girder web. Compare with the results from pt 1 and code formulations. It is especially of interest to see if the girder may carry large shear forces in by tension field redistributing axial force and bending moment to the girder flanges,

3) To the extent possible conduct alternative analysis with USFOS using the same finite element mesh. Initial imperfection may have to be introduced differently.

4) Perform nonlinear analysis of a secondary girder with class 4 cross-section. The girder may have cut-outs and/or patch loads. The loads shall be applied proportionally for various load combinations. Determine the ultimate strength of the girder. Compare numerical results with NS-EN 1993-1-5

5) Perform nonlinear finite element analysis with ABAQUS or USFOS of a hybrid plate girder-truss-work section in a platform deck. The truss-work shall be modelled with shell finite elements including secondary stiffeners. Special attention shall be placed on modelling boundary conditions and introducing initial imperfections to trigger local buckling of plate girder. The truss-work may be modelled with beam elements. The truss work shall be subjected to combined bending, shear and locally distributed forces. The ultimate strength for various load shall be determined. Comparison shall be made with capacities obtained with conventional design formulas, as given in DNV-RP-C201 Buckling Strength of Plated Structures and NS-EN 1993-1-5 Design of steel structures, Plated structural elements.

6) If time permits, establish a model of a larger part of the deck structure, based on beam representation of the deck girders combined with crude shell modelling of the stiffened plates.

The plating shall be meshed one or a few all no be included. The effect of omitting the stiffeners shall be discussed. The ultimate strength of the deck shall be assessed

7) Conclusions and recommendations for further work

Literature studies of specific topics relevant to the thesis work may be included.

The work scope may prove to be larger than initially anticipated. Subject to approval from the supervisors, topics may be deleted from the list above or reduced in extent.

In the thesis the candidate shall present his personal contribution to the resolution of problems within the scope of the thesis work.

Theories and conclusions should be based on mathematical derivations and/or logic reasoning identifying the various steps in the deduction.

The candidate should utilise the existing possibilities for obtaining relevant literature.

Thesis format

The thesis should be organised in a rational manner to give a clear exposition of results, assessments, and conclusions. The text should be brief and to the point, with a clear language. Telegraphic language should be avoided.

The thesis shall contain the following elements: A text defining the scope, preface, list of contents, summary, main body of thesis, conclusions with recommendations for further work, list of symbols and acronyms, references and (optional) appendices. All figures, tables and equations shall be numerated.

The supervisors may require that the candidate, in an early stage of the work, presents a written plan for the completion of the work. The plan should include a budget for the use of computer and laboratory resources which will be charged to the department. Overruns shall be reported to the supervisors.

The original contribution of the candidate and material taken from other sources shall be clearly defined. Work from other sources shall be properly referenced using an acknowledged referencing system.

The report shall be submitted in two copies:

- Signed by the candidate
- The text defining the scope included
- In bound volume(s)
- Drawings and/or computer prints which cannot be bound should be organised in a separate folder.

Thesis supervisor: Prof. Jørgen Amdahl

Deadline: June 10, 2014

Jørgen Amdahl

Trondheim, January 14, 2014

Remark: As the project goes on, more time is devoted into the first three tasks in the list. In agreement with Professor Amdahl, the research about the first three tasks are carried out in depth and a plenty of work is completed for this purpose.

Summary

As for the increasing demands of offshore oil and gas, the new platforms are designed in more and more serious conditions. The safety check and modification of the complex structure has become a hot subject. Normally, the deck girder can be regarded as the combination of truss works and girders, which will suffer from the axial compression from global bending as well as shear force due to the local equipment loads.

The main goal of this paper is to make contributions to predict the ultimate strength and post-buckling behavior of this kind of hybrid deck girder. Comparison among various cases is the main methodology for drawing a conclusion.

The linear eigenvalue analysis is aimed to introduce the initial imperfection into the structure. The effects of imperfection on the ultimate strength are found to be small for this kind of robust structure. The way how the stiffener strength and boundary conditions influence the ultimate capacity is also investigated. In addition, two nonlinear finite element software (Abaqus and USFOS) provide similar pre- and post-buckling behavior, while the deviation for the ultimate strength is in a quite large but acceptable level. The simplified estimate according to design standards is also investigated here and the comparison with finite element analysis shows that the regulations can give a quite good prediction about the ultimate capacity of stiffened plates and primary girder section.

Contents

List of Figures

List of Tables

Nomenclature

$\bar{\lambda}$	reduced slenderness ratio
γ	Flexural rigidity of stiffener
γ^*	Optimum flexural rigidity of stiffener
γ_m	Material factor
λ	Load proportional factor
λ_i	Eigenvalues
ν	Poisson's ratio
ω_i	out-of-straightness amplitude
σ_U	Ultimate plastic stress
σ_y	Yield stress
σ_t^y	Tension field web membrane stress
σ_{yw}	Yield stress of web material
τ_{cr}	Critical shear stress of web
θ	Inclination of web tension field
υ_i	Eigenvactors

E	Elastic modulus
E_s	Secant modulus
h, t	Plate thickness
K	Constant stiffness
k	Buckling coefficient
$K_I(r)$	Tangent or incremental stiffeness
l	Structure length
M	Bending moment
M_p^*	Flange strength parameter $=M_{pf}/d^2 t\sigma_{yw}$
M_{pf}	Plastic moment of the flange plate
M_{ult}	Ultimate bending capacity
R	External loads
r	displacement
T	Shear stress
T_{ult}	Design shear capacity
V_s	Ultimate shear capacity of girder
V_{yw}	Shear force to produce yielding of web

Chapter 1

Introduction

Nowadays, there are a plenty of demands of new platforms to support the exploration of oil and gas offshore. At the meantime, the modification of existing platforms is also a new hot branch in the structure analysis field.

The hybrid deck girder, which consists of truss works and girders, is a typical type of platform deck. The girder will suffer from both local, lateral loads as well as axial stresses form the global bending moment.The ultimate strength analysis of the platform deck is an essential part in the design stage to ensure the structural stability. The buckling of girders and braces within the truss work may exert the dramatic effects on the their own resistance for failure, while the effects on the whole system may be small since the adjacent members can take the force for the buckled members.

As mentioned above, the complexity of structure increases the difficulties to estimate the ultimate strength and corresponding post ultimate behaviors. In addition, the design principle will tend to provide the conservative estimate in the design state. Although the nonlinear finite element method performed by the advanced software such as Abaqus and USFOS can always predict the structure behavior well, it is hard to predict the deformation in advance due to complexities.

Compared with truss works, there are more difficulties in predicting the behavior of the stiffened girders. There are a lot of researches with regards to the stress estimation. Wagner [1] developed the tension field theory for evaluating the critical shear buckling stress for web or girders. In addition, Tang et al [2] conducted several tests to study the effects of the longitudinal and transverse stiffeners on the girders.

In this thesis, some contributions are expected to make to predict the ultimate strength and post-buckling behavior of hybrid deck girder. For example, the effects of the stiffeners on the girders will be investigated to provide a clear insight into the role of the stiffener strength played in structural ultimate capacity. The check of the difference between the DNV regulations and finite element analysis will be also studied to see the conservative effects from the design principles. Furthermore, results from two commercial finite element software (Abaqus and USFOS) will be compared to see the deviations in terms of the results for the ultimate analysis. In order to provide a clear overview about this project for readers, the main work done in this thesis is listed below.

- Effects of initial geometric imperfection on ultimate capacity – Section 7.2
- Effects of boundary conditions on ultimate capacity – Section 7.3
- Effects of secondary stiffeners on ultimate capacity –Section 7.4
- Comparison between two software (Abaqus and USFOS) – Section 8.4
- Capacity check of stiffened plates ´ – Section 9.1&9.2
- Capacity check of primary girder – Section 9.4

Chapter 2

Review of Frame Failure Mechanism

2.1 Introduction

In practice, structures are usually designed for the coexisting of shear force, bending moment and even other types of loads. Evans [3] stated the complexity of estimate about the ultimate strength for webs under both shear forces and bending moments. Compared with one frame under pure bending moment, a frame under shear force will reduce its bending capacity. Similarly, the occurrence of bending moment makes the full shear capacity not available any longer. The various proportionality of the stress will lead to different collapse mechanisms.

Additionally, the initial imperfection will also exert an influence on the ultimate capacity of the structure. The imperfection assumed as the out-of-straightness during manufacturing can be simply expressed by one reasonable practical factor and the element length. As for the buckling issues, the regulations from DNV will demonstrate the problems in details.

2.2 Bending and shear interaction

The interaction between bending and shear on the ultimate strength of one plate girder is plotted in Figure 2.1. The line OC is the critical line to define the border of different failure mechanisms. The region OCS means the girder will fail in shear mechanism and the collapse in the other part belongs to the flange failure.

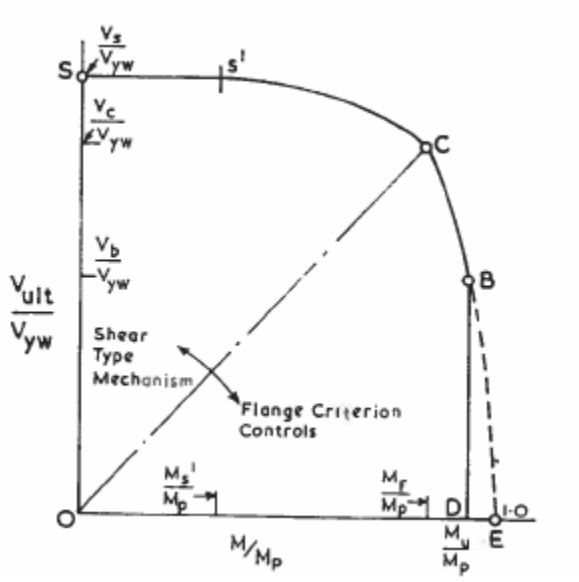

Figure 2.1: Diagram showing interaction between shear and bending effects [14]

Evans et al [4] carried out a study to estimate a value of the applied critical bending moment changing the mechanism from web to flange. Their conclusion is that the critical bending moment is approximately equal to the plastic bending capacity of the girder with the flanges only.

Daley [5] presented an equation to show the relationship of this interaction, where α is a parameter which depends on the cross-section and the value is equal to or greater than one.

$$(\frac{M}{M_{ult}})^2 + (\frac{T}{\alpha.T_{ult}})^2 = 1 \tag{2.1}$$

The Figure 2.2 is plotted based on the equation and it is markable that the section with $\alpha > 1$ will reserve some bending strength at the point of full shear.

Theoretically, the vertical part of the girder is responsible for resisting the shear force, the height including the top and bottom flanges instead of the web's height is treated as the height resisting shear force. As the shear capacity of web is used up, the moment capacity of section reduces until the level of residual section modulus, which is defined by the free flange contribution only. From the figure 2.2, a flat bar has no residual capacity, whereas a stiffener with flange area retain almost 1/3 of initial moment capacity.

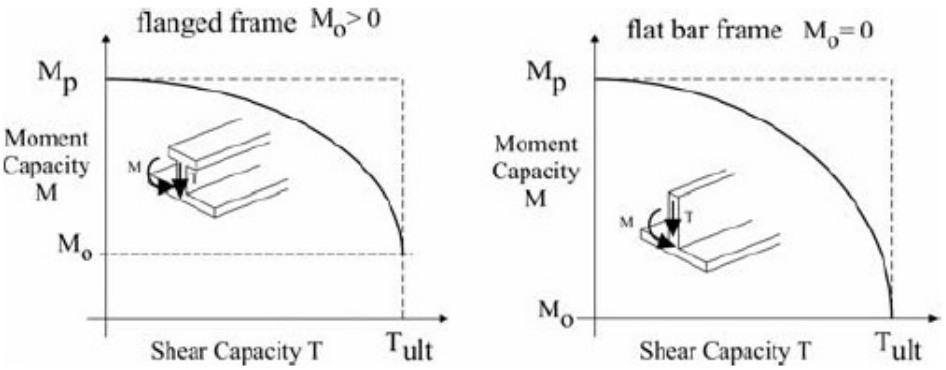

Figure 2.2: Bending/shear interaction diagrams for different cross-section [5]

When the web is fully yielded and a shear hinge starts to form, the flanges can still provide additional load capacity. In a truly pure shear collapse, even the whole area of flanges should be expected to reach the yield stress. However, bending hinges in the flanges will occur at a lower level of energy compared to the energy needed for pure shear collapse.

Graciano [6] studied the interaction between concentrated loads, shear and bending (shown in Figure 2.3). He stated that the total patch loading resistance will be dramatically reduced because of the coexisting of bending and shear and bending action has a major influence on the reduction of patch capacity.

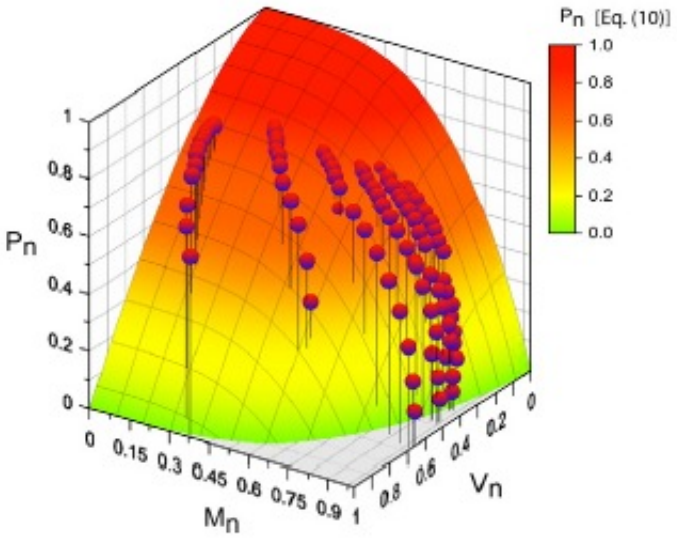

Figure 2.3: Intercation surface among concentrated loading p_n, shear V_n and bending M_n [9]

2.3 Collapse mechanism

In this sectin, the response mechanisms for the case with symmetric central loads are studied and possible response mechanisms are listed below. As for the case with asymmetric loads, please refer to IACS framing requirements.[7]

- 2 shear hinge
- 3-hinge bending/shear
- 4-hinge bending/shear

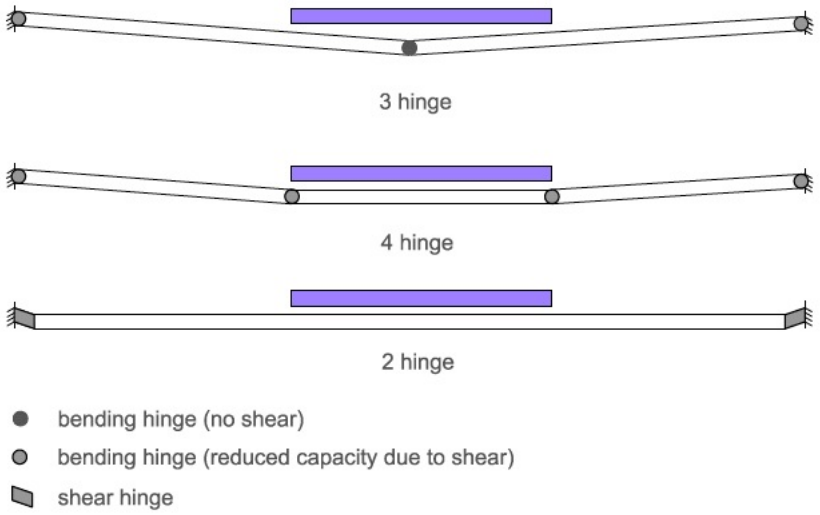

Figure 2.4: Typical symmetrical collapse mechanisms

Among different mechanisms, the mechanism requiring the lowest load capacity should be the dominant one, which mainly depends on the shape of cross-section, the load length and the load magnitude. The 3-hinge bending/shear is usually chosen as the dominant mechanism, even though it normally needs a larger collapse load than the 4-hinged mechanism. Through several finite element analyses, Daley [5] proved that the difference in the collapse loads of 3-hinged and 4-hinged mechanisms is in an acceptable range. The 2-hinged mechanism can be avoided by adjusting the web area to be larger than the minimum permissible web area in the pure shear force. The shear area is shown in equation 2.2.

$$A_0 = \frac{1}{2} P.b.S.\frac{\sqrt{3}}{\sigma_y} \tag{2.2}$$

The 3-hinged mechanism is therefore usually adopted in the design state, and in this project we can see the 2-hinged mechanism caused by simulated shear force later.

2.4 Initial imperfection

Initial imperfections have a significant impact on the physical buckling strength of structures subjected to compression. Likewise, in a numerical simulation of system collapse, buckling is often highly dependent on the initial deformation. There are two main sources of imperfections:

- Geometric deviations
- Residual stresses

Geometric imperfections refer to variations in the data of cross-section and axial out-of-straightness. The variations in cross-section data is mainly caused by the manufacturing of the profile, while the axial out-of-straightness is particularly due to structure fabrication. Additionally, welding can induce residual stress, which arises from both the manufacturing of the profile and the structure fabrication.

Generally, there are some difficulties in knowing the magnitude and direction of imperfections. Design column curves, which contains the effects of true imperfections and residual stresses, are often simulated very well by means of an equivalent imperfection. Very often this imperfection is approximately equal to the tolerance level for out-of-straightness specified by the code. For example, the expression for equivalent imperfection based on some codes (ECCS, Euro3) is shown below.[8]

$$w_i / l = 0.0015(1 - 0.2/\bar{\lambda}) \tag{2.3}$$

where w_i is the out-of-straightness amplitude

l is the element length

$\bar{\lambda}$ is reduced slenderness ratio

The equivalent imperfection is assumed to take the effects of both geometry deviations and residual stresses into account. The second part in the bracket in the equation 2.3 can be neglected for simplified cases.

Graciano [9] pointed out the reduction of capacity caused by initial imperfection is normally less than 12% of the resistance with respect to perfect model. Additionally, for most cases, the initial imperfection can be directly modelled by the shape of a sinus-wave or the first eigenmode from eigenvalue analysis.

2.5 Regulation check according to DNV RP

DET NORSKE VERITAS (DNV) describes two different, but equally acceptable methods, for buckling and ultimate strength assessment of plated structures in DNV RP C201[10].

The first method, as given in Part 1, is a conventional buckling code for stiffened and unstiffened panels of steel, which is applicable for plates, stiffeners and girders.

The second method, as given in Part 2, is a computerized semi-analytical model called PULS (Panel Ultimate Limit State). It is based on a recognized non-linear plate theory, Rayleigh-Ritz discretizations of deflections and a numerical procedure for solving the equilibrium equations.The method is essentially geometrically non-linear with stress control in critical positions along plate edges and plate stiffener junction lines for handing material plasticity.

The Excel program developed by DNV for buckling resistance includes check of unstiffened plates, check of stiffeners from both the stiffener and plate sides, and check of the girder section if there is.

The methodology for buckling check of stiffened plates are explained in the DNV RP C201 in details [10]. Results from DNV Excel program and PULS will be discussed in the chapter 9.

Chapter 3

Review of Researches on Plate Girder

Plate girders are usually used in the ships, platforms and drilling rigs. The combination of the shear force, axial force and bending moment will decide the critical load and corresponding buckling modes. The vital geometrical parameters are the web thickness, the flange area and the strength of longitudinal and transverse stiffeners. In this chapter, some previous researches relating to the strength of plate girders are reviewed.

3.1 The tension field concept

The tension field formed in the web plate can help the plate girders to reserve considerable strength in the post-buckling region. When a plate girder is subjected to shear forces, the development of stress in the web can be treated as two steps: [11]

Step 1: Initially, the tension and compression stress are equal and the directions are perpendicular to each other.

Step 2: When the compressive stress reaches the principle value for buckling, it can't take any more pressure in that direction. While the in the tension direction, there is no buckling problem and the additional stress can be tolerated by the tension band.

The experimental results published by Evans et al [12] are superimposed in the Figure 3.1 below showing the principal strain and stress in the web during the development of tension band.

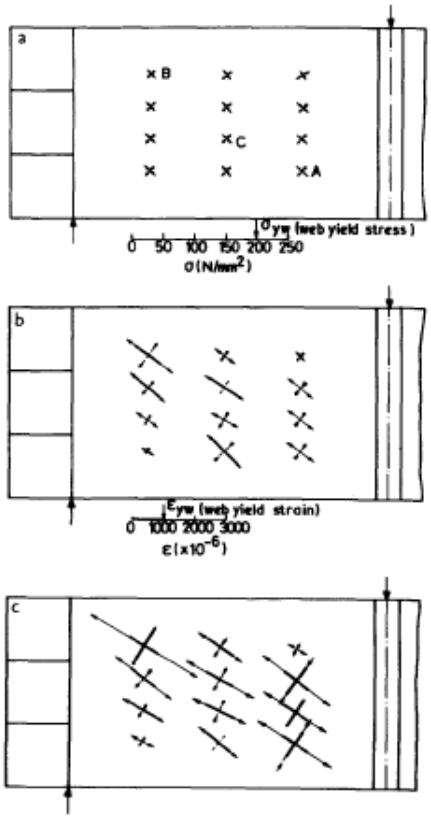

Figure 3.1: Principal stresses and strains in the web panel LS3-A with $0.29V_{max}$, $0.97V_{max}$ and web strains on failure plateau [12]

3.1.1 Web shear capacity

In the unbuckled region, the shear capacity can be expressed as

$$\tau_{cr} = \frac{\pi^2 E}{12(1-\upsilon^2)}(\frac{h}{b})^2 k \tag{3.1}$$

where the buckling coefficient k, for simply supported edges is given by

$$\begin{aligned} k &= 5.34 + \frac{4}{(a/b)^2} && for\, a/b \geq 1 \\ k &= 4 + \frac{5.34}{(a/b)^2} && for\, a/b \leq 1 \end{aligned} \tag{3.2}$$

3.1.2 Tension band capacity

Membrane stress tends to occur and tension band will fail when it exceeds the yield stress. Using the two-dimensional stress components in web (shown in Figure 3.2).

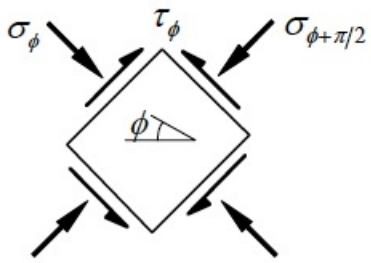

Figure 3.2: Stress state in a web plate [11]

Applying the von Mises' yiled criterion, we have the membrane stress

$$\sigma_t^y = \sqrt{\sigma_{Yw}^2 - 3\tau_c r^2(1-\frac{3}{4}sin^2 2\phi)} - \frac{3}{2}\tau_{cr} sin2\phi \tag{3.3}$$

Rockey [13] developed the tension field mode which can predict the failure mode accurately with predominated shear forces.

Referring to the mathematical transformation[14], the total shear capacity can be obtained as

$$\frac{V_s}{V_{yw}} = \frac{\tau_{cr}}{\tau_{yw}} + \sqrt{3}sin^2\theta(cot\theta - \frac{b}{d})\frac{\sigma_t^y}{\sigma_{yw}} + 4\sqrt{3}sin\theta\sqrt{(\frac{\sigma_t^y}{\sigma_{yw}}M_p^*)} \tag{3.4}$$

The total shear capacities can be treated as three components:

- the first term is the buckling strength.
- the second term represents the contribution from the tension field in the post-buckling stage.
- The third term indicates the contributions from the flanges.

The inclination of the tension field has to be decided before calculating the shear capacity. Evans put forward an empirical formulae that the value of inclination of the tension field causing the ultimate shear loads tends to be roughly 2/3 of the inclination angle described by the diagonal line in the web.[3]

$$\theta \approx \frac{2}{3} tan^{-1}(\frac{d}{b}) \tag{3.5}$$

3.1.3 Extreme cases with weak and strong flanges

So far, the discussion is about the case that the tension stress is anchored at both the top flange and the vertical stiffener, but for the extreme cases, the layout of tension field may be different from the case above.

If the flange of the girder is very weak, the contribution from the flanges may be very small and becomes negligible. In such a case, the tension filed can only be anchored at the vertical stiffeners as shown in Figure 3.3

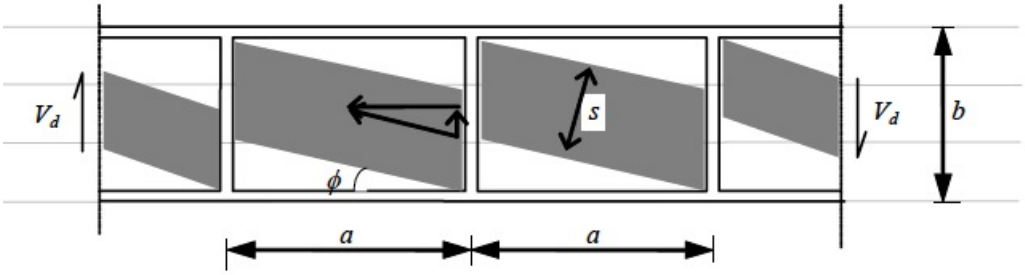

Figure 3.3: Formulatin of tension field for the cases with weak flanges [11]

This way to calculate ultimate strength for weak flange is also called Basler's theory [15] and the expression of ultimate shear capacity is shown in equation 3.6.

$$\frac{V_s}{V_{yw}} = \frac{\tau_{cr}}{\tau_{yw}} + \sqrt{3} sin^2\theta (cot\theta - \frac{b}{d}) \frac{\sigma_t^y}{\sigma_{yw}} \tag{3.6}$$

If the flange becomes very strong, the hinge of the tension field will also anchor on the flange side.Then the expression becomes

$$\frac{V_s}{V_{yw}} = \frac{1}{4}\frac{\tau_{cr}}{\tau_{yw}} + \frac{\sqrt{3}}{2}\sqrt{(1-\frac{1}{4}(\frac{\tau_{cr}}{\tau_{yw}})^2)} + 4\sqrt{3}(\frac{b}{d})M_p^* \tag{3.7}$$

3.2 The effects of stiffeners

3.2.1 Transverse stiffeners

The transverse stiffeners on the web are designed for increasing the shear resistance. Theoretically, we can image that the transverse stiffeners will divide the whole web panel into several sub-panels with smaller aspect ratios.

Tang et al [2] conducted 9 tests with various aspect ratios (0.62-1.24) to analyze the effects of space between transverse stiffeners. The webs with very large slenderness ratios (over 800) guarantee the development of considerable strength during the post-buckling. His experimental results can be concluded that

- The tension field mechanism can predict quite accurate results for the plate girders with adequate transverse stiffeners. The maximum derivation among the nine tests is 15%.
- The empirical formulae about the inclination of the tension field works well
- The transverse stiffeners will obviously improve the strength of the plate girder. Even though some stiffeners may be not adequate enough, they also provide a significant improvement in the ultimate capacity.

3.2.2 Longitudinal stiffeners

The longitudinal stiffeners are designed to improve the buckling capacity of the web panel, mainly for the bending capacity.

Tang et al [12] conducted 18 plate girder tests with strong, intermediate, weak stiffeners, as well as some cases without stiffeners. The results for different stiffeners are plotted in Figure 3.4. Some conclusions can be summarized as follows

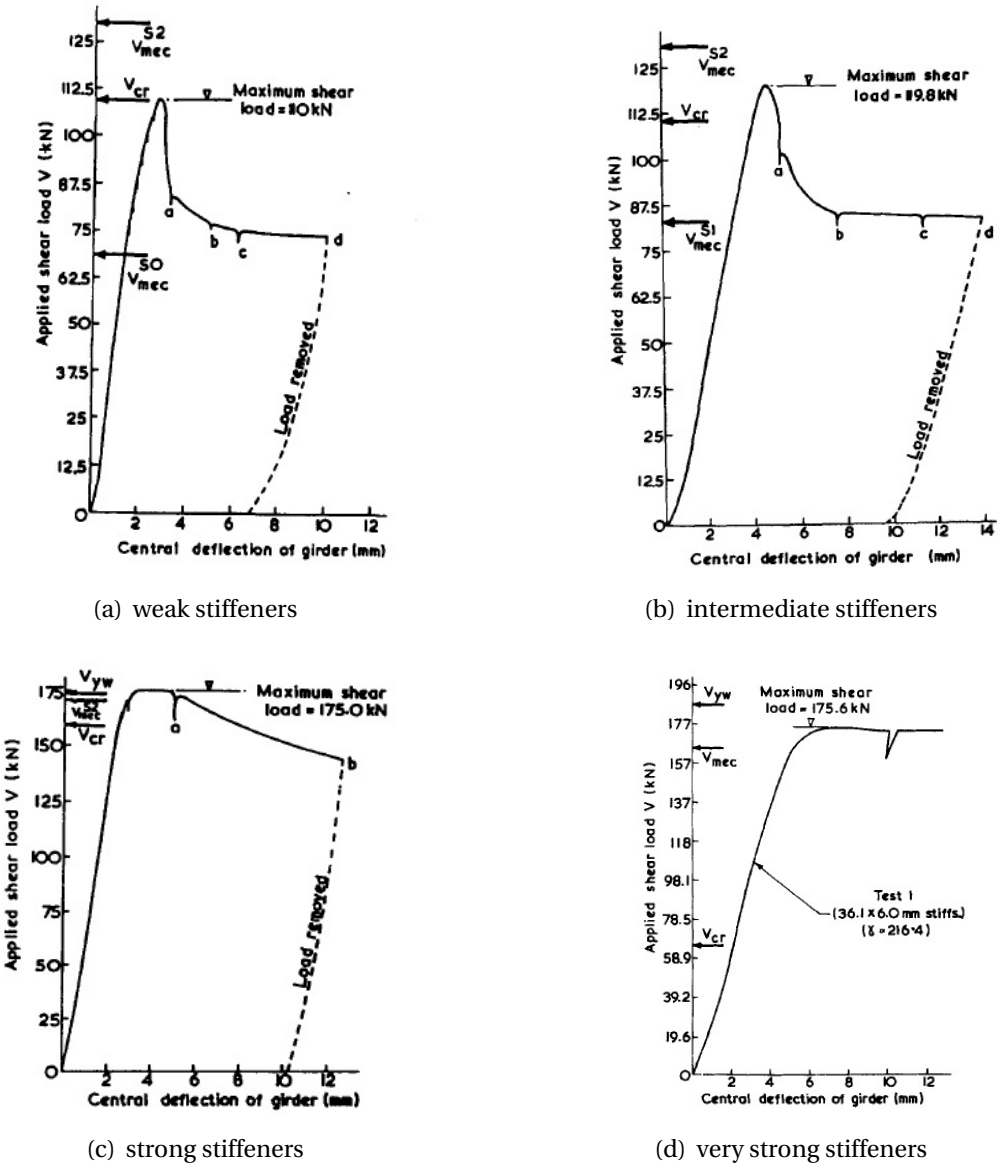

(a) weak stiffeners

(b) intermediate stiffeners

(c) strong stiffeners

(d) very strong stiffeners

Figure 3.4: load/deflection plot with various stiffeners [12]

- For all the cases, tension field mechanism can always predict ultimate failure capacity in a reasonable range.
- The bending capacity in the panels with adequate stiffeners is less than that in the unstiffened panels.
- The plate girder with weak longitudinal stiffeners shows a sharp load reduction after collapse, while the girder with stronger stiffeners tends to have a gentler drop-off.

- The plate girders with inadequate stiffeners (weak and intermediated) will collapse unstably, and then the value of the load capacity in the reduced level is approximately equal to the ultimate capacity of an unstiffened web.

3.2.3 Stiffener requirements

Transverse stiffeners must be capable of supporting the tension field. They are designed to resist buckling, while the optimum rigidity of stiffeners refers to the minimum requirement of the stiffener to remain stable during buckling. Mossonnet [16] pointed out the required rigidity of stiffeners to remain fully effective during the post-buckling process to the ultimate load has to be several times larger than $\gamma*$.

$$\gamma = k \times \gamma* \tag{3.8}$$

For simple cases, k can be found directly from the previous research[17].

One plot about the stiffener deflection in the post-buckling is shown below. The horizontal coordinate represents the ratio between applied shear force and critical shear force, while the vertical axis is the ratio between stiffener deformation and web thickness.

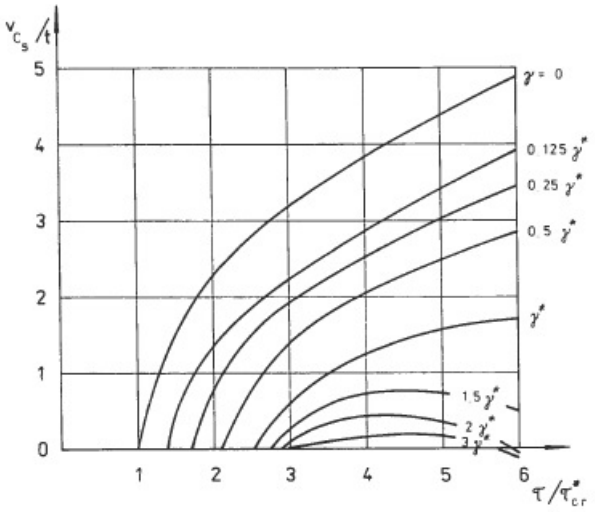

Figure 3.5: Deflection of the transverse stiffener in terms of stiffener rigidity and load factor [18]

In order to gain a clear understanding about the function of stiffeners in the post-buckling region, three contours plots of the web deflections with different stiffener rigidities are shown in Figure 3.6. [18]

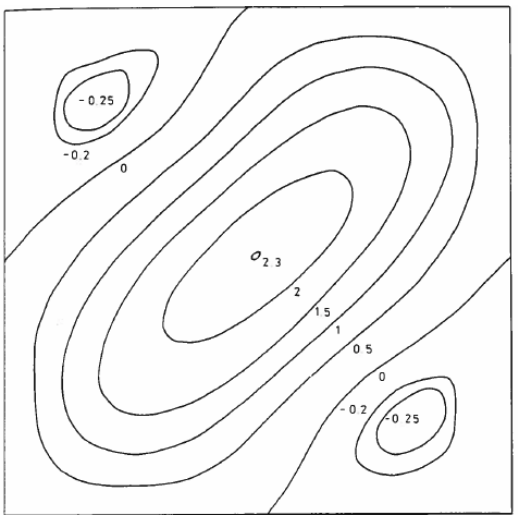

(a) (c)$\gamma/\gamma* = 0, \tau/taucr = 2$

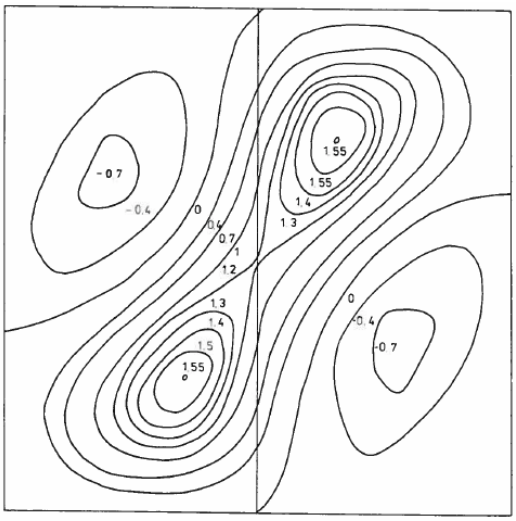

(b) (c)$\gamma/\gamma* = 1, \tau/taucr = 3.8$

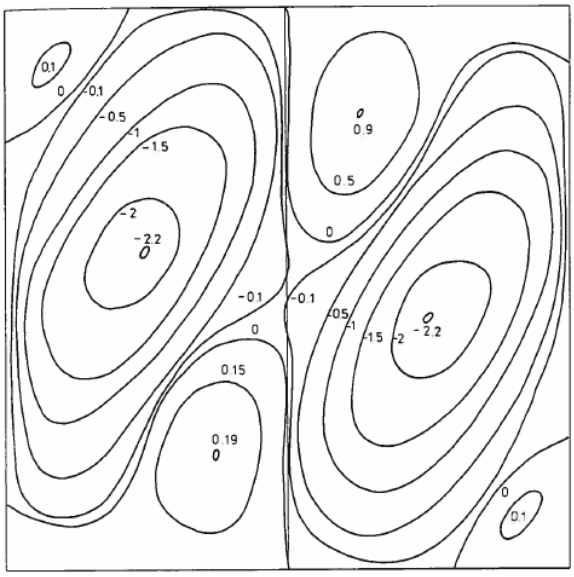

(c) buckled pattern of a web in shear and fitted with one central transverse stiffener: (c)$\gamma/\gamma* = 3, \tau/taucr = 5.9$

Figure 3.6: load/deflection plot with different rigidities [18]

From the Figure 3.6 , it is obvious that the strength of stiffeners will affect the forming of tension field, either locally with strong stiffeners or globally with week stiffeners.

A lot of previous researches recommended value for the flexural rigidity. For example, the tests conducted by M. Skaloud [18] showed that when the $\gamma * / \gamma$ is around 7, then the deflections of the longitudinal stiffener are so small that the sub-panel can be treated as the rigid supports, however, the further research showed that when the flexural rigidity reaches a certain value, a considerable increase of the stiffness rigidity results merely in a slight growth in the ultimate capacity. In practice, the recommended values for k should be 3 and 4 for transverse and longitudinal stiffeners respectively.

According to researches so far, the ratio k is mainly affected by:

- The type of the stiffener
- The cross-section of the stiffener
- The ratio between the depth and thickness of the web

Chapter 4

Review of Non-linear Finite Element Method

4.1 Introduction

This chapter mainly refers to the compendium about finite element method.[19].

Since M. J. Turner generated and idealized the direct stiffness method in the middle of 20th century, finite element method has developed to be the most popular numerical technique for approximate solutions in the structural analysis field. The three basic principles behind the finite element methods are listed

- Equilibrium (expressed by stress)
- Kinematic compatibility (expressed by strains)
- Stress-strain relationship

When the displacements are comparatively small and the material is assumed to be linear and elastic, then linear finite element method can be adopted. In reality, the true failure modes at the ultimate stress or structural post-buckling behavior are essential for design in the ultimate limited states or accidental limited states, the assumptions for linear analysis needs to be modified and nonlinearities should be taken into account.

Nowadays, nonlinear analyses are wildly used in stress analyses during the assessment of existing structures. Nonlinearities in the finite element method will definitely increase the computational time, but this issue tends to be overcame by the new generation of robust and powerful computers.

4.2 Nonlinearities of nonlinear analysis

4.2.1 Geometry nonlinearity

The geometrical nonlinearity of a bar system and the stiffness relationship is a third degree polynomial, plotted in Figure 4.1.

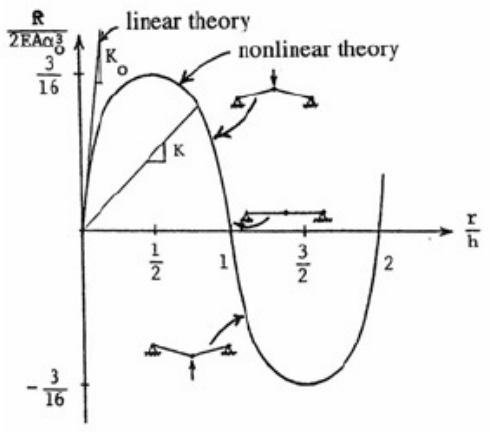

Figure 4.1: Load-deflection characteristics for a two-bar system [19]

The resultant stiffness can be regarded as the sum of the linear stiffness term and an additional correction term because of nonlinear geometrical effects. Mathematically, the linear stiffness relationship can be expressed as

$$R = Kr \tag{4.1}$$

where R is external loads

K is a constant stiffness based on the linear strain stress relationship

r is displacement

The expressions of the stiffness relationship with geometrical nonlinearities is modified

$$R = K(r).r \tag{4.2}$$

where K(r) is instantaneous stiffness based on the current displacement

In order to solve equation 4.2, it can be written based on a finite incremental form

$$\Delta R = K_I(r).\Delta r \tag{4.3}$$

where ΔR and Δr finite increments in loads and displacements

$K_I(r)$ is tangent or incremental stiffness

As for the relationship among different stiffness concepts (K_O, K_G, K_I, K), one plot is shown in Figure 4.2

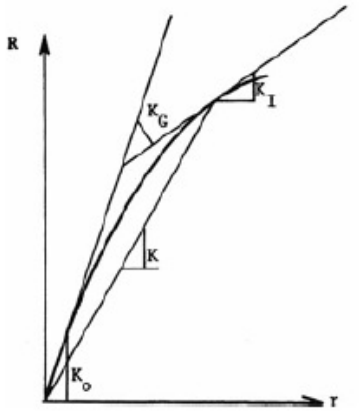

Figure 4.2: Explaination of various stiffness [19]

(K_O, K_G, K_I, K) refers to linear, geometrical, incremental and secant stiffness respectively.

4.2.2 Material nonlinearity

After exceeding the proportionality limit (σ_p), the linear relationship between stress and strain expressed by Hook's Law is not accurate any longer. The typical material properties is shown in the Figure 4.3.

The elastic strain is expressed by Hooke's law:

$$\varepsilon_e = \sigma / E \tag{4.4}$$

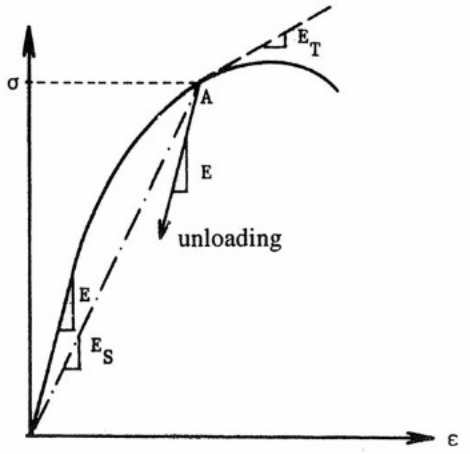

Figure 4.3: Definition of material properties [19]

Nonlinear material properties can be described by the following definitions. The stress at the point A can be shown as:

$$\sigma = E_S \varepsilon \tag{4.5}$$

where E_S is the secant modulus, which depends on the current stress strain.

When load is applied at point A, the increment of stress, $\Delta\sigma$ can be expressed by:

$$\Delta\sigma = E_T \Delta\varepsilon \tag{4.6}$$

By unloading at point A, Hooke's law applies:

$$\Delta\sigma = E\Delta\varepsilon \ \ (unloading) \tag{4.7}$$

The elasto-plastic material behaviors can be described by three rules in non-linear FEM:

- A initial yield stress: define the condition of the criterion for yielding
- A hardening rule: describe the modification of the yield due to strain hardening during plastic deformation
- Flow rule: allow determination of plastic strain increment at each point in the load history.

4.2.3 Boundary nonlinearity

Nonlinearity may also related to the boundary condition, for example, press a cylinder roller onto a flat plane by a certain displacement (shown in Figure 4.4). The boundary nonlinearity can occur even if the material is perfectly linear and the displacement is infinitesimal. This kind of nonlinearity is mainly caused by the nonlinear changes of contact area.

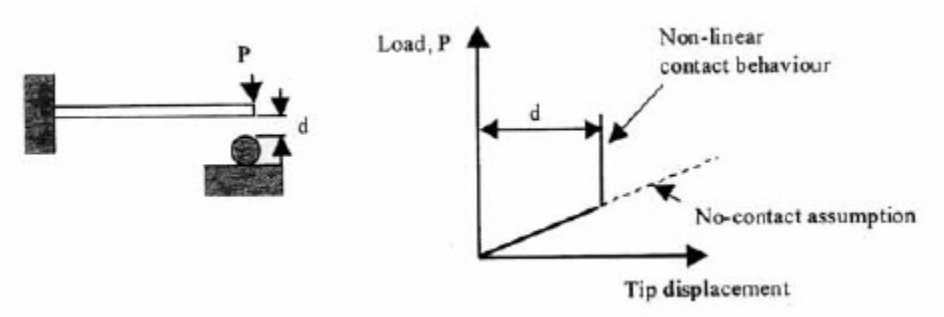

Figure 4.4: Example of boundary nonlinear [19]

This type of nonlinearity is not important in this project. For the nonlinear analyses in this project, the other two nonlinearities will be introduced.

4.3 Solution techniques

4.3.1 General

The characteristic features of various types of nonlinear response are illustrated in Figure 4.5.

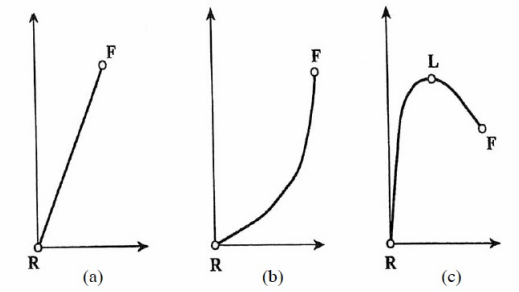

Example problem

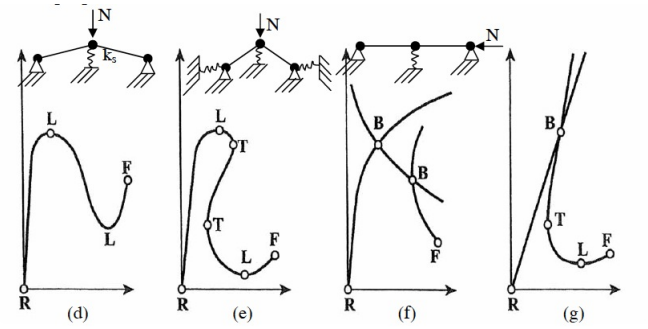

Figure 4.5: Characteristic features of nonlinear response[19]

Basic response patterns: (a) Linear until brittle failure,
(b) Stiffening or hardening,
(c) Softening.

where F and L donate failure and limit points respectively

More complex response patterns: (d) snap-through
(e) snap-back,
(f)&(g) bifurcation combined with limit points and snap-back

where B and T identify bifurcation and turning points respectively.

For nonlinear analyses, the solution is not unique any more, which means that the solution achieved may not necessarily be the solution sought. Three basic methods from various solutions will be described here

- Euler-Cauchy method
- Newton-Rapshon iterative method
- Combined method

Mathematical knowledge and physical insight into the structural nature are usually combined to obtain a qualified solution with satisfied accuracy.

4.3.2 Basic solution techniques

Euler-Cauchy method

This method provides a displacement increment which is based on the external loading increment. Then the total displacement is obtained by adding the new displacement increment. For step No. (m+1) the mathematical expressions are shown below

$$\begin{aligned} \Delta R_{m+1} &= R_{m+1} - R_m \\ \Delta r_{m+1} &= K_I(r_m)^{-1}\Delta R_{m+1} \\ r_{m+1} &= r_m + \Delta r_{m+1} \end{aligned} \tag{4.8}$$

The load should be added to the desired level. The method is illustrated for a single degree of freedom in Figure 4.6.

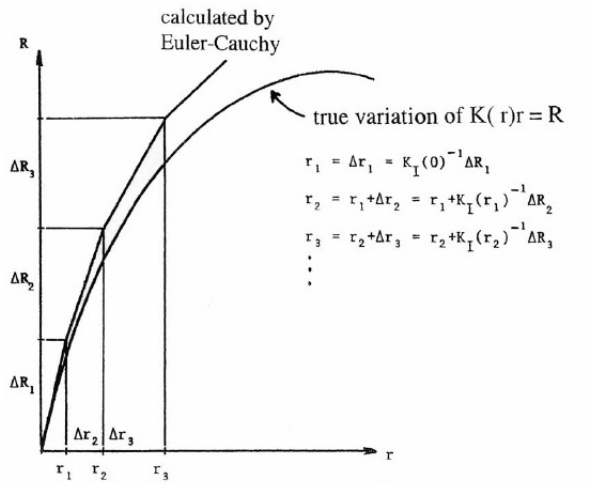

Figure 4.6: Euler-Cauchy increment [19]

In this method, the stiffness in the previous step will be used for calculating the increment of displacement in the next step. Then the deviation between approximate and true values occur as shown in Figure 4.6. The accuracy can be increased by adopting small load increment.

Newton-Raphson method

The main principle behind this method is the iteration shown in Figure 4.7.

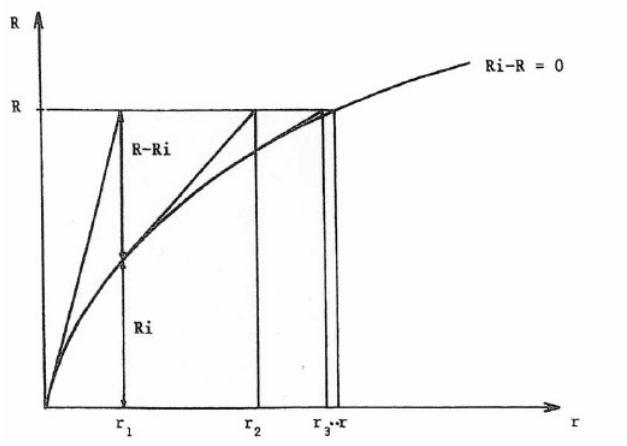

Figure 4.7: Newton-Raphson iteration [19]

The displacement increment at each step is based on the deviation between the approximate and true values at that step. The mathematical expression is that

$$R - R_{int} = K_{I(n)} \Delta r_{n+1} \tag{4.9}$$

Since the updated K_I at each step lead to an iterative procedure for calculating ΔR_{n+1}, this method is quite time-consuming. In order to reduce the unnecessary calculations, the modified Newton-Raphson iteration is put forward to update K_I less frequently. Figure 4.8 demonstrates two alternative methods to modify Netwon-Raphson methods.

The modified Newton-Raphson method can dramatically save the computational time, while the successive estimation in Newton-Raphson methods may result in slow convergence rate or no convergence at all. Additionally, the reasonable convergence criterion is expected to be given to stop the calculation procedure.

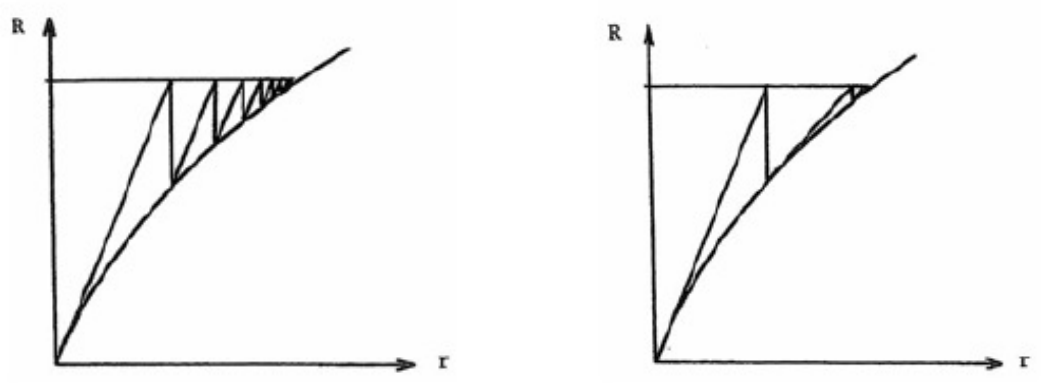

(a) No updating of K_1 (b) K_1 updated after 1. iteration

Figure 4.8: Modified Newton-Raphson methods for single degree of freedom [19]

Combined methods

The two methods mentioned above are often combined. The external load is used to control the increments and during each increment, iteration is used to obtain equilibrium. The combination of Euler-Cauchy method and a modified Newton-Raphson iteration is illustrated in Figure 4.9

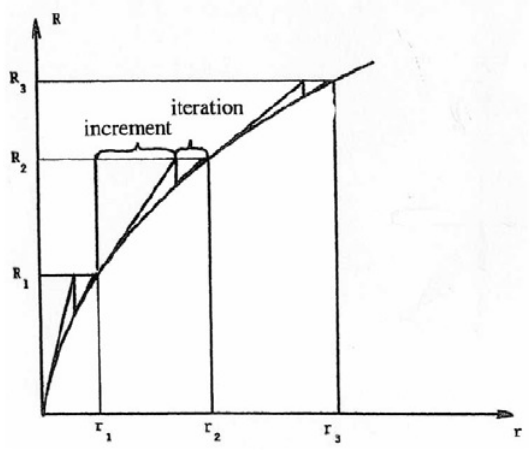

Figure 4.9: Combined incremental and iterative solution procedure [19]

The procedure is completed by applying load based on equation 4.8 followed by iteration at each level by using equation 4.9. Commonly, a modified Newton-Raphson method is used keeping the gradient K_I constant during several iteration cycles. Convergence criterion is also needed to stop Iteration.

4.3.3 Advanced solution procedures

In terms of the unstable problems, the load-displacement response may be similar with the sketch in figure 4.5(d) - 4.5(g). During the response, the variation of load is not monotonically increasing with displacement increment. Any extreme point in the load-displacement curve will need special technique to get acceptable results. Under this occasions, arc-length method shall be adopted.

As the deflection weakens the structural capacity, the external loads should be automatically made adjustments to fit the internal reaction forces. A displacement vector Δr and a load increment parameter $\Delta\lambda$ are used to describe the increment in load-displacement space, such that $\Delta R = \Delta\lambda R$. Consequently, this will result in one more equation to be solved for the equation matrix. The advantage of this method is that the additional equation helps the solution matrix to avoid 'singular', while this new equation may also cause asymmetric troubles. Several existing methods can help to solve the arc length. Two of them are plotted in Figure 4.10.

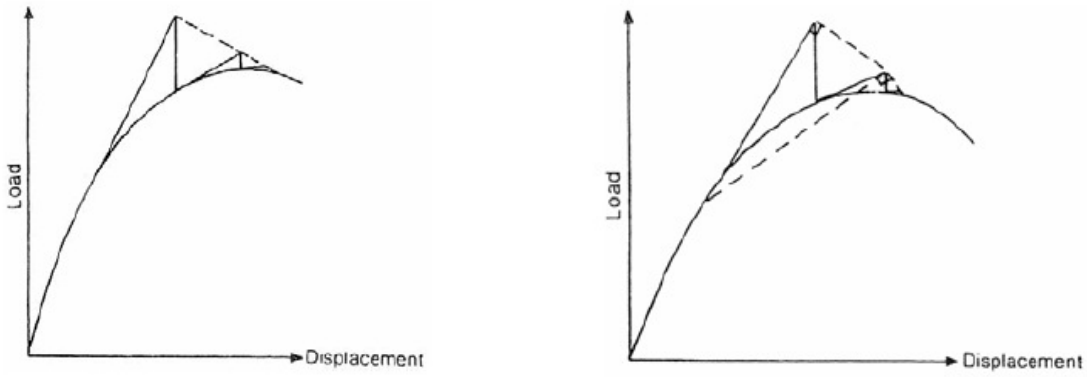

(a) Riks-Wempner's method (b) Ramm's method

Figure 4.10: Arc-length control method[19]

In Ramm's method, the iterative corrector is perpendicular to the tangental plane at the current step, while it is orthogonal to the incremental vector $(\Delta r_0, \Delta r_0)$ in the Riks methods.

Fried [20] shown another alterative method, naming orthogonal trajectory iteration method.Additionally, Crisfield [21] gave the example of very complicated iterative path.

Chapter 5

Modelling of Platform Girder in Abaqus

5.1 Introduction

The platform main deck is primarily regarded as a truss work where the top flange consists of a stiffened girder. The stiffened girder is subjected to axial compression from global bending as well as shear force due to local equipment loads. In this project, part of girder section from the platform deck is taken and analyzed. Figure 5.1 below shows a part of the drawing about the platform deck.

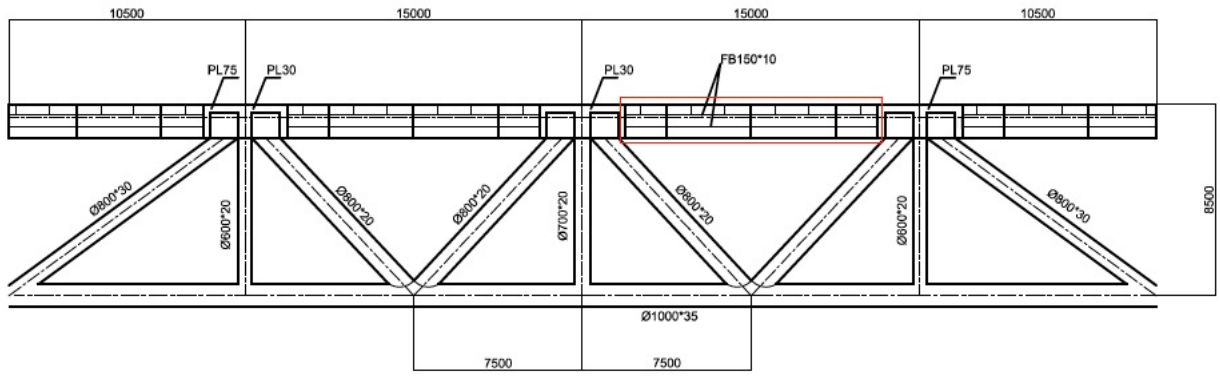

Figure 5.1: Drawing of the platform deck

The red rectangular in Figure 5.1 indicates the girder section to be analyzed in this paper. The girder section is stiffened by longitudinal stiffeners and secondary girders. Two extra section are added at the ends to modify the connections. The simplified girder section and its corresponding dimensions are shown in the Figure 5.2.

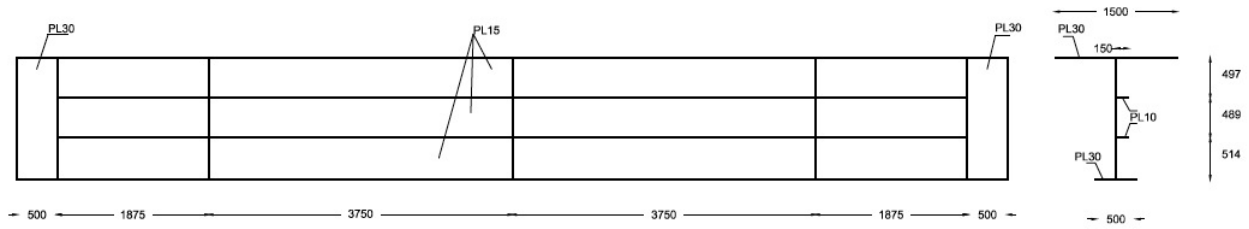

Figure 5.2: Drawing of the girder section

The girder has two flat bars almost equally spaced. In order to increase the strength, it has been proposed to replace the flat bars with T-profiles. The effects of this will also be investigated and the dimensions of the stiffeners used in this paper are listed below. The yielding stress of the material used in this girder section is 420 MPa.

Table 5.1: Dimensions of stiffeners in this project

Stiffener type	h	b	f	t
Flatbar	150	10	N/A	N/A
T-profile	300	10	130	20

5.2 Geometry model

Based on the girder section shown in Figure 5.2, the similar modelled structure in Abaqus is shown in Figure 5.3.

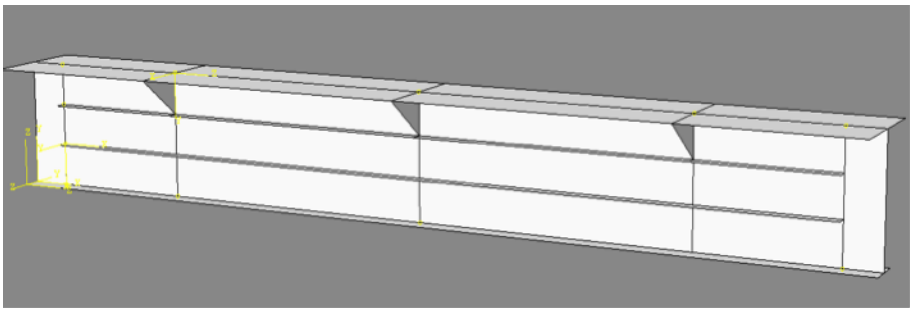

Figure 5.3: Girder section model in Abaqus

In the simplified model, the secondary girders are not induced, however, their effects on the web are simulated by additional boundary conditions to restrain the lateral displacement of the web

at the locations of the secondary girders. Furthermore, the triangular supports for the flanges are appended to prevent deformation of the flanges. The effects of the flange supports will be discussed in the buckling mode analysis and the ultimate strength analysis later.

5.3 Finite element model

Abraham stated that for design purpose, the shell elements in the analysis will present more conservative results than the solid elements. [22] The shell elements (S4R) are selected to model the whole structure.

The Figure 5.4 below illustrates the differences between a conventional shell and a continuum shell element.

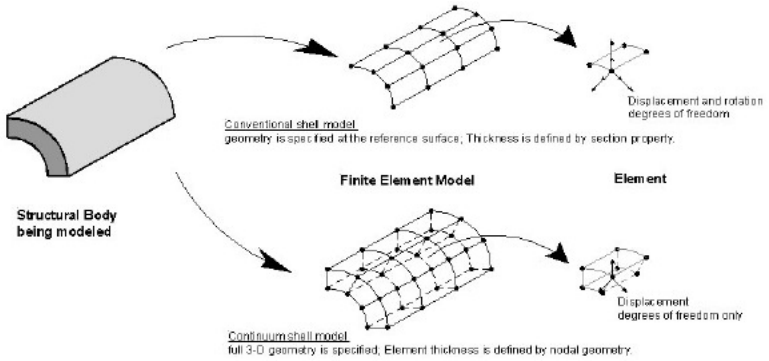

Figure 5.4: Conventional and continuum shell elements [23]

Conventional shell elements normally discretize a body by defining the geometry at a reference surface. In this method, thickness is defined by the section property. This type of elements have both translational and rotational degree of freedom. In contrast, continuum shell elements discretize an entire three-dimensional body. The thickness can be obtained from the nodal positions of elements.[23]

The reason of adopting the conventional S4R element is that it can be valid to model both thin and thick elements. Empirically, S4R elements can provide quite reasonable and accurate results for most cases. Moreover, the reduced integration method not only suits well for cases with

nonlinear membrane strain, but also helps to decrease the calculation time. The difference among S4R, S8R and S4 will be analyzed later in this paper.

5.4 Material properties

The yield stress of the material is provided to be 420 MPa and Young's Modulus is given to be 2.1E+05MPa. For nonlinear analysis, the strain hardening will also be taken into account. The hardening properties of the actual material are not known. In lieu of this, a relatively moderate hardening was assumed as the blue line in figure 5.5

In general, the methods to describe nonlinear material properties can be divided into two categories (nominal and true). The true strain and stress are employed in Abaqus to define the material nonlinearity, while USFOS will use nominal strain and stress. The explanations of conversion from nominal values to true values are attached in the Appendix A.

The assumed engineering properties and the corresponding true values are plotted in the Figure 5.5. The straight line with the slope of the young's modulus represents the elastic properties, which is followed by plastic nonlinear properties.

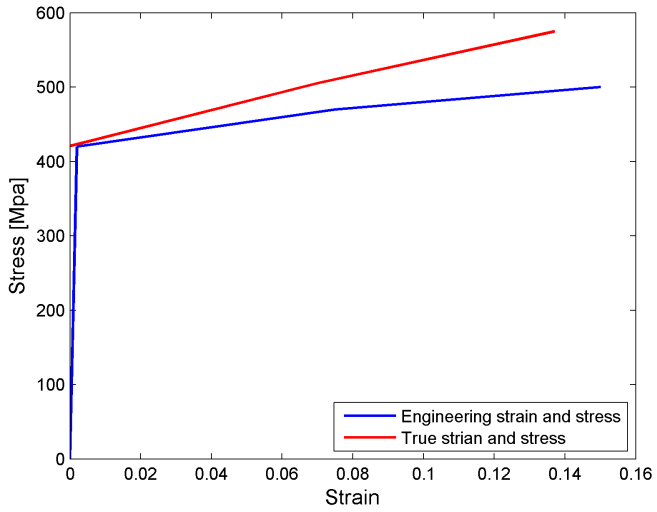

Figure 5.5: Material properties expressed by true and engineering strain and stress

5.5 Loads in Abaqus

Various load conditions listed below will be studied in this paper from the simple single loads to the combination loads.

- Pure compression
- Pure shear
- Combination of shear and compression

For the cases under compression, the forces are modelled by using normal 'shell edge load' applied on the edge of the shell elements (shown in Figure 5.6).

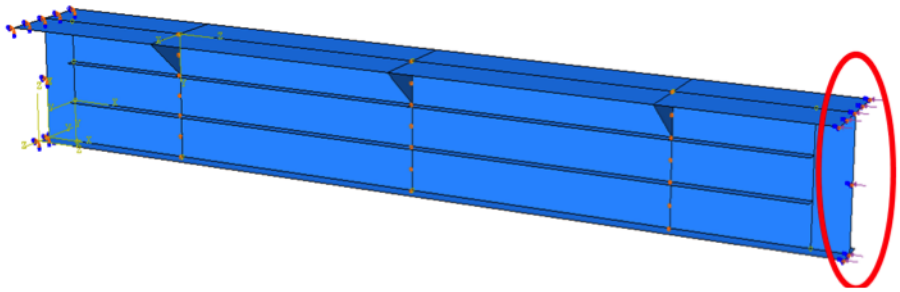

Figure 5.6: Applied compression at the ends in Abaqus

For cases under shear force, three concentrated loads together with proper boundary conditions are utilized to model the shear force. The Figure 5.7 illustrates the applied concentrated loads.

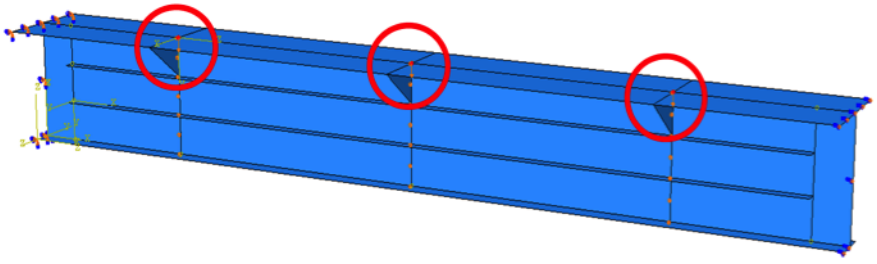

Figure 5.7: Applied shear in the middle in Abaqus

Since the shear 'shell edge load' will lead to asymmetric deformation and obviously cause the largest bending moment at the clamped ends. Instead, we decide to choose the concentrated loads leading to the largest bending moment in the mid-span and the tension fields at the ends

5.6 Boundary conditions

As mentioned that the secondary girders are not included in this simplified girder model,its effects are modeled by extra boundary condition shown by the arrows in Figure 5.8. At the locations of the secondary girders, the web is restrained against the lateral displacement.

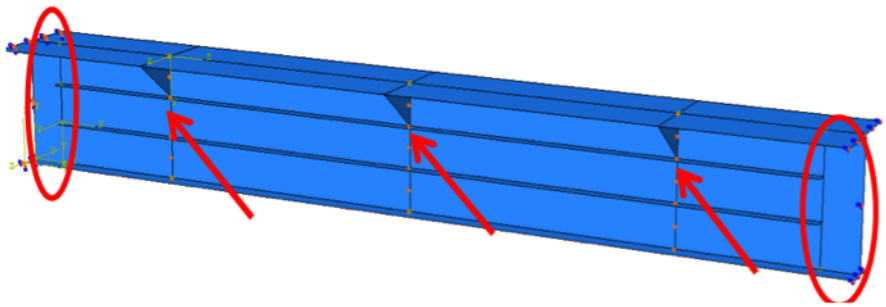

Figure 5.8: Boundary conditions in Abaqus

In terms of the ends of the girder section, clamped ends will be regarded as the most proper boundary conditions due to the the fixity at the ends. Two extra sections (in red cylinders in figure 5.8) without stiffeners are added at both two ends to avoid concentration loads under shear force. The way to model boundary conditions for this case in Abaqus is explained below.

- Clamped ends
  - Compression

    The end under compression is only free to move in the load direction, while the other end is fully fixed for six degrees of freedom.

  - Shear

    All ends are fully fixed for all degrees of freedom.

- Simply supported ends
  - Compression

    Both ends are only free to move in the compression direction, one point on the neutral axis at each end is set to rotate about the outward axis. One extra point in the middle is fixed in the compression direction. (figure 5.9(a))

  - Shear

    One point on the neutral axis at each end is set to be free to move in the longitudinal direction, and to rotate about the outward axis, but the freedom in the shear force direction has to be fixed. (Figure 5.9(b))

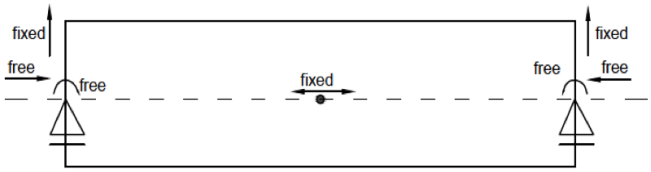

(a) Compression case

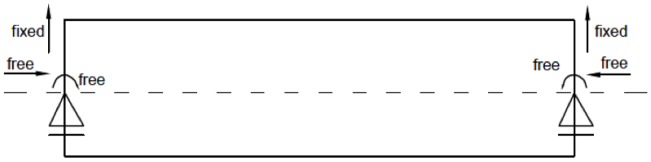

(b) Shear case

Figure 5.9: Modelled simply supported boundary conditions

When both loads are applied, the proper combination of shear and compression boundary conditions should be chosen. The effects of boundary conditions will be investigated by comparing cases with two simply supported ends and one clamped, one simply supported end.

Chapter 6

Eigenmode Analyses

6.1 Introduction

In nonlinear analysis it is necessary to introduce geometric imperfections to trigger buckling in a realistic manner. This may be done in several ways, the eigenmodes for linear buckling will be used in this paper.

Abaqus can help to run the linear eigenvalue analysis and suitable buckling eigenmodes will be picked out from the results.

The linear buckling analysis will consist of another two steps in addition to the initial step. The first step consists of a pre-loading step with the characteristic load pattern. Next, the buckling step will introduce a small perturbation load and then calculate eigenvalues and eigenvectors based on the equation 6.1.

$$(K_0 + \lambda_i K_\Delta)v_i = 0 \tag{6.1}$$

Where K_0 is the stiffness matrix caused by the preload

K_Δ is the stiffness matrix due to incremental load

λ_i and $v_i$are eigenvalues and eigenvectors

6.2 Eigenmodes under compression

Initially, the top flanges were free to move without triangular supports. The first eigenmode (Figure 6.2(a)) is dominated by flange buckling, while the web buckling mode (Figure 6.2(b)) can be found at a higher eigenmode.

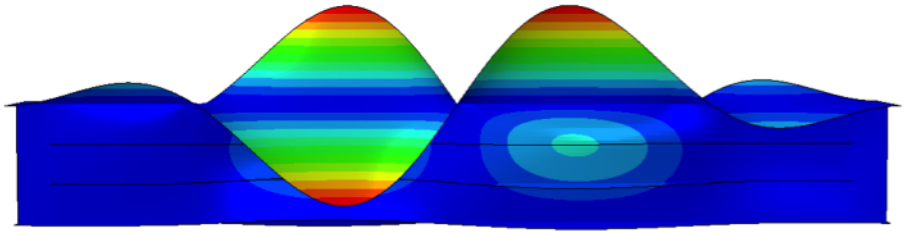

(a) Flange domiated eigenmode

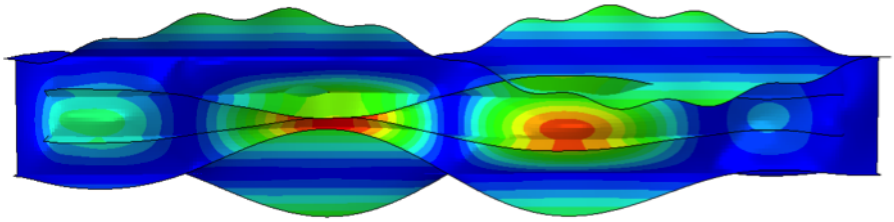

(b) Web dominated eigenmode

Figure 6.1: Important eigenmodes for the case without flange supports

Later, the flange supports are introduced to simulate the effects of secondary girder to prevent the unrealistic deformation of the top flanges.The most suitable and reasonable eigenmodes (Figure 6.2) are selected from the output results.

Due to the large cross-section area in the top flange and possibility of the flange failure, the buckling mode in the flange seems to be as same important as the buckling mode in the web. The combined eigenmodes in the web and flange are adopted to model the imperfections. Through the two figures above, the flange supports can prevent the flange deformation obviously when the web buckling mode is dominated.

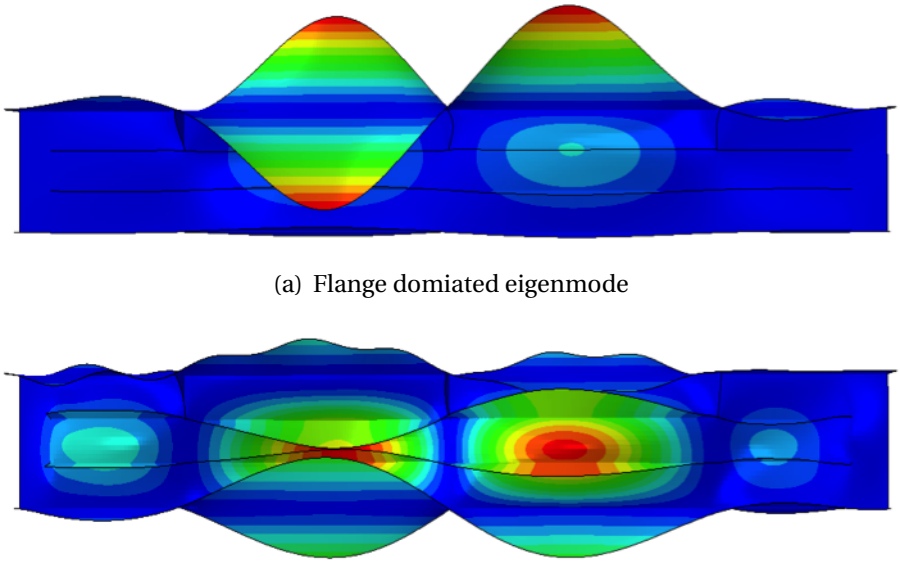

(a) Flange domiated eigenmode

(b) Web dominated eigenmode

Figure 6.2: Important eigenmodes for the case with flange supports

6.3 Eigenmodes under shear

Theoretically, the shear force will cause extremely high stress in the extra web section and failure mode will occur there as well, but these corresponding eigenmodes are not the expected ones. So two methods are put forward to enhance the strength the added web sections at the ends in order to gain the reasonable eigenmodes.

* Method 1: A new more rigid material for the web sections at the ends

A new material property for the two added web sections is defined in this method. The Young's Modulus is ten times larger than original value for other parts and the yield stress is enhanced to be 1000 times larger. The potential satisfying eigenmodes are listed in Figure 6.3.

* Method 2: Define web sections at the ends as rigid elements in Abaqus

In Abaqus, elements can be set as rigid element using the command 'constraint'. Then the elements can be regarded as infinite rigid elements shown in Figure 6.4.

The potential eigenmodes (18th eigenmode and 19th eigenmode) for the method 2 under pure shear forces are shown in Figure 6.5.

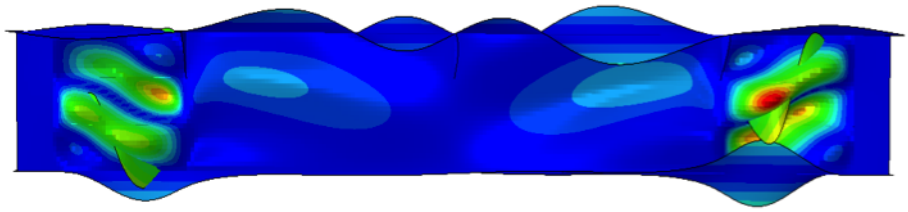

(a) 2nd eigenmode

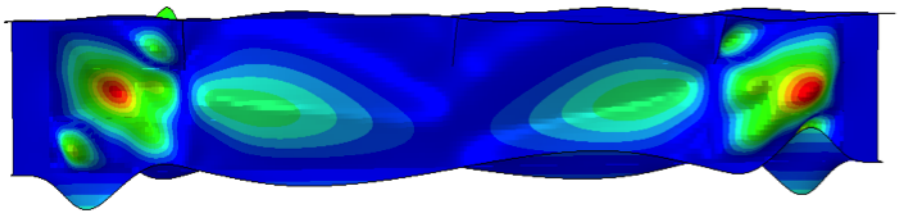

(b) 13rd eigenmode

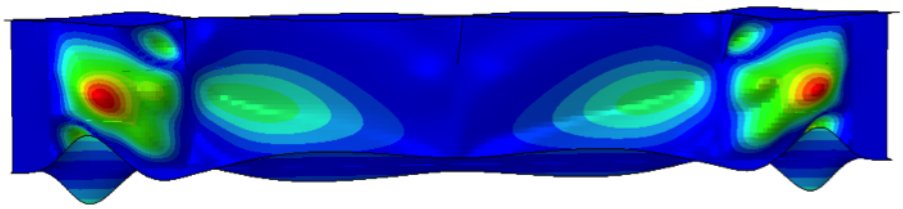

(c) 14th eigenmode

Figure 6.3: Potential eigenmodes for method 1 under pure shear

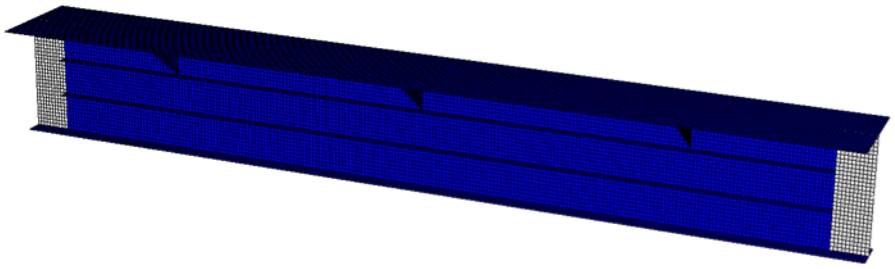

Figure 6.4: Method 2: model with infinite rigid elements at the ends in Abaqus

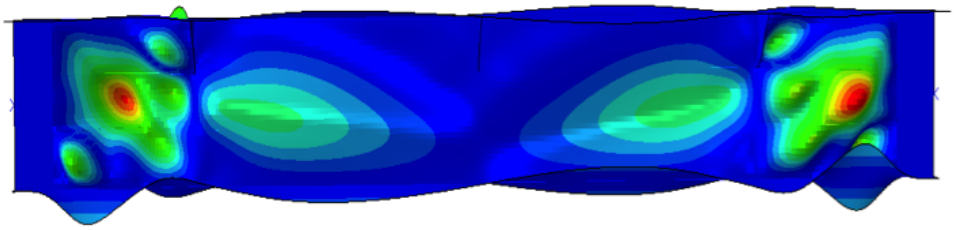

(a) 18th eigenmode

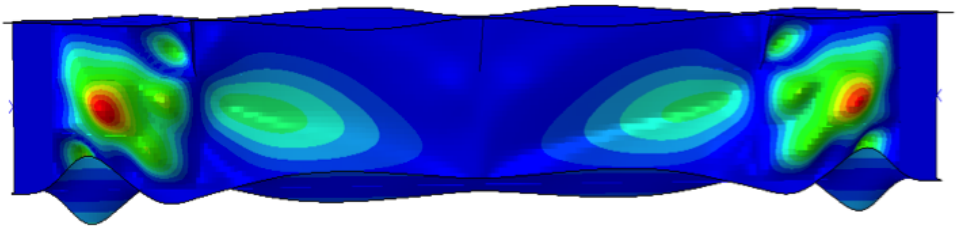

(b) 19th eigenmode

Figure 6.5: Potential eigenmode for method 2 under shear

The 2nd eigenmode (Figure 6.3(a)) in the method 1 is used to analyze the effects of the eigenmode on the ultimate strength later. Two eigenmodes in each method with symmetric and asymmetric deformed eigenmodes are selected to study influences of the deformed shape on the ultimate capacity.

From the eigenmode analysis, we can conclude that these two methods seem to give quite similar buckling modes. Specifically, the 18th eigenmode in method 2 is alike 13th eigenmode in method 1, and 19th eigenmode and 14th eigenmode are quite similar. The web will mainly resist shear forces, and for this shear load case, the tension fields at the ends occur easier than that in the middle panel.

6.4 Eigenmodes under combination of compression and shear

As for the results of the eigenvalue analysis for combination of compression and shear, no shear dominant eigenmode can be found; however, the dominated eigenmodes in the top flange and web section are quite similar with those under pure compression. The well-shaped eigenmodes

for combination of shear and compression are shown in the Figure 6.6.

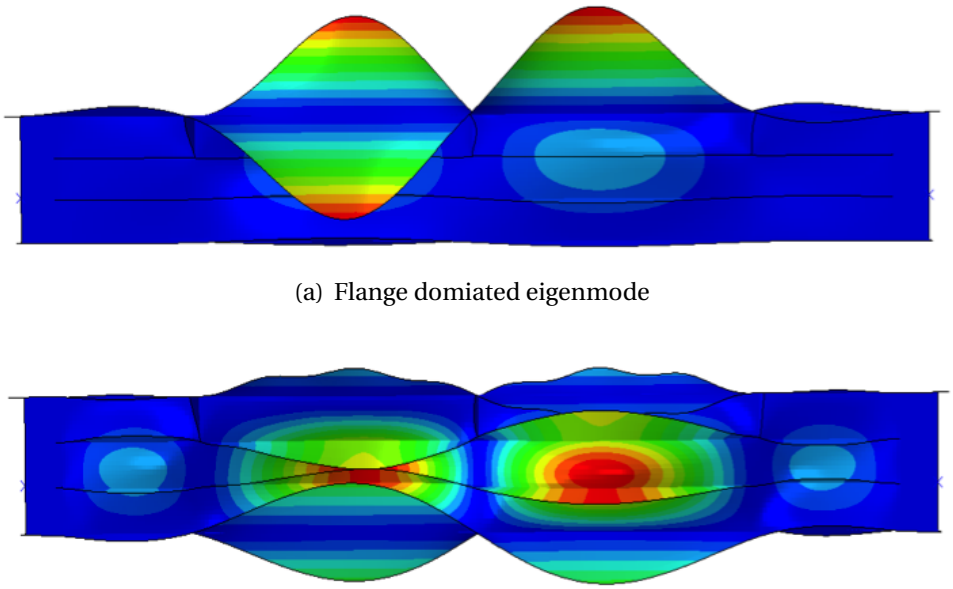

(a) Flange domiated eigenmode

(b) Web dominated eigenmode

Figure 6.6: Important eigenmodes for the case under shear and compression

According to Figure 6.6 and Figure 6.2, the conclusion is that the effects of shear on the eigenmode analysis are negligible, compared with compression. Additionally, in some cases, it is also feasible to apply eigenmodes from the cases under pure compression when running analyses under pure shear forces.

When analyzing the effects of stiffeners, the stiffeners are changed to T-profile with double height. The buckling eigenmodes in the flange and web are shown in Figure 6.7(a) and Figure 6.7(b) respectively.

Since the height of stiffeners is doubled, the local stiffener buckling will become more noticeable. Due to the effects of stronger stiffeners, the buckling mode on the web tends to be replaced by the local ones.

Furthermore, the stiffeners are strengthened by the bracketed supports at a distance of every 1875 mm. Then the larger deformation in the stiffeners shown in the Figure 6.7(b) is successfully constrained and the buckling eigenmode of the web is not important any more. The important eigenmode for this case is shown in the Figure 6.8.

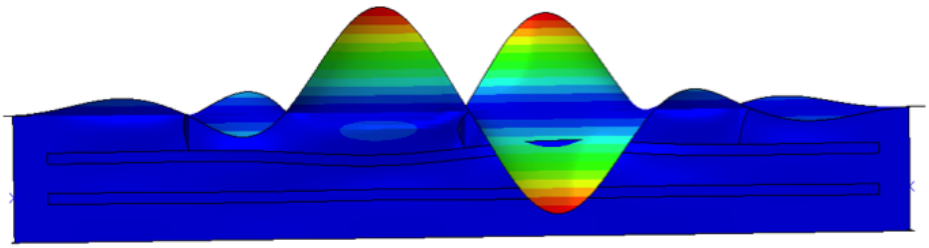

(a) Flange domiated eigenmode

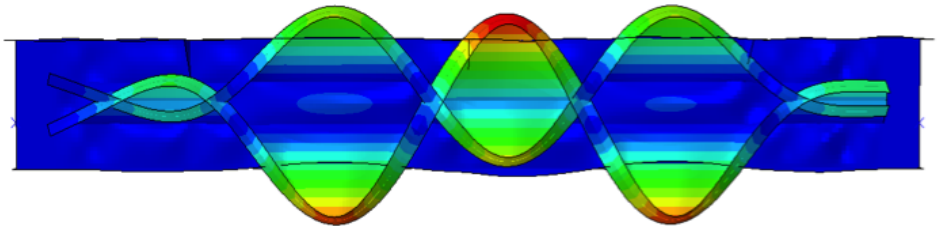

(b) Web dominated eigenmode

Figure 6.7: Important eigenmodes for the case with T-profile stiffeners under combined loads

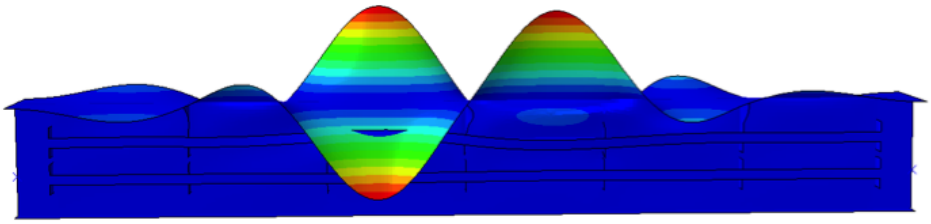

Figure 6.8: Important eigenmodes for the case with supported T-profiles under combined loads

In conclusion, we can find the following points from the eigenmode analyses:

- The buckling mode in the pure compression will dominate the deformation under the combined shear force and compression.
- The reinforced stiffeners will prevent the local deformation and affect the eigenmodes dramatically.
- Eigenmodes depend on the geometrical layout of the structure and the type of applied force, but has nothing to do with the magnitude of forces.

Chapter 7

Ultimate Strength Analyses with Abaqus

7.1 Introduction

In Abaqus, the method of riks is used to perform the post-buckling analysis. The features of riks method are listed based on the tutorial documents with regard to Abaqus:[23]

- is generally used to predict unstable, geometrically nonlinear collapse of a structure.
- includes nonlinearities form boundary conditions and material.
- is often applied after an eigenvalue buckling analysis to investigate a structure's collapse.
- can be used for the cases with snap-through problems

In the Riks analysis, the load during a step is always proportional and the current load magnitude is defined by:

$$P_{total} = P_0 + \lambda(P_{ref} - P_0) \tag{7.1}$$

where P_0 is the 'dead load', which exists at the beginning of the step and never be redefined.

P_{ref} denotes the reference load defined in the Riks step.

λ is the load proportionality factor.

The load proportionality factor is the output at each increment as part of the solution.

The Riks method performs well in post-buckling problems, no matter how stable the post-buckling behavior is. However, since there is some discontinuous response at the point of buckling, the exact post-buckling problem can be analyzed directly. One alternative is to introduce an initial geometrical imperfection, then the problem will have continuous response instead of bifurcation and some responses in the buckling mode will occur before reaching the critical load.[24]

In this chapter, the effects of different eigenmodes and the magnitude of initial imperfection will be estimated under different load conditions. The effects of different boundary conditions and stiffeners will also be analyzed as well.

7.2 Effect of initial imperfectons

Initial imperfections are modelled with distorted coordinates using the eigenmodes from Chapter 6. Originally, for one eigenmode, the maximum amplitude is somewhat arbitrarily selected to be 10mm. This corresponds to 2% of stiffener spacing. For two included buckling modes„ the deflection about 0.15% of length is used to model the initial geometric imperfection (equation 2.3).

Here we assume that the boundary conditions are clamped for all the cases, and the effects of boundary condition will be investigated in the next section.

7.2.1 Pure compression

As for the cases under compression, the buckling of the top flange seems to be critical. The effects of the flange supports will be studied here as well. All the cases about compression are listed in Table 7.1. All the corresponding stress distribution at the ultimate strength can be found in the Appendix B.

The results of ultimate strength analysis for the first four cases are plotted in Figure 7.1 and 7.2 with flange dominated and web dominated eigenmodes respectively.

Table 7.1: Case list under pure compression

Case No.	Flange support	Eigenmodes	Imperfection (mm)
1	No	Flange dominated	10
2	Yes	Flange dominated	10
3	No	Web dominated	10
4	Yes	Web dominated	10
5	Yes	Two eigenmodes	5 for web & 5 for flange
6	Yes	Two eigenmodes	10 for web & 10 for flange
7	Yes	Two eigenmodes	15 for web & 15 for flange
8	Yes	Two eigenmodes	No imperfections

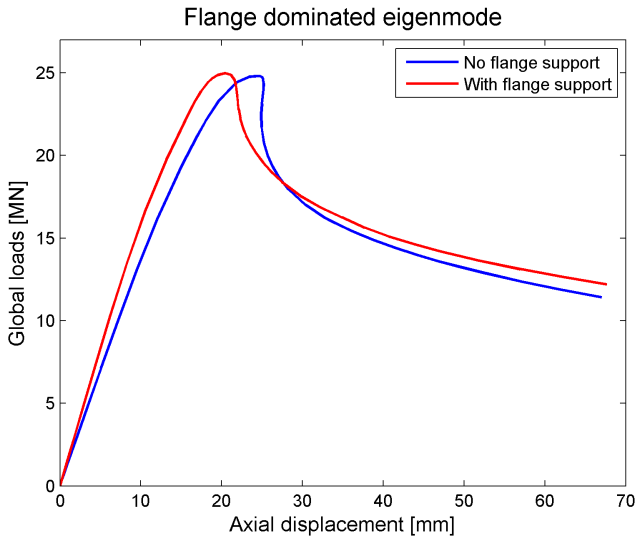

Figure 7.1: Effect of flange supports with flange dominated eigenmodes

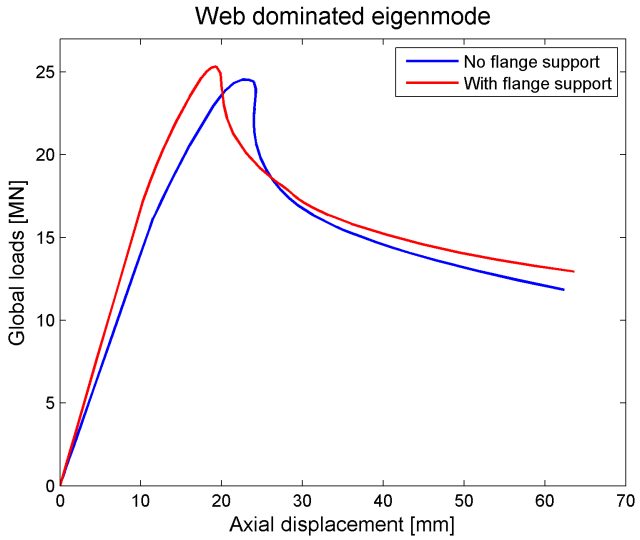

Figure 7.2: Effect of flange supports with web dominated eigenmodes

From the results, it is obvious that no matter what kind of eigenmode is introduced, the additional flange support can enhance the total strength of this girder, but the increment in ultimate capacity is limited.

The differences between the ultimate loads with web and flange dominated eigenmodes are small, two reasons may be concluded as follows:

- The ultimate strength is quite robust to different eigenmodes.
- Due to large slenderness, the top flange is as sensitive as the web to buckle.

Based on the results above, the buckling modes of the top flange and web almost have the same importance. In order to model the realistic imperfection of the plate girder, two eigenmodes will be used together to modify the initial imperfection in both flange and web.

Theoretically, the 5 mm imperfections for two eigenmodes (case 5 in Table 7.1) can give a good estimation for this 12-meter-long structure. The failure mode for the case 5 at the ultimate strength is shown in figure 7.3 (Case 5 in Appendix B).

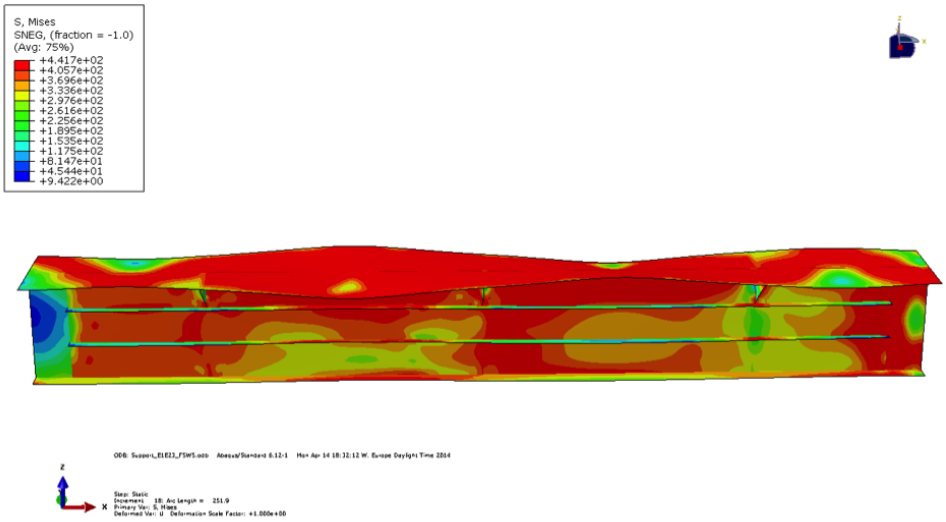

Figure 7.3: Von Mises stress distribution at the ultimate strength under pure compression(case no. 5)

For the failure process, the stiffener will reach its buckling capacity at first and the stiffened plate tends to buckle, which will weaken the whole structure, then the top flange will collapse together with the web section. The structure fails due to buckling.

In order to investigate the effect of initial imperfections under pure compression, more cases with buckling eigenmodes from web and flanges (case 6-8 in table 6.1) are designed and the results with respects to the load/deflection relationship are shown in the Figure 7.4.

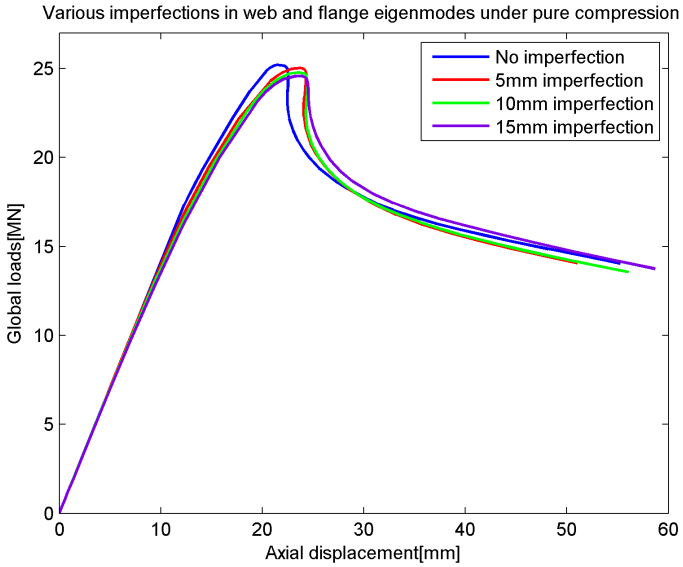

Figure 7.4: Effect of imperfections under pure compression

According to the collapse behavior and the results shown in the figure above, we can draw the following conclusions:

- Initial imperfection will definitely decrease the ultimate capacity.
- The larger the initial imperfection is, the more nonlinear the response becomes.
- Nonlinear analysis of this structure is robust to the initial imperfections under pure compression.

7.2.2 Pure shear

As two methods for analyzing pure shear force and their corresponding potential eigenmodes are studied in the last chapter, the influences of these two methods and different eigenmodes on the ultimate stress of the plate girder will be discussed here. The cases under pure shear force are listed in Table 7.2 and the corresponding stress distribution at the failure step are attached in Appendix B.

Table 7.2: Case list under pure shear

Case No.	Method No.	Eigenmodes	Imperfection (mm)
9	1	2	5
10	1	13	5
11	1	14	5
12	2	18	5
13	2	19	5
14	2	19	10
15	2	19	15
16	2	19	No

☞ **Methods**:

Method 1: A new rigid material for the web sections at the ends

Method 2: Define web sections at the ends as rigid elements from Abaqus

The first five cases are designed for investigating the effects of two methods and different eigenmodes. The results of ultimate analysis are plotted in Figure 7.5.

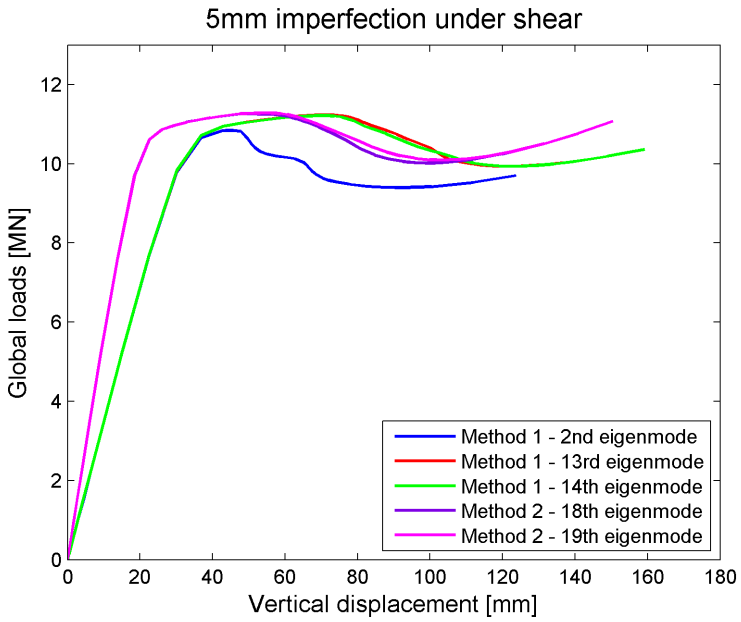

Figure 7.5: Comparison of ultimate capacity for two methods

As for the method 1, the eigenmodes 13 and 14 can provide a larger strength capacity than eigenmode 2 after the initial yielding. The method 2 with the infinite rigid elements can take almost the same global loads as method 1, but the larger inclination of slope indicates that the whole structure becomes more rigid due to infinite rigid elements.

According to figure 75, the curves for eigenmode 13 and 14 almost overlap each other, so do the curves for eigenmodes 18 and 19. Given the certain magnitude of largest deflection, the symmetric and asymmetric imperfections tend to give the same level of ultimate capacity.

The failure modes for eigenmode 18 and 19 are shown in Figure 7.6. The symmetric imperfection cause the symmetric failure modes, while the asymmetric imperfection will lead to asymmetric stress distribution during collapse.

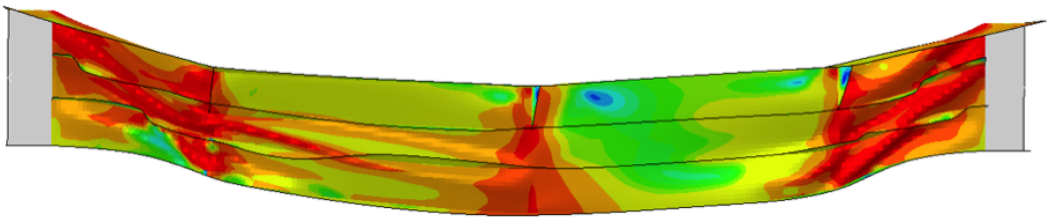

(a) Failure mode of eigenmode 18 (asymmetric)

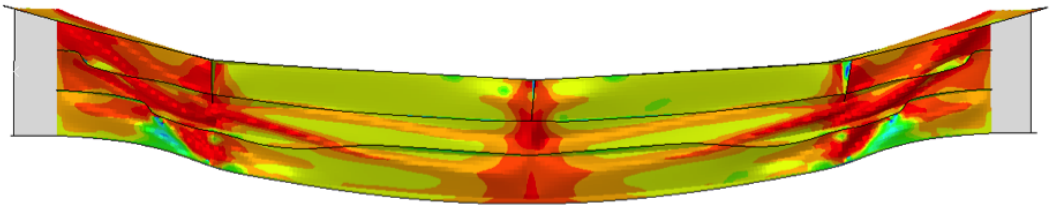

(b) Failure mode of eigenmode 19 (symmetric)

Figure 7.6: Comparison between failure modes based on different eigenmodes

Additionally, in contrast to method 1, the method 2 can show proper stress distribution for the main body of the girder, references about the stress distribution at the ultimate strength can be found in Appendix B. The Von Mises stress distribution for the ultimate strength with eigenmode 19 is shown in Figure 7.7 (Case 13 in the Appendix B).

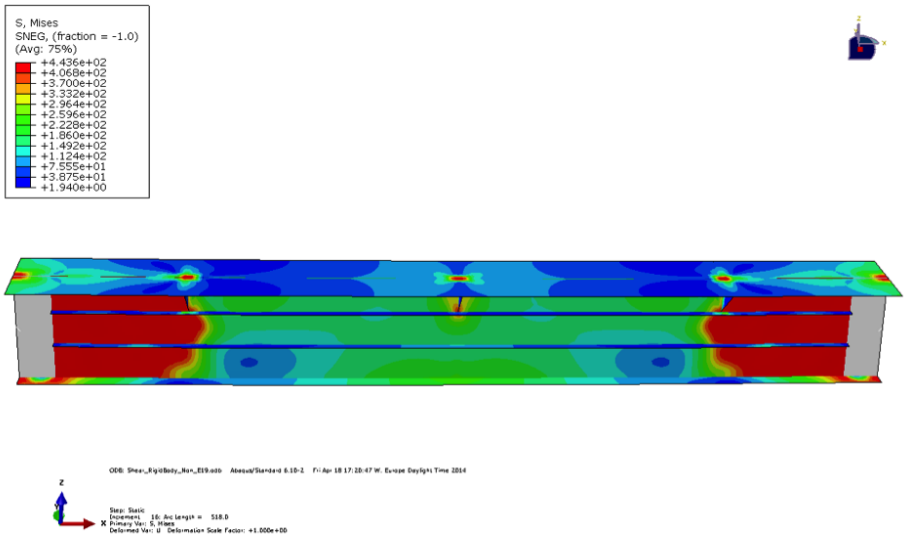

Figure 7.7: Von Mises stress distribution at the ultimate strength under pure shear(case no. 13)

The stress in the web section at the ends are higher than other section due to the membrane stress near the fixed boundary conditions and the tension field will appear when the shear buckling capacity is fulfilled.

The strain stress relationship is elastic until the occurrence of the first yielding, which is followed by the hardening in the plastic zone. Then the whole structure begins to collapse and the membrane stress forms the tension fields at the ends to bear more loads.

The sensitivity of ultimate capacity of the structure to the initial imperfection under the pure shear is discussed by case 13-16, which is shown in Figure 7.8 in next page. Based on the ultimate capacity study under shear force, the following conclusions are summed up:

- Initial imperfection will definitely decrease the shear ultimate capacity.
- The larger the imperfection is, the smaller the hardening zone is.
- Regardless of imperfections, the post-buckling behaviors due to the membrane stress are almost the same.
- The magnitude of deformation determines the reduction of the capacity, while the effects of the direction of the deformation are tiny.

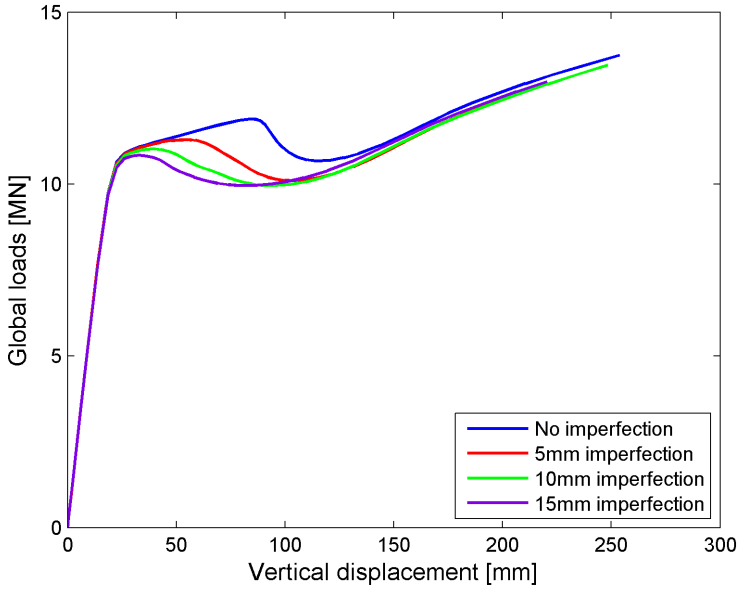

Figure 7.8: Effects of imperfections under pure shear

7.2.3 Combined shear and compression

As discussed in last chapter, the eigenmodes for combined compression and shear are similar with those under pure compression. Based on the buckling mode analysis, the shear eigenmodes are not dramatically important to cause the structure to collapse under combined forces. So we introduce the imperfections in the flange and web from the buckling analysis under combined forces.

The Table 7.3 illustrates the various composition of shear and compression in the combined cases.

Table 7.3: Compositions of shear and compression in the combined loads

Case No.	Shear (of ultimate stress)	Compression (of ultimate stress)
Pure shear	100%	0%
Shear dominated	80%	20%
Both equal	50%	50%
Compression dominated	20%	80%
Pure compression	0%	100%

The cases 17-21(shown in Table 7.4) are designed for analyzing the relationship between the ultimate capacity of the girder and the proportion of shear and compression for the combined force. The remaining cases 22-32 are used to discuss the effects of imperfections under the combined loads. All these cases adopt the buckling eigenmodes for combined force mentioned in Chapter 6.

Table 7.4: Case list under combined loads

Case No.	Stress composition	Imperfection (mm)
17	Pure shear	5 for web & 5 for flange
18	Shear dominated	5 for web & 5 for flange
19	Both equal	5 for web & 5 for flange
20	Compression dominated	5 for web & 5 for flange
21	Pure compression	5 for web & 5 for flange
22-26	As cases 17-21	10 for web & 10 for flange
27-31	As cases 17-21	15 for web & 15 for flange

In the nonlinear analysis for the ultimate strength, the excitation forces dominate the failure modes of structures. Like the case 18, the case with dominated shear force motivates the shear failure modes (Figure 7.9).

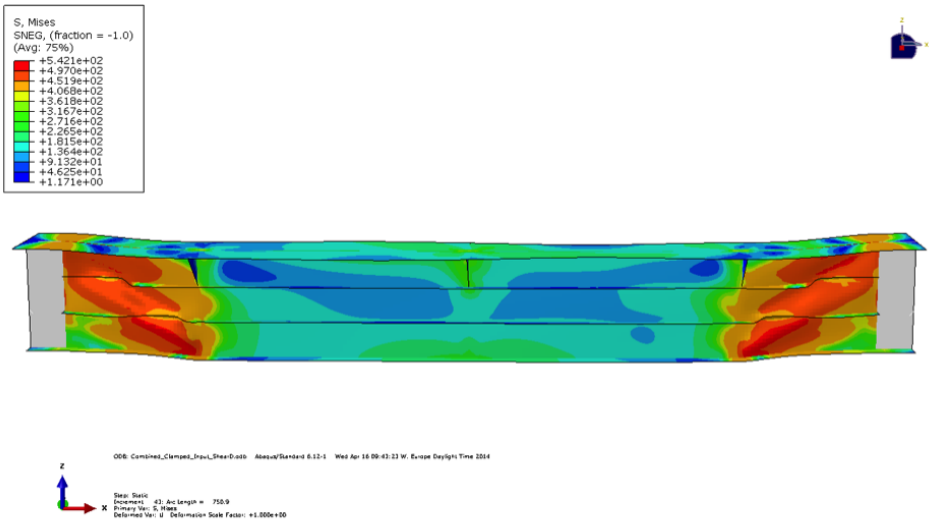

Figure 7.9: Failure modes of case 18 at post-buckling: shear dominated

Similarly, the bending failure modes will be triggered due to the dominated compress force in case 20 (Figure 7.10).

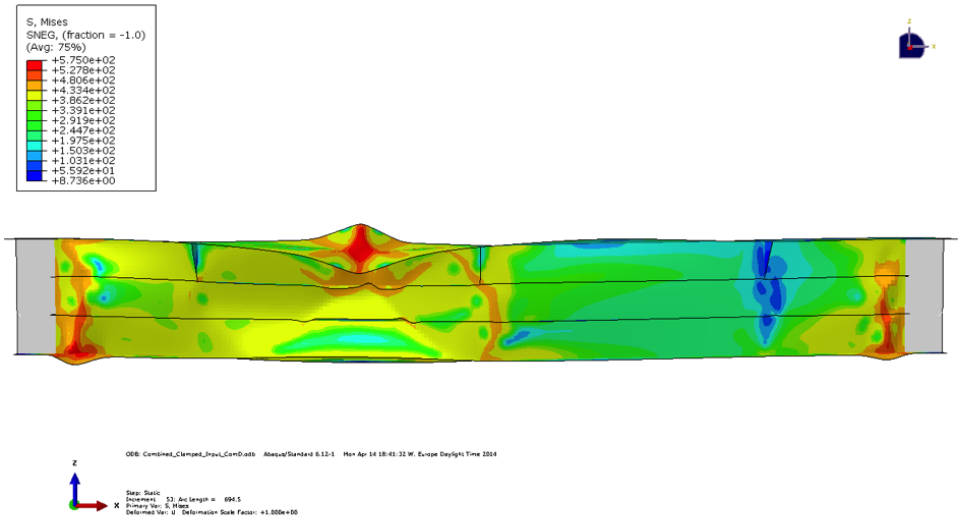

Figure 7.10: Failure modes of case 20 at post-buckling: compression dominated

The ultimate strength of the structure with various combined forces are shown in Figure 7.11. The interaction of shear and compression on the ultimate strength of the structure can be expressed roughly by the parabola curve, which means the ultimate capacity can be treated as the sum of the capacity utilizations under different loads, but the failure mechanism will greatly depend on the dominated load.

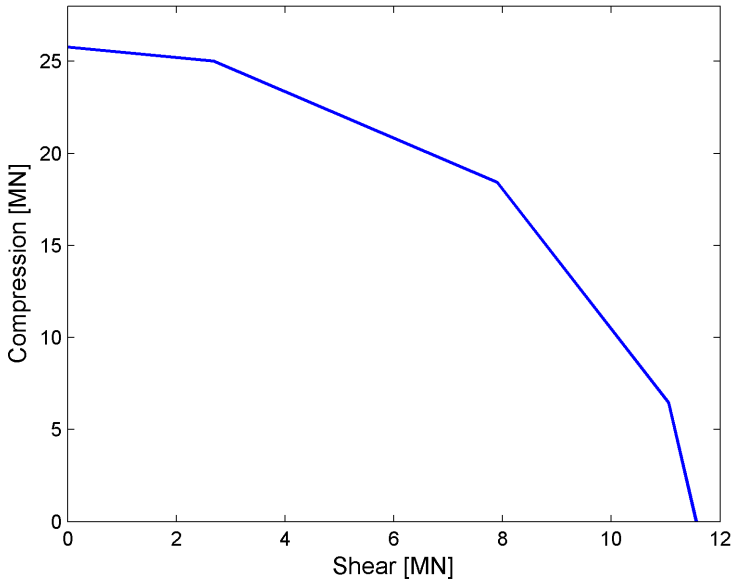

Figure 7.11: Interaction of compression and shear for ultimate capacity

The effects of the initial imperfections on the ultimate capacity are studied by introducing 0mm, 5mm and 10mm imperfection based on the eigenmode analysis under combined forces. It means that no shear eigenmode is included and the results are plotted in Figure 7.12.

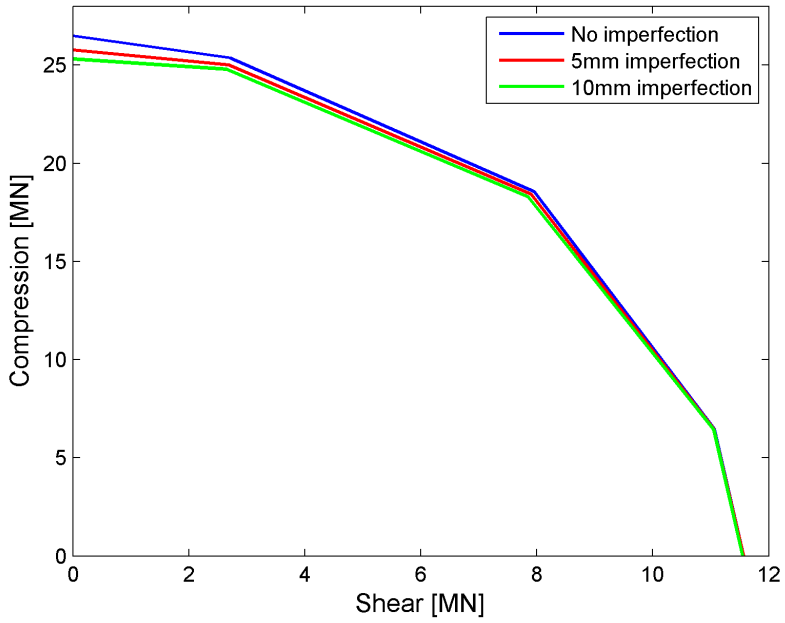

Figure 7.12: Effects of imperfections under the combined loads

The conclusions from the studies with regards to the ultimate strength under combined forces with various composition, some conclusions are given below to explain the phenomenons in this section.

- Although eigenmodes under combined forces are almost the same as those under the pure compression and no shear buckling mode is introduced, it is still valid for shear dominating cases to fail in a shear mechanism .
- The effects of geometric imperfection become noticeable gradually when the compression starts to dominate.
- Since no shear buckling mode is taken into account for the combined cases, the ultimate capacity under pure shear is almost the same with different initial imperfections
- The utilization can be treated as the sum of the capacity utilization under different loads, but the failure mechanism will depend on the dominated load.

7.3 Effect of boundary conditions

7.3.1 Introduction

The boundary conditions for a given problem can be formulated to solve the differential equations. The boundary condition is related to the prescribed displacements and stresses. In this paper, three different boundary conditions are analyzed under the combined loads.

- Clamped at two ends
- Simply supported at two ends
- Clamped at one end and simply supported at the other one

The cases designed for comparing the different boundaries are tabulated in Table 7.5.

Table 7.5: Case list for various boundaries

Case No.	Boundary conditions	Stress composition
17-21	Two clamped ends	pure shear, shear dominated, both com dominated, pure compression
32-36	One clamped end and one simply supported end	As cases 17-21
37-41	Two simply supported ends	As cases 17-21

7.3.2 Comparison of three boundary conditions

For the cases with dominant shear, dominant compression and equal shear & compression, the stress distribution at the step of ultimate stress are shown in Figure 7.13- 7.15 for different boundary conditions.

From the figures 7.13- 7.15, we can conclude that the clamped ends will the concentrated stress and then fail near the ends. The failure for the simply supported case occurs in the middle of the plate girder. For the shear dominated cases, the failure will occur in a shear failure mechanism, while the bending failure mode takes place when the compression tends to dominate.

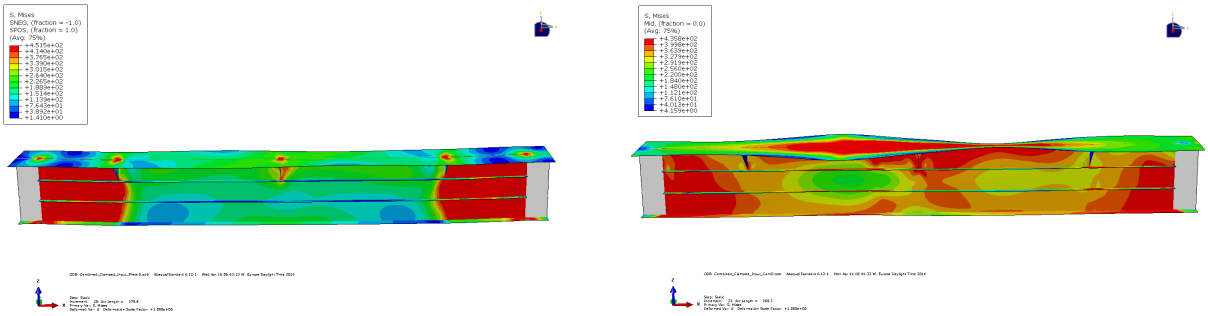

(a) Shear dominated (case 18 App. B) (b) Compression dominated (case 20 App. B)

Figure 7.13: Stress distribution at the ultimate step for two clamped ends

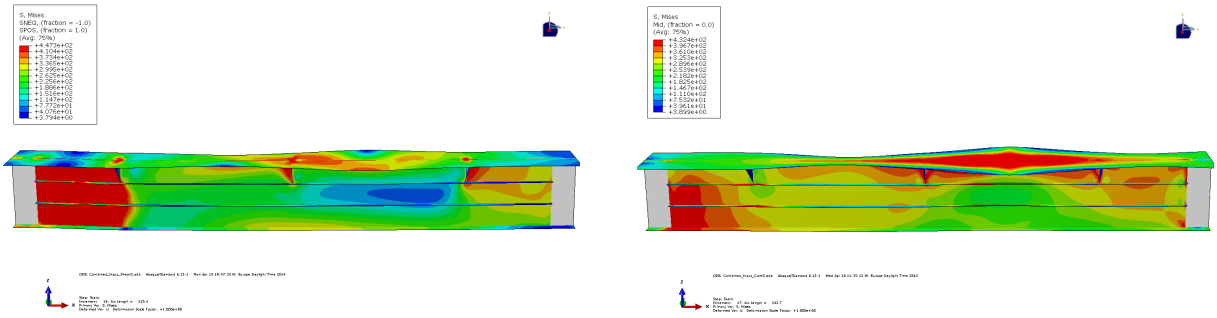

(a) Shear dominated (case 33 App. B) (b) Compression dominated (case 35 App. B)

Figure 7.14: Stress distribution at the ultimate step for combined boundary conditions

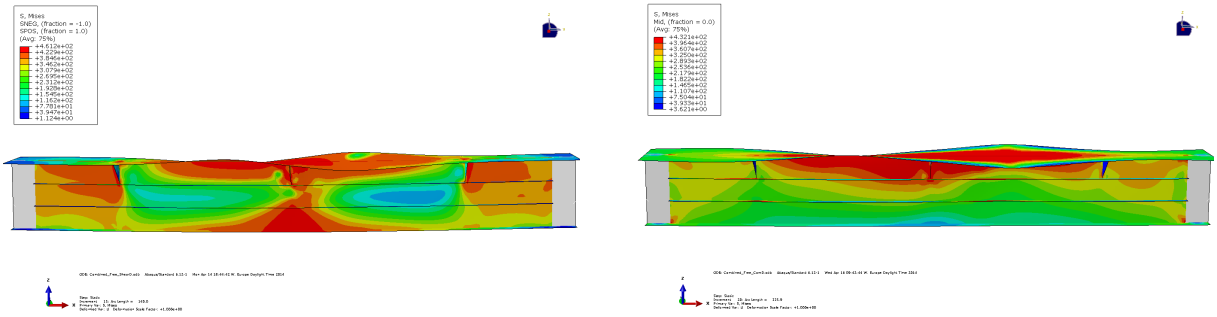

(a) Shear dominated (case 38 App. B) (b) Compression dominated (case 40 App. B)

Figure 7.15: Stress distribution at the ultimate step for two simply supported ends

One markable conclusion from the figures above is that clamped boundary conditions tend to have membrane stress concentration near the ends, while simply supported case prefer to fail in the middle section. Results about the effects of boundary conditions on the ultimate capacity of the girder section are shown in Figure 7.16 below.

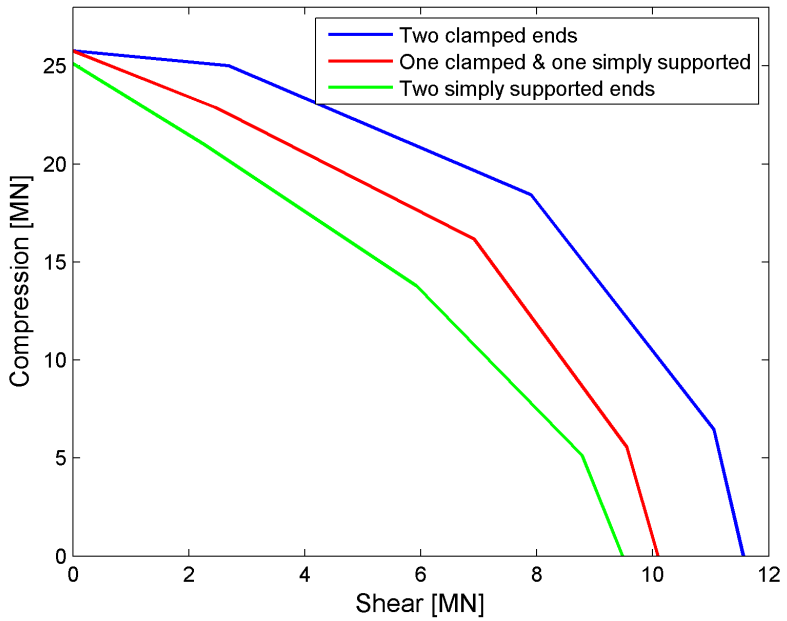

Figure 7.16: Effect of boundary conditions with the same imperfection

◇ Shear dominated cases

Clamped boundary conditions possesse more resistance, the main reason is the membrane stress at the fixed ends can make contributions to the ultimate capacity. Another reason is that the flange can contribute to resist more loads after the web is utilized in the shear failure mechanism.

◇ Compression dominated cases

The effects from the boundary conditions are quite small, even negligible because of the limitations from boundary conditions. Specifically speaking, when the compression is quite large and uniform distributed, the displacement of the whole end is totally the same in the direction of compression force and no rationality takes place at the simply supported ends. This corresponds to the clamped ends under pure compression

7.4 Effect of secondary stiffeners

7.4.1 Introduction

As studied by previous researches, the stiffeners help to increase the structural strength and affect the stress distribution. The magnitude of the enhancement depends on the strength of stiffeners. In order to increase the strength, the flat bar in the previous cases are replaced by strong T-profile stiffeners, and T-profile stiffeners with stiffener supports. The dimensions of the stiffeners are illustrated in Table 5.1.

The cases for analyzing the stiffeners are tabulated in Table 7.6. Case 17-21 means the previous cases with various composition under the combined forces. Case 42-46 are designed for study the difference between different stiffeners and case 47-51 are used to analyze the effects of the supports for stiffeners. The stress distribution of all the cases at the ultimate step can be found in Appendix B.

Table 7.6: Case list for stiffener effects

Case No.	Stiffener types	Stress composition
17-21	Flat bars	pure shear, shear dominated, both com dominated, pure compression
42-46	T-profile	As cases 17-21
47-51	T-profile with supports	As cases 17-21

7.4.2 T-Profile stiffeners

From the eigenmode analysis, the buckling of the double-height stiffeners tends to become dominant and replaces the buckling of the web. So it will be introduced as the initial geometric imperfection into the ultimate analysis here. The failure modes of the flat bar and T-profile stiffener in the shear dominated cases are given in Figure 7.17 .

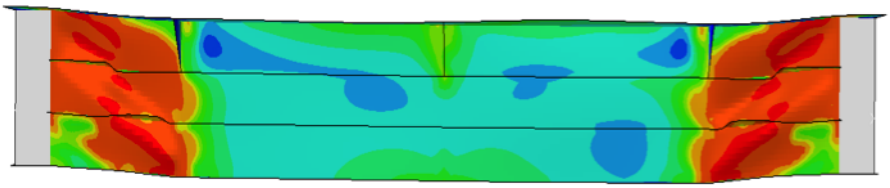

(a) Failure mode of flatbar stiffener

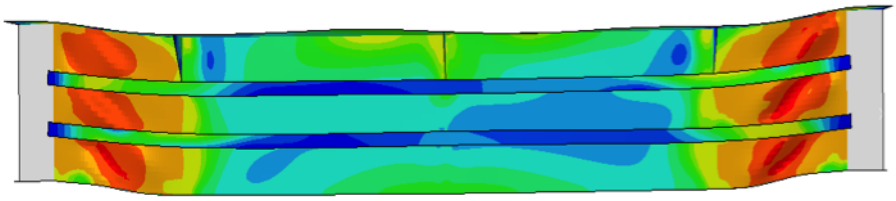

(b) Failure mode of T-profile stiffener

Figure 7.17: Comparison of failure modes caused by stiffeners under shear dominated

From Figure 7.17, we can observe that the strong T-profile stiffeners remain stable and the tension fields take place between the stiffeners, while the flat bar stiffeners are wrapped during the forming of the tension field.

7.4.3 T-Profile stiffeners with supports

The stiffeners on the web are reinforced by the brackets every 1875mm. In order to simplify the modelling, the brackets are builded as rectangular webs as shown in the figure below.

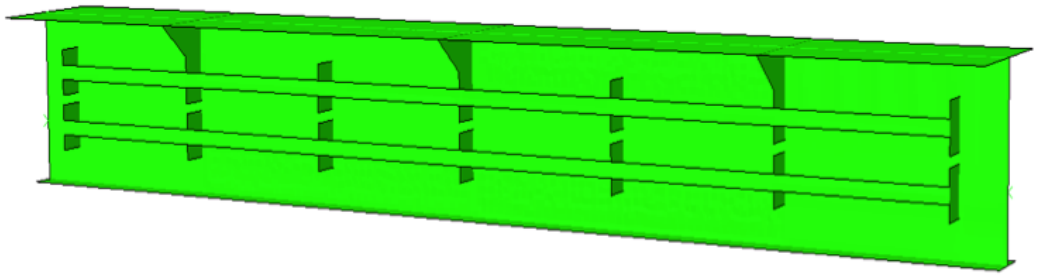

Figure 7.18: Plot of the girder with stiffener supports

From the eigenmode analysis, the stiffener supports enable stiffeners to be strong and stable, and then the deformations in the web and stiffener are not important anymore. Instead, the deformation and failure tends to take place locally. The failure modes of shear and compression dominant cases are shown in Figure 7.19.

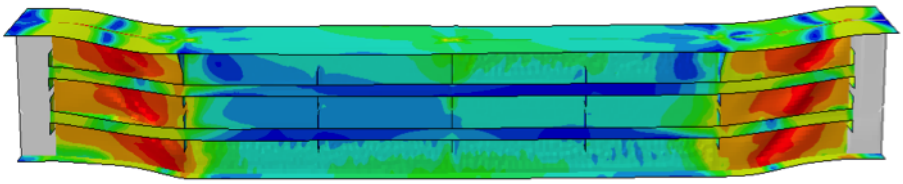

(a) Shear dominated case

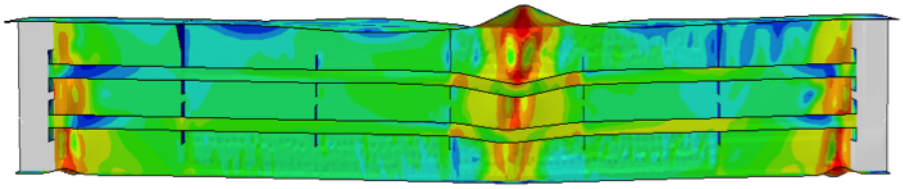

(b) Compression dominated case

Figure 7.19: Failure modes for T-profile stiffeners with supports

On the basis of the results form nonlinear analysis, the increment of the ultimate capacity due to changes of stiffener strength is listed in Table 7.7, 7.8.

Table 7.7: Increment of ultimate strength due to strong stiffeners

Stress case	Flat bar(MN)	T-profile(MN)	Increment(%)
Pure shear	11.565	12.004	3.80
Pure com	25.787	29.641	14.95

Table 7.8: Increment of ultimate strength due to stiffener support

Stress case	T-profile(MN)	T-profile support(MN)	Increment(%)
Pure shear	12.004	12.374	3.08
Pure com	29.641	30.459	2.76

In order to show the results in a intuitionistic and clear way, the plot of ultimate strength with various stiffeners is shown in Figure 7.20

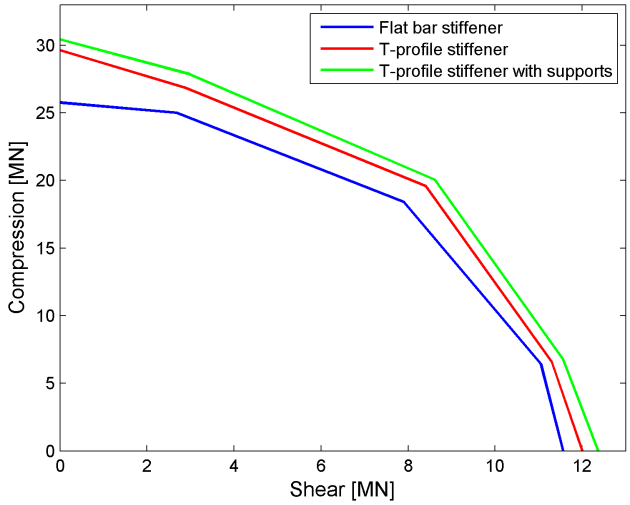

Figure 7.20: Effect of secondary stiffener strength on ultimate capacity

For the effects of secondary stiffeners on the ultimate strength, several conclusions can be drawn as follows:

- In contrast to flat bars, the stronger T-profile stiffener can improve the ultimate strength dramatically, from around 15% under pure compression to 3.80% under pure shear. This is because the longitudinal stiffeners can increase more bending capacity compared with shear capacity.
- The stiffener supports can improve the ultimate capacity of the structure at almost the same level (3%) for all the cases.
- Strong stiffeners can effectively prevent the global buckling or failure. Instead, the deformation will occur locally between the stiffeners.

Chapter 8

Ultimate Strength Analyses with USFOS

8.1 Introduction

As a leading computer program, USFOS is designated for nonlinear static and dynamic analysis of frame structures. As described in the USFOS manual,[25] the nonlinear analysis can be concluded as the basic following steps:

- Incremental load is applied in steps
- The nodal coordinates and element stiffness are updated after each step
- In each load step, the plastic capacity will be checked in each element to see whether the critical value is exceeded or not. If the capacity is fully occupied, the load step will be scaled to make the force comply 'exactly' with the yield condition
- When the force in the element reaches the yield surface, a plastic hinge occurs. Since the element later may be unloaded and become elastic, if so, the plastic hinge can be removed.
- The load step is reversed if global instability is detected

As for the load increment in each step, the sign of the load increment and size of the load increment will needed to be considered.

In USFOS, the current stiffness parameter and the tangential stiffness matrix determinate decide the sign of the load increment. For load step no. i, the Current Stiffness is defined by

$$S_p^i = \frac{\triangle r^{1^T} \triangle R^1}{\triangle r^{i^T} \triangle R^i} [\frac{\triangle p^i}{\triangle p^1}]^2 \tag{8.1}$$

For most problems, the current stiffness parameter mentioned in the user manual [26] can give a good indication about the sign of the load increment. In regards the spring-back problems, more corrections are needed.

As for the size of the load increment, it is the outcome of several functions and they can be concluded as followings:

- The history specifications in the user's load control file
- Occurrence of plastic hinges
- Exceedance of the maximum displacement increment defined by user
- The incremental procedure defined by 'arc length'
- Adjustments during equilibrium iterations

Additionally, the advanced technique, arc length iteration procedure, is used to overcome the instabilities of the iteration when passing limiting points and bifurcations. More details can be found in the USFOS User's manual.[26]

8.2 Introducing imperfection from Abaqus

The function 'Struman' in the USFOS can help to create the input model file in USFOS based on the input file for Abaqus. As for the initial imperfection, it is not feasible to run the eigenvalue analysis in USFOS, while one possible way is to export the geometry containing the imperfections from Abauqs and then use the function 'Struman'.

The geometries for all steps can be found from the output file (odb.) in Abaqus, (File->Import->Part->*.odb), next select "Import deformed configuration" option and choose the original increment step as the initial imperfection. (shown in Figure below).

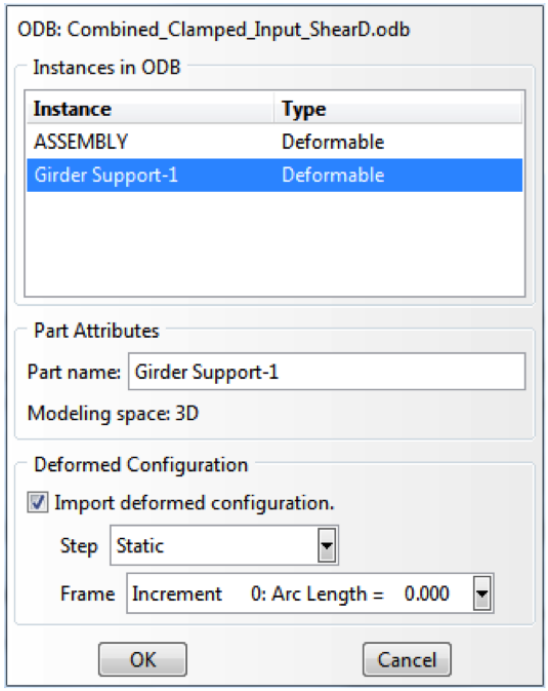

Figure 8.1: Export the deformed geometry from Abaqus

8.3 Defining model parameter in USFOS

Unlike Abaqus, USFOS uses the engineering strain and stress. The characteristic values for this material are assumed reasonably based on experience and can be found in the table in step (i) in appendix A. The blue line in Figure 5.5 shows a clear impression about this material engineering properties.

In terms of defining the material properties, it is hard to define the nonlinear material plasticity in the USFOS. In USFOS, the material plasticity is simply defined by hardening parameter given in equation 8.2, which is treated as a reference value after yielding.

$$Hardening = \frac{\sigma_U - \sigma_Y}{0.15 \times E} \tag{8.2}$$

The cases in USFOS are listed in Table 8.1. In order to calibrate results from Abaqus accurately, all parameters should set to be the same as those in Abaqus. The imperfection is the output from Abaqus and boundary conditions for all these cases are assumed to be fully clamped.

Table 8.1: Case list in USOFS

Case No.	Applied loads	Imperfection (mm)	Boundary
52	Pure shear	5 for web & 5 for flange	Clamped
53	Shear dominant	5 for web & 5 for flange	Clamped
54	Equally combined	5 for web & 5 for flange	Clamped
55	Compression dominant	5 for web & 5 for flange	Clamped
56	Pure compression	5 for web & 5 for flange	Clamped

The compression forces are applied as the nodal loads at one end of the model and three concentrated loads at the same location are used to simulate the shear effects. In order to compare the largest load proportional factor for collapse, the applied global load in USFOS should be made sure to be equal to the load sum in Abaqus. The Figure 8.2 illustrates the way of the loads applied in USFOS

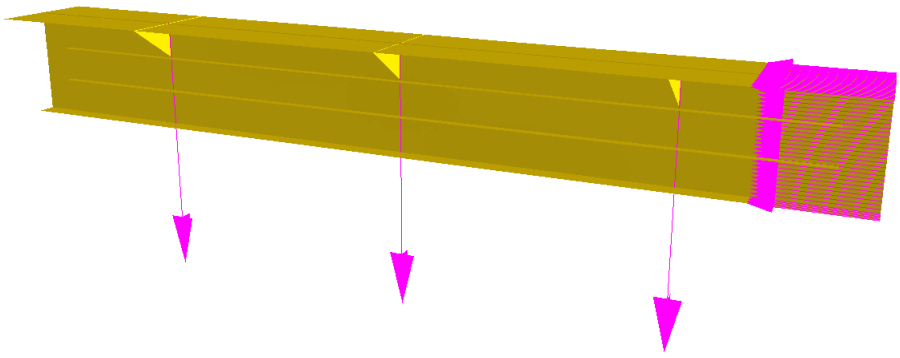

Figure 8.2: Load application in USFOS

8.4 Results comparison between USFOS and Abaqus

The Von Mises stress distribution at the step of the ultimate strength and curves for the relationship between global load and displacement are shown in Figures 8.3 - 8.5 for the cases with large shear, large compression and two equal components respectively.

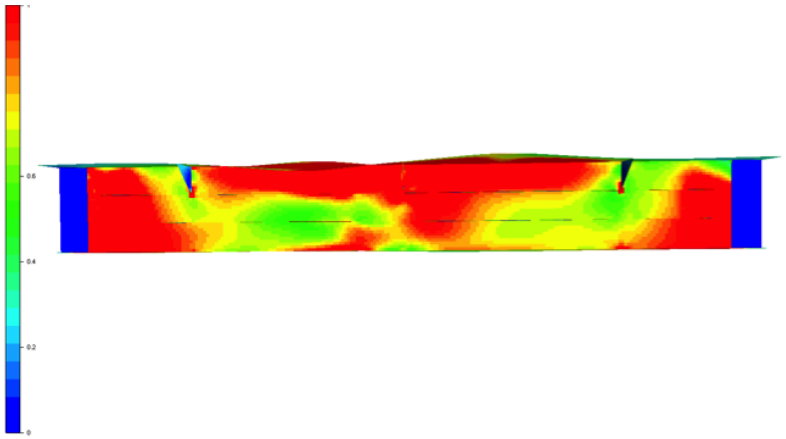

(a) Stress distribution in USFOS

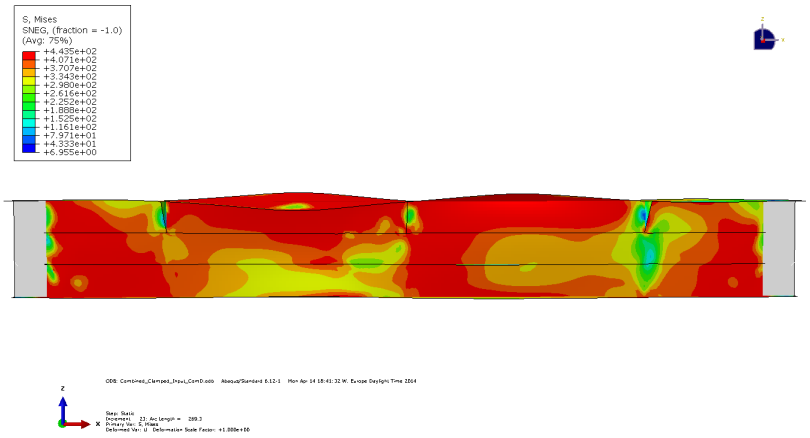

(b) Stress distribution in Abaqus

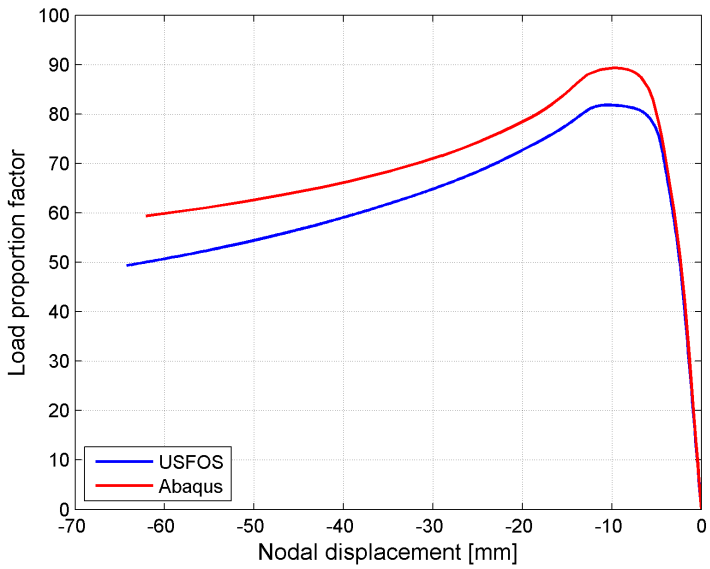

(c) Load/deflection curves

Figure 8.3: Results comparsion for compression dominated cases

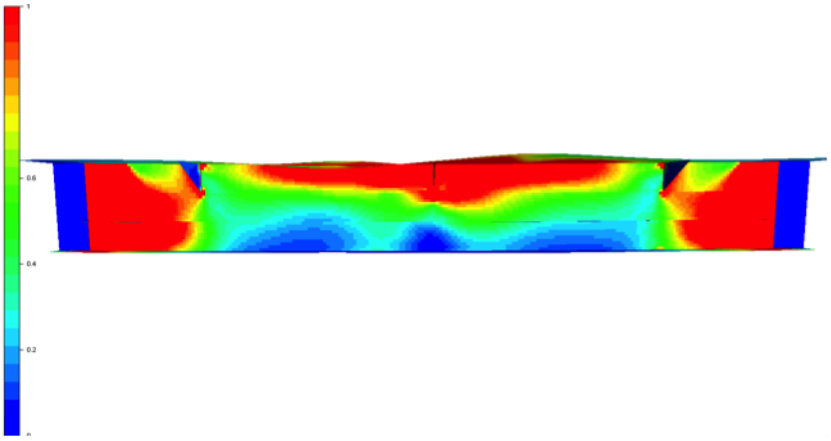

(a) Stress distribution in USFOS

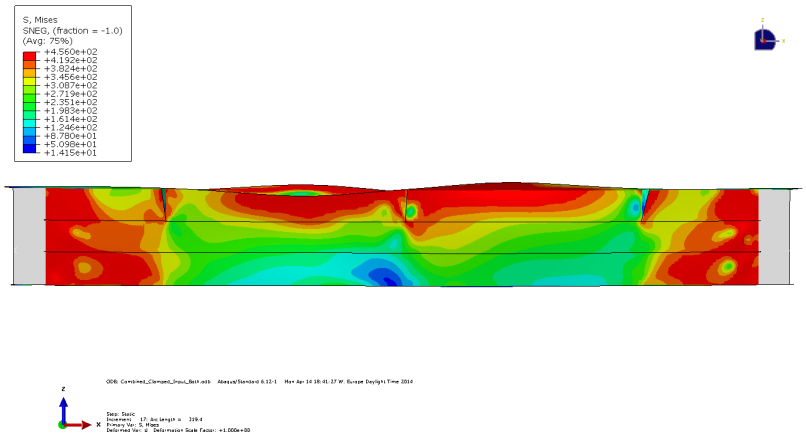

(b) Stress distribution in Abaqus

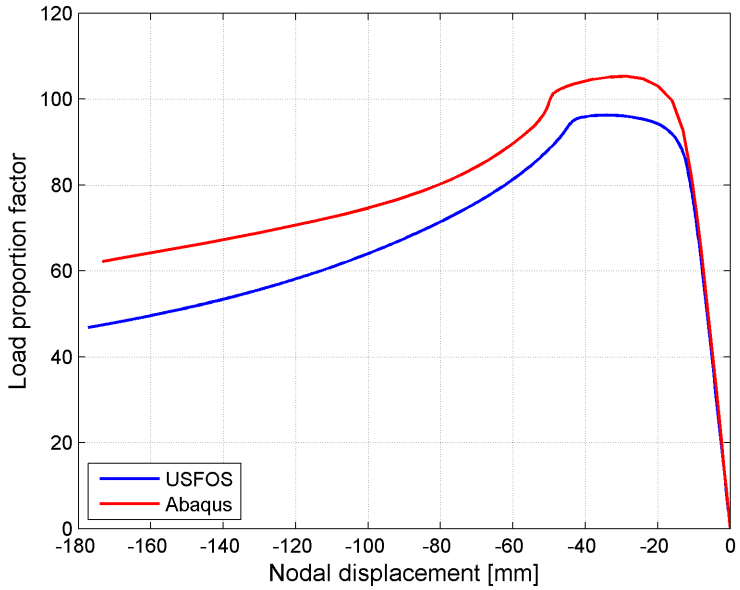

(c) Load/deflection curves

Figure 8.4: Results comparsion for compression dominated cases

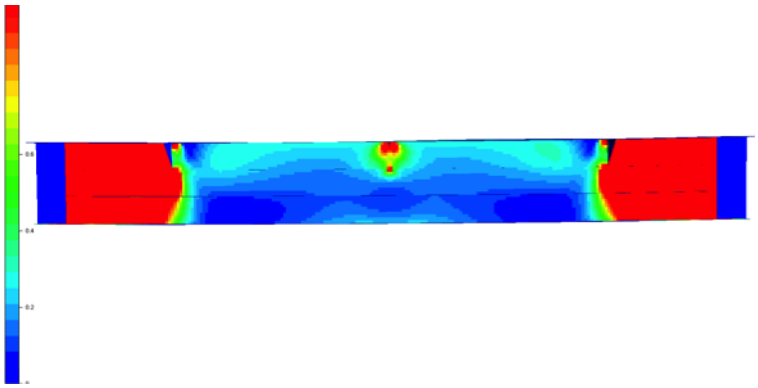

(a) Stress distribution in USFOS

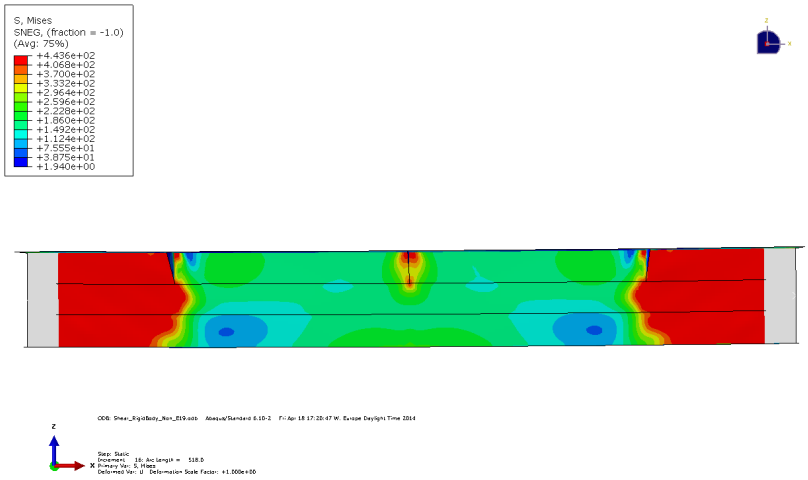

(b) Stress distribution in Abaqus

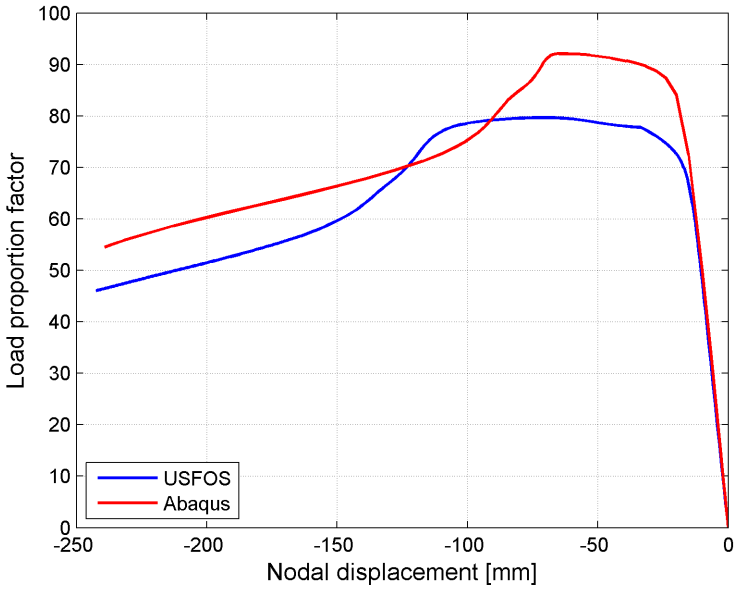

(c) Load/deflection curves

Figure 8.5: Results comparsion for compression dominated cases

From the figures above, we can conclude that Abaqus and USFOS describe similar stress distribution when the structure collapses. Additionally, the load deflection relationship before and after the ultimate stress almost has the same tendency, but a dramatic deviation exists between peak stresses estimated by these two software.

From the Von Mises stress distribution for various loads, we can see that the stress contours from two software are quite similar under compression, while the difference becomes obvious when shear force is dominant. The reason should be that shell elements can provide very good estimation for buckling problems caused by bending, which has been proved by previous researches. The performance of shell element under shear may be not very stable and the deviation exists between these two softwares.

Given the same global load, the corresponding largest load proportional factors describing the ultimate capacity for different load cases between various load cases is shown in Figure 8.4. As for the specific values, they are tabulated in Table 8.3 in the next page.

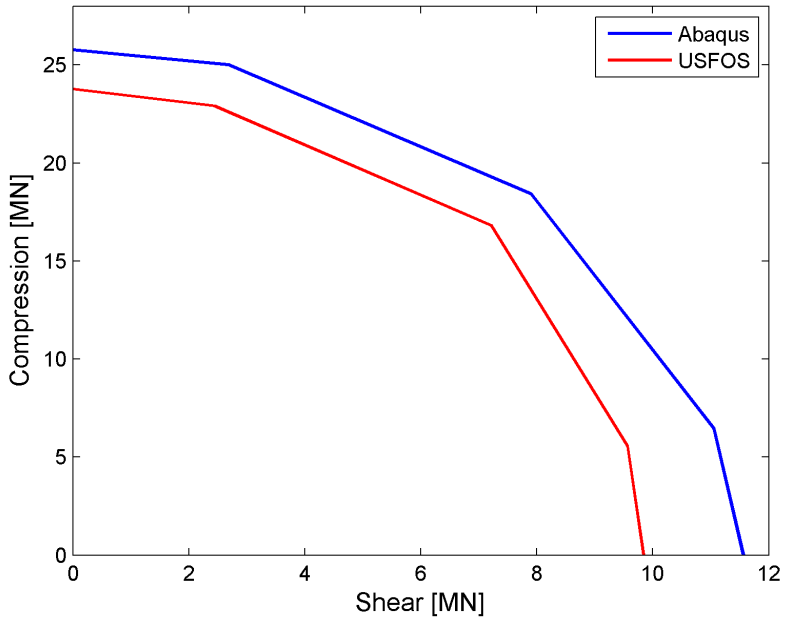

Figure 8.6: Comparison of ultimate strength between USFOS and Abaqus

Table 8.2: Difference between LPF in two softwares

	Full shear	Dominant shear	Equal both	Dominant compression	Full compression
Abaqus	77.098	92.118	105.323	89.359	73.678
USFOS	65.633	79.729	96.18	81.853	67.967
Difference(%)	14.87	13.45	8.68	8.40	7.75

The two softwares can provide very similar failure mechanism and post-buckling behavior, while the range of the difference about the peak collapse loads varies from the 14.87% to 7.75%. For the big differences in the ultimate capacity, three possible reasons are checked as follows .

- **Check the applied total force**

The purpose of the reaction check is to guarantee that the force with the structure is equal to the applied force enlarged by the load proportional factor. The reaction check is completed at the ultimate strength step for the pure compression case. The total reaction force in USFOS can be found in the result file, while the total reaction force in ABAQUA has to be found out by summing the nodal reaction force at the end (shown in Figure 8.7).

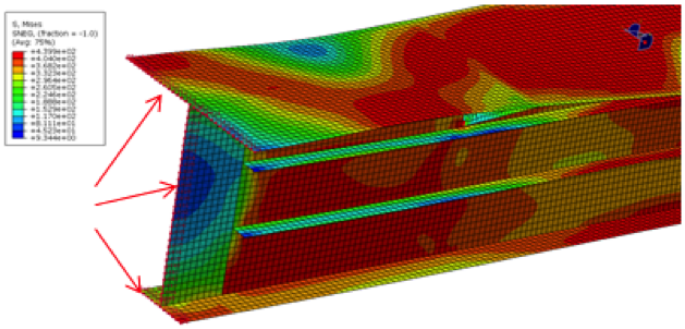

Figure 8.7: Check nodal reaction force in Abaqus

The procedure of summing the nodal force in Abaqus is attached in Appendix C. The difference between the force in the structure and the applied force is tabulated in the table below.

Table 8.3: Check the applied total force at the ultimate capacity

	Reaction force (N)	Applied force (N)	Difference (%)
Abaqus	25684440	25684400	1.56E-04
USFOS	23790000	23792300	9.67E-03

The differences between the applied and reaction forces are so small that we can conclude that with regards to the big difference between the ultimate capacity, there are no errors relating to the applied or reaction forces.

- **Check the type of shell element**

In Abaqus, there are various types of shell elements and integration analytical methods, while USFOS has only one type of shell element. Two more types of elements (S4 and S8R) in Abaqus are adopted to check the effects of the different element types. S8R represents an 8-node doubly curved thick shell element with reduced integration and S4 stands for a 4-node doubly curved general purpose shell element with finite membrane strains. The results of the largest load proportional factor relating to ultimate capacity is given in the table below.

Table 8.4: Check load proportional factor with different elements types

Element type	Full shear	Dominant shear	Equal both	Dominant com	Full com
S4R	77.098	92.118	105.323	89.359	73.678
S8R	76.372	91.374	105.633	89.844	75.020
S4	75.690	90.846	107.282	90.509	75.493

From the table, we can notice that the different types of elements have slight effects on the ultimate load proportional factor. Elements S4R will provide a little more shear capacity, while the bending resistance is higher when adopting elements S4. Compared with the load proportional factor from USFOS, we can conclude that the shell elements in USFOS are closer to the elements S4 in Abaqus. In addition, the different types of shell elements won not be the reason to cause the huge difference between Abaqus and USFOS.

- **Check material plastic properties**

Abaqus can define suficient hardening in the plastic zone (blue line in Figure 8.8), while USFOS can only accept one hardening parameter (red line in Figure 8.8). The differences for the plasticity after yielding can be found in the figure below. Another material with higher hardening parameter is defined in USFOS (green line in Figure 8.8) in order to check the effects from the plastic material properties.

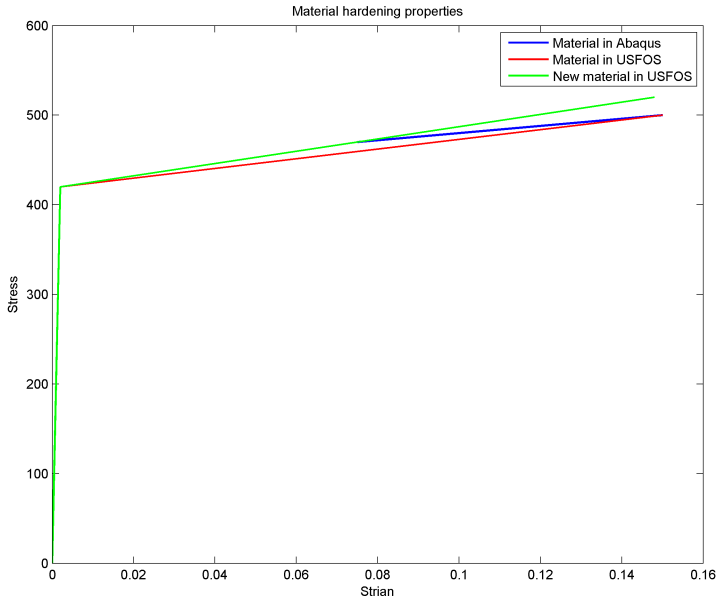

Figure 8.8: Material hardening in USFOS and Abaqus

The ultimate load proportional factor with these two plastic properties under different forces are listed in the table below.

Table 8.5: Check load proportional factor with different plasitc material

Material	Full shear	Both equal	Full compression
Original	65.633	96.18	67.967
New	65.639	96.196	67.977

The difference between the original and new materials is quite small, so we can conclude the plastic behavior of the material is not dramatic for the ultimate capacity analysis and the plastic

properties is not the reason causing the deviation between these two software. The results are obtained based on the cases considered in this project.

Except the possible reasons above, we can only assume the difference is the algorithm between these two software when calculating the ultimate stress. The average difference among all the cases from these two software is approximate 10%. Although this value is a little larger than the normal industrial range, it is still in an acceptable level after considering the nonlinear finite element methods in two different software. One possible explanation is that Abaqus tends to provide non-conservative results, while USFOS will normally estimate the consequences conservatively.

Chapter 9

Capacity Check based on Design Standards

9.1 Introduction

The simplified calculation method mentioned in the design standards, for example DNV RP C201 [10] can provide an estimate with respect to the buckling strength of the structure. If setting the material factor from 1.15 to 1.0, calibration with the finite element method can check the feasibility of these formulae to estimate the structural ultimate capacity.

In this chapter, the EXCEL spreadsheet and software PULS based on the DNV standards are used to check the ultimate strength of the stiffened web. In addition, another check for the whole girder section is also completed referring to the DNV RP C201 [10]. The results are listed and explained in the following sections, and the calculation procedures are attached in the Appendix D & E.

9.2 Capacity check of stiffened plates according to DNV RP C201

The DNV EXCEL spreadsheet, ' buckling of stiffened plate panel ' is adopted to check the ultimate capacity of stiffened web. The comparison between the results from this simple program and finite element method is shown in Table 9.1. Furthermore, the calculation in the EXCEL is attached in the Appendix D.

Table 9.1: Capacity check for stiffened web with DNV EXCEL spreadsheet

	Case	DNV EXCEL(MN)	Abaqus(MN)	Difference(%)
Flatbar	Shear	10.899	11.565	-5.76
	Compression	24.735	25.787	-4.08
T-profile	Shear	10.899	12.374	-11.92
	Compression	28.694	29.641	-3.19

From Table 9.1, it is easy to notice for the cases with compression, the difference between the DNV simplified method and nonlinear finite element method is very small, 4.08% and 3.19% respectively for two cases with flat bar and T-profile stiffeners. This means that the simplified method can give a good estimate for the ultimate capacity under compression by changing the material factor from 1.15 to 1.0.

For the shear cases, the deviation between the results is a little larger. The reason may be that the applied shear in Abaqus is simulated by the concentrated loads instead of the real shear at the end of the web. In addition, from the EXCEL spreadsheet, we can notice the failure load for these two cases under shear doesn't change at all. The reason should be that the ultimate shear capacity is mainly affected by the transverse stiffeners instead of longitudinal stiffeners. So the reinforced longitudinal stiffener will not improve the shear capacity in a large level.

9.3 Capacity check of stiffened plates according to PULS

PULS is a software based on the DNV standards used for estimating the ultimate capacity for simply structures. Here it is used to check the ultimate capacity of the stiffened web without flanges. The table with the output results from PULS is shown below.

The results obtained from PULS are almost the same as those from the simple EXCEL program except the case with T-profile stiffener under pure compression. Like the EXCEL program, in PULS different stiffeners provide the same shear capacity. Compared with results in EXCEL, the T-profile stiffener can increase more resistance for the compression, when strong stiffeners are used.

Table 9.2: Capacity check for stiffened web with PULS

	Case	DNV PULS (MN)	Abaqus(MN)	Difference(%)
Flatbar	Shear	10.899	11.565	-5.76
	Compression	24.513	25.787	-4.94
T-profile	Shear	10.899	12.374	-11.92
	Compression	32.490	29.641	+9.61

The global buckling mode in PULS is shown in the figure below, the location of stiffeners is not exactly the same as the layout of model, so corresponding buckling mode and failure mode are different from that in Abaqus. This may be the reason of the deviation between the DNV recommended method and nonlinear finite element method.

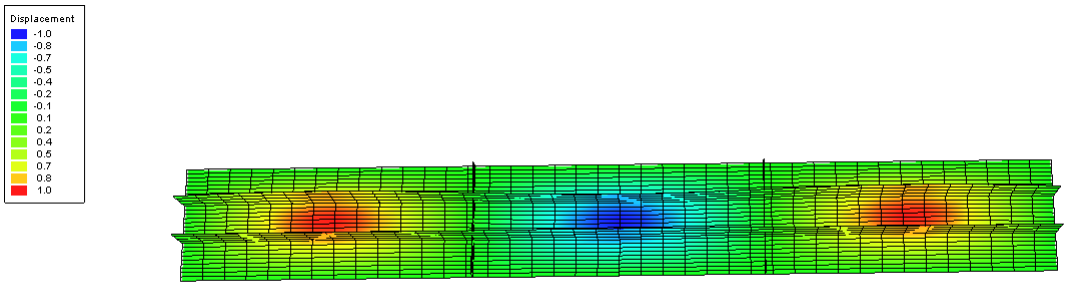

Figure 9.1: Global buckling mode in PULS

The algorithm in the PULS is almost the same as EXCEL. So almost the same conclusion can be found that PULS can also give a good estimate for the ultimate resistance under the pure compression, while when the shear force is considered, some errors are introduced. These differences are either caused by the special way to apply shear force in this paper or due to the algorithm behind PULS. Compared with DNV EXCEL program, PULS is more user-friendly and often used as a post-processor with other programs, while EXCEL spreadsheet is more direct to give solutions.

9.4 Capacity check of primary girders according to DNV-RP-C201

For the check of the primary girders, it is necessary to obtain the top and bottom stress at the mid-span and end sections by finite element methods. For the capacity check at different sections, another parameter z^* is regarded as the distance from the neutral axia of the effective section to the working point of the axial force. z^* is varied to select the maximum utilization. Simplified z^* can be treated as 0 for the conservative estimate. Here one assumption is made that z^* is equal to -150mm.

On the basis of the section force from the FEM analysis at the collapse step, the maximum utilization factors checked by different equations under external excitations are very close to 1. The two main checked sections are given below.

- 1.059 at the end supports
- 1.001 in the middle section

From the utilization factor, the capacity of the middle section and supports are fully occupied and the supports seem to fail more easily. The values are quite close to 1.0, which means that this calculation procedure can provide a reasonable estimation for the capacity of the whole girder section based on some reasonable assumptions. The detailed calculation procedure is shown in the Appendix E.

9.5 Conclusions with regards to capacity check

On the basis of the complex hand calculation referring to DNV CP R201 together with the results from DNV EXCEL spreadsheet, the calibration with the results with regards to nonlinear finite element methods seems to provide some positive results. The conclusion for the check in this chapter can be concluded as follows:

- ◇ The EXCEL spreadsheet and PULS can provide reasonable estimation about the ultimate capacity of stiffened plates with some differences, especially for the case under pure com-

pression. The reason should be that the compression will lead to the buckling issue which is as the DNV standards assumed. When the large shear is applied, the buckling may not be the dominant failure mode any more, which will cause some deviations.

- The way, concluded from the DNV RP C201, to estimate the primary girder based on the stress from nonlinear finite element method works well to provide a good prediction about the utilization ratio of the structure.

- From Table 9.1 (negative differences) and the results for the primary girder check (utilization 1.059 and 1.001), it is obvious that DNV standards tend to provide a conservative result compared with nonlinear finite element method. This conclusion fits well with the main characteristics of design standards,

Chapter 10

Conclusion

The nonlinear finite element analyses in this girder section provide the ultimate capacity and its corresponding post-ultimate behavior. Cases are studied to investigate the various effects in details.

Based on the specific discussion about the results in this paper, the following conclusions can be summarized from different aspects.

- Simplified method from DNV RP C201 can give a good estimate about the ultimate capacity for the girder or plated structures. The conservative difference is around 4 % for the cases under compression, while more considerations are needed when shear is introduced. The dominated compression will lead to the buckling failure and DNV rules can estimate the buckling strength accurately, but dominated shear force will cause shear failure mechanism. In this circumstance, the DNV RP C201 will have difficulties in predicting the ultimate strength as accurate as the cases under pure compression.

- Reinforced stiffeners can improve the ultimate capacity at a certain,but small level. In contrast to flat bar stiffener, T-profile stiffener can improve 14.95% in compression resistance, while only 3.80% in shear resistance.

- Boundary conditions influence the ultimate capacity, especially for shear dominated cases. This may result from the flange contribution under shear. In addition, simply supported boundary conditions can provide conservative results and the clamped ends can provide 21.9% more shear capacity compared with simply supported ends.

- For the nonlinear ultimate analysis, the effects of initial imperfections are not dramatic

for robust structures. Compared with other cases, the effects of the imperfections under pure shear are more markable.

- Some differences, varying from the 14.87% under pure shear to 7.75% under pure compression, exist between two nonlinear programs in predicting the ultimate strength. Although the tolerance is larger than the industrial criteria, it is still acceptable.

- From the eigenvalue analysis, the combined case has almost the same buckling eigenmode with the case under pure compression. Shear failure mechanism can occur, even though no shear buckling mode is introduced.

- The eigenvalue analysis is essential for introducing the geometric imperfections into the structure. The buckling modes depend on the type of applied force, the layout of the structure and so on. Choosing the most suitable buckling mode is significantly important.

- In view of the previous case studies, the shell elements perform quite well in the buckling problems, while the performance is not very stable when shear, internal pressure or other load conditions are applied. In this project, compared with dominating shear force, dominated compression always leads to results, which fits better with theoretical knowledges. This may prove the limitations of the shell elements.

Chapter 11

Recommendation for Further Work

During the case studies for the ultimate strength and post-ultimate behavior of the special girder section, several conclusions are found through comparisons. Since the huge amount of work and limited time, several recommended further checks are listed below based on the obtained results so far. In addition, the remaining tasks in the original task list will be left as the further work to be finished.

- For the deviation between the results from Abaqus and USFOS, more studies and cases should be designed to find out the reasons or the explanations about the differences.
- The feasibility of the simplified method based on the DNV RP C201 should be further modified for the shear dominated cases. For example, the effects of the longitudinal stiffeners on the ultimate shear capacity should be taken into account.
- The increment of ultimate strength due to stiffeners should be calculated according to previous researches. The comparison with nonlinear finite element method is also expected to see how the simplified method works.
- Perform nonlinear analysis of a secondary girder with class 4 cross-section. The girder may have cut-outs and/or patch loads. The loads shall be applied proportionally for various load combinations. Determine the ultimate strength of the girder. Compare numerical results with NS-EN 1993-1-5
- Perform nonlinear finite element analysis with ABAQUS or USFOS of a hybrid plate girder-truss-work section in a platform deck. The truss-work shall be modelled with shell finite elements including secondary stiffeners. Special attention shall be placed on mod-

elling boundary conditions and introducing initial imperfections to trigger local buckling of plate girder. The truss-work may be modelled with beam elements. The truss work shall be subjected to combined bending, shear and locally distributed forces. The ultimate strength for various load shall be determined. Comparison shall be made with capacities obtained with conventional design formulas, as given in DNV-RP-C201 Buckling Strength of Plated Structures and NS-EN 1993-1-5 Design of steel structures, Plated structural elements.

Appendix A

Define material nonlinearity in Abaqus

The steps transforming from the measured normal stress strain data (step (i)) to the stress strain relationship (step (vii)) in Abaqus are listed below.

(i) This data is based on the nominal (engineering) stress and strain.

Nominal stress (MPa)	Nominal strain
0.00E+00	0.00E+00
4.20E+02	2.00E- 03
4.70E+02	7.50E- 02
5.00E+02	1.50E- 01

(ii) Abaqus expects the stress strain data to be entered as true stress and true plastic strain.

(iii) To convert the nominal stress to true stress, use the following equation.

$$\sigma_{tru} = \sigma_{nom}(1 + \epsilon_{nom}) \tag{A.1}$$

(iv) To convert the nominal strain to true strain, use the following equation

$$\epsilon_{tru} = ln(1 + \epsilon_{nom}) \tag{A.2}$$

(v) To calculate the modulus of elasticity, divide the first nonzero true stress by the first nonzero true strain.

(vi) To convert the true strain to true plastic strain, use the following equation

$$\epsilon_{pl} = \epsilon_{tru} - \frac{\sigma_{tru}}{E} \tag{A.3}$$

(vii) The results as the material input in Abaqus should be

True stress (MPa)	Plastic strain	Elastic modulus (Mpa)
4.2084E+02	0.000E+00	2.1063E+05
5.0525E+02	6.992E- 02	
5.7500E+02	1.037E- 01	

Appendix B

Von Mises stress distribution at the step of ultimate capacity for all cases

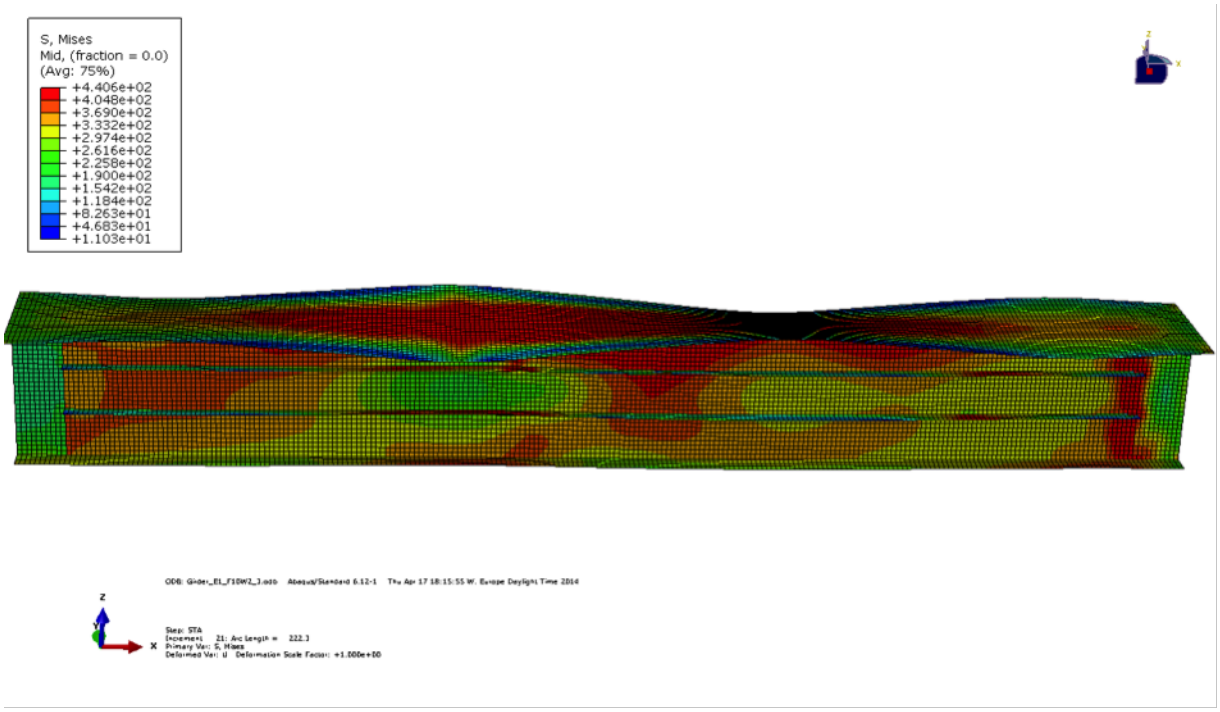

Figure B.1: Case 1

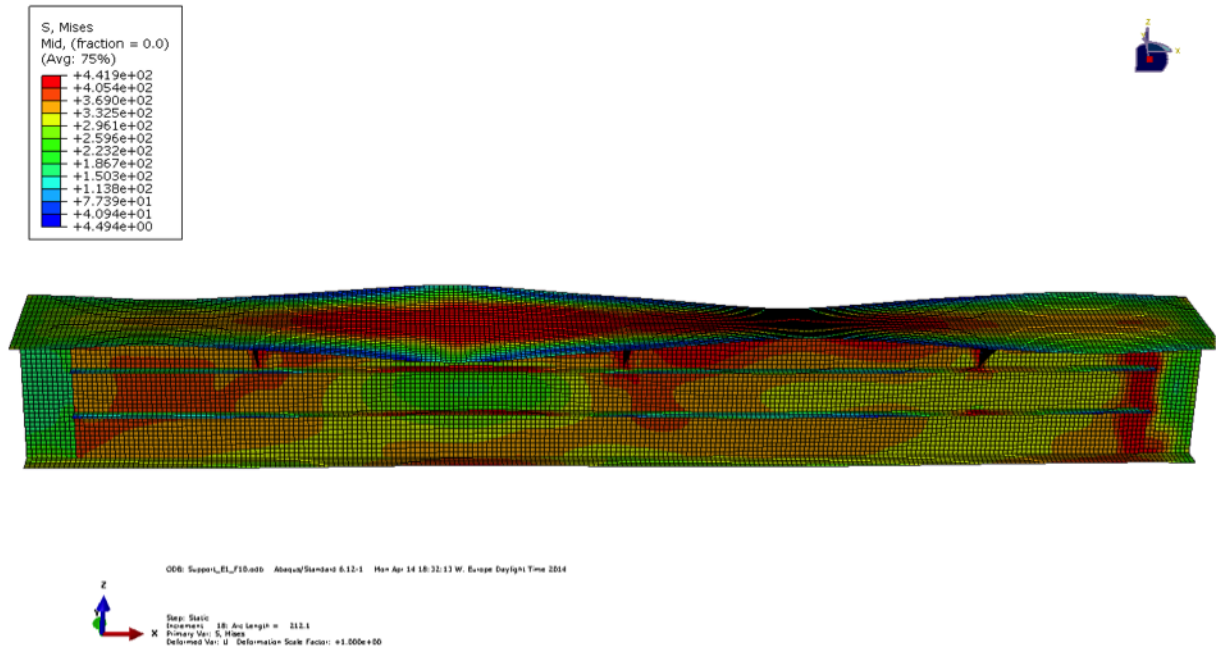

Figure B.2: Case 2

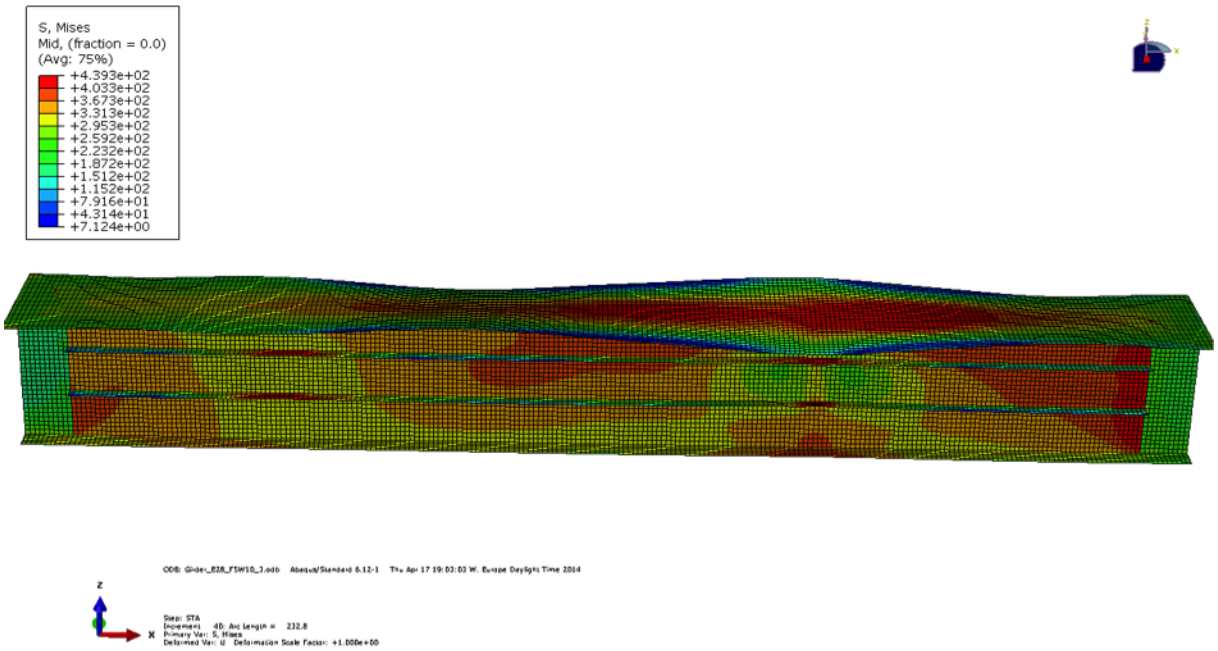

Figure B.3: Case 3

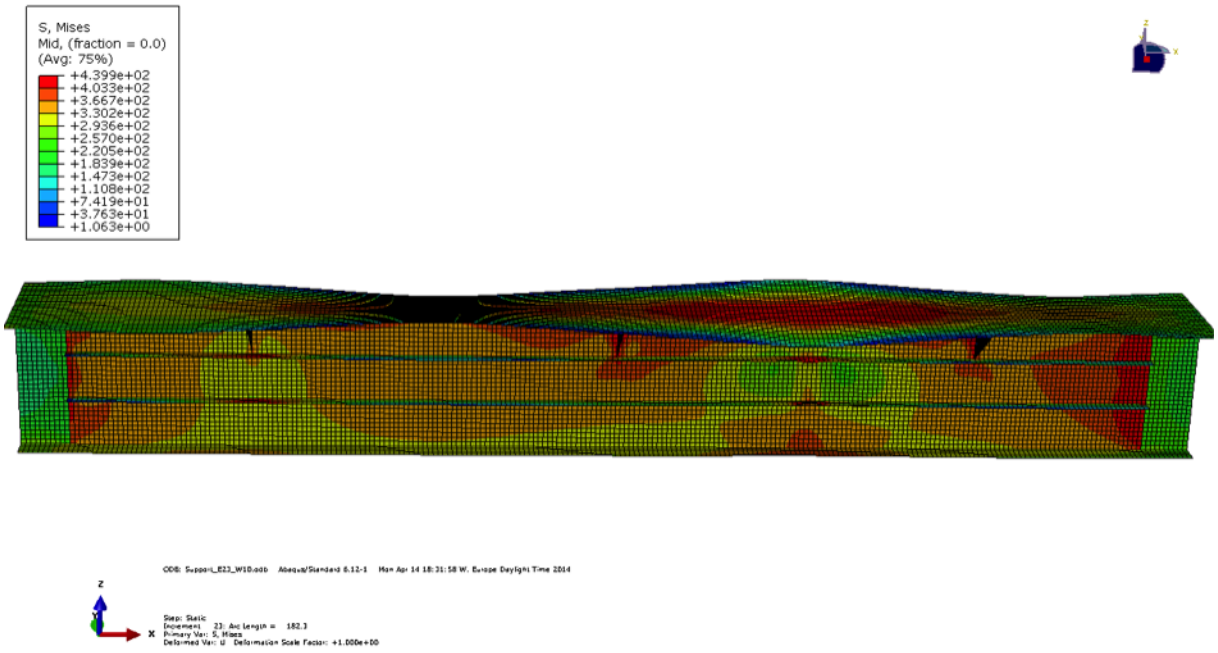

Figure B.4: Case 4

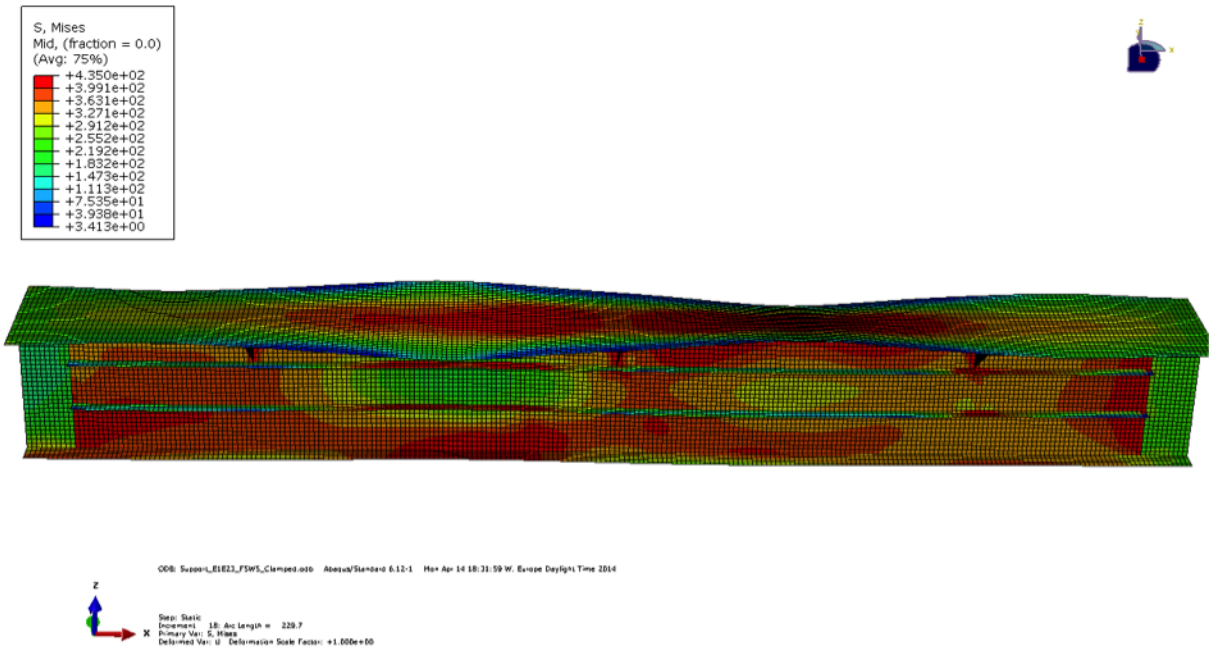

Figure B.5: Case 5

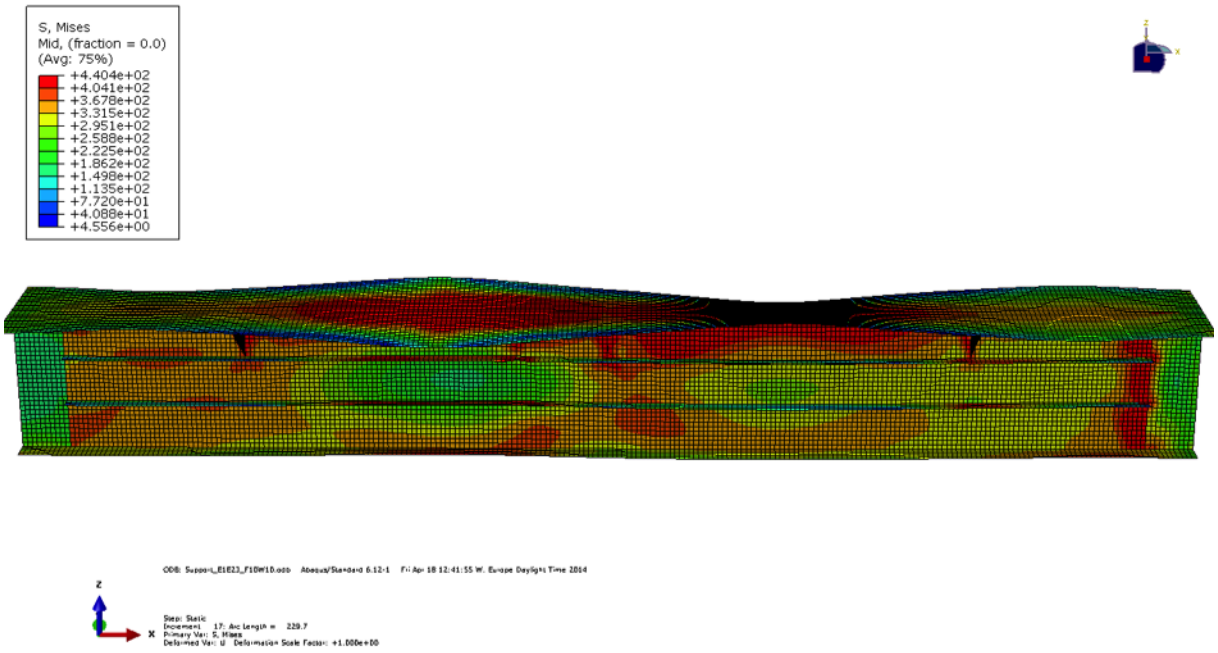

Figure B.6: Case 6

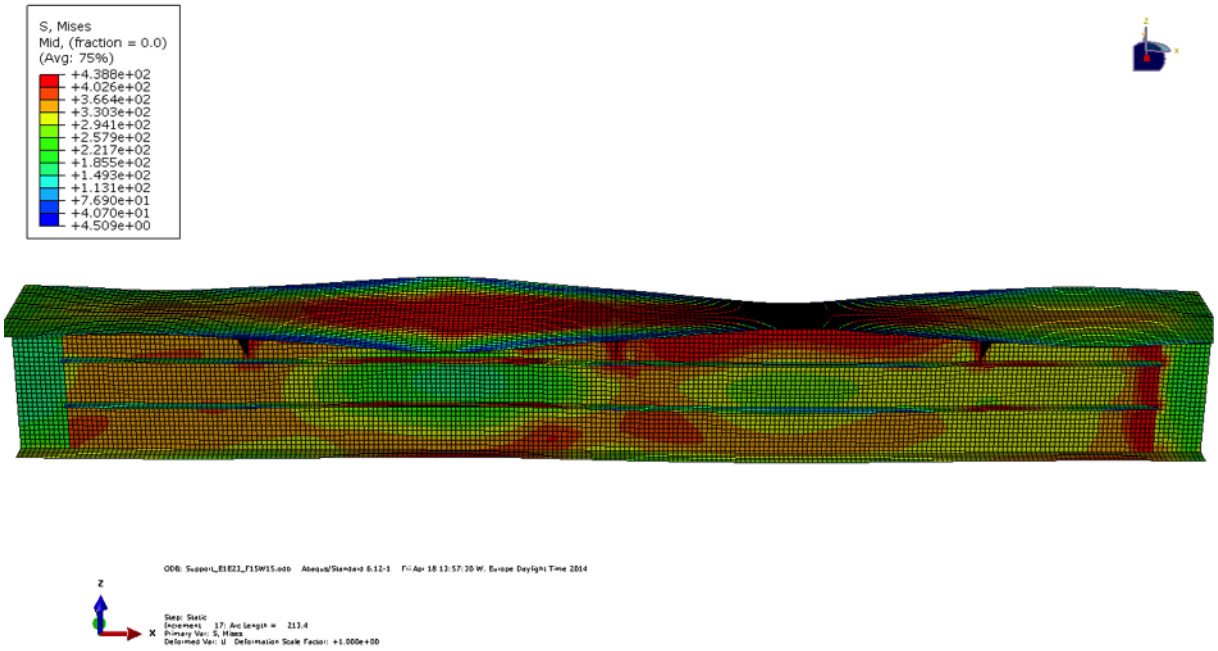

Figure B.7: Case 7

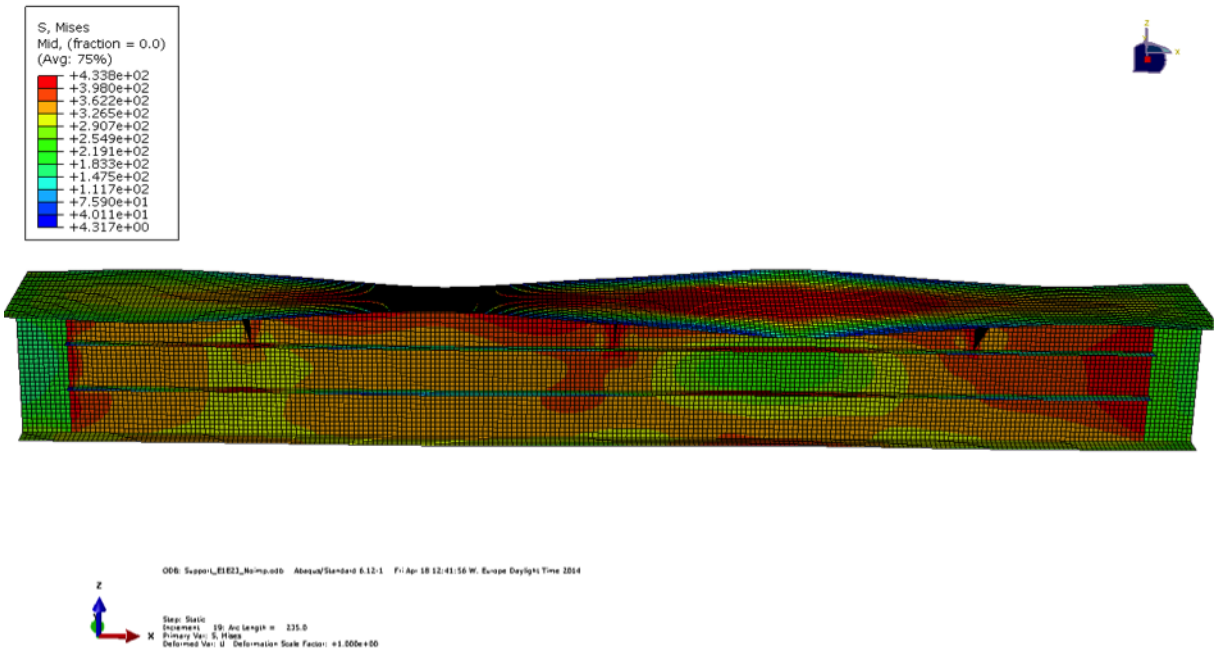

Figure B.8: Case 8

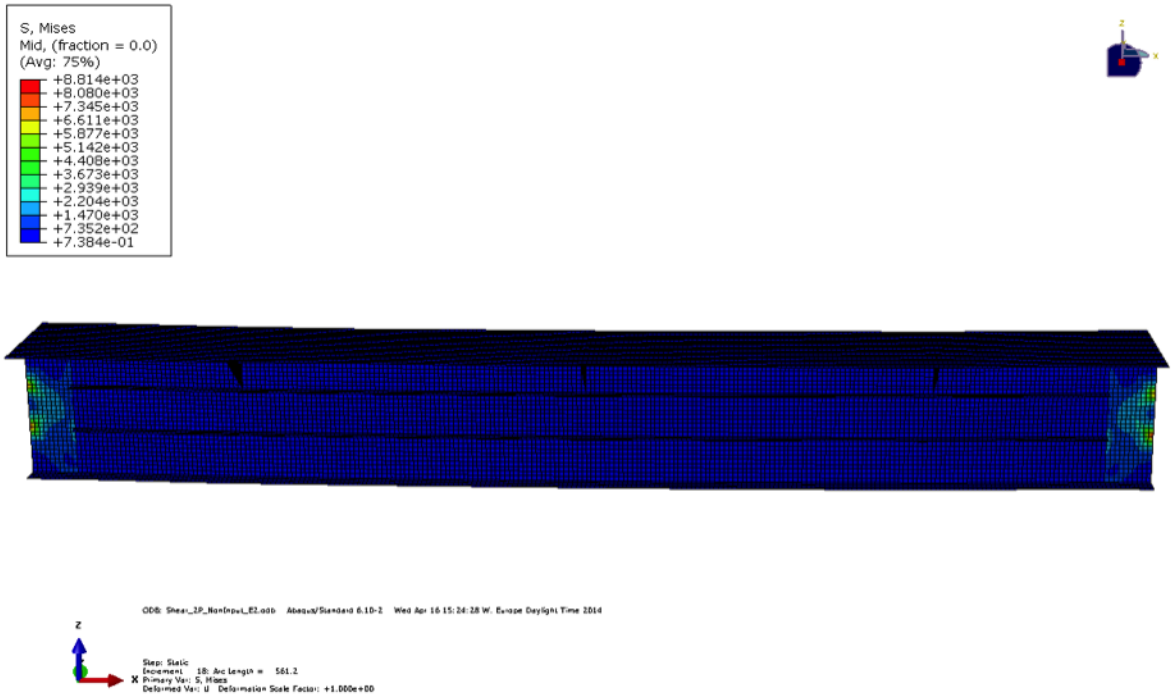

Figure B.9: Case 9

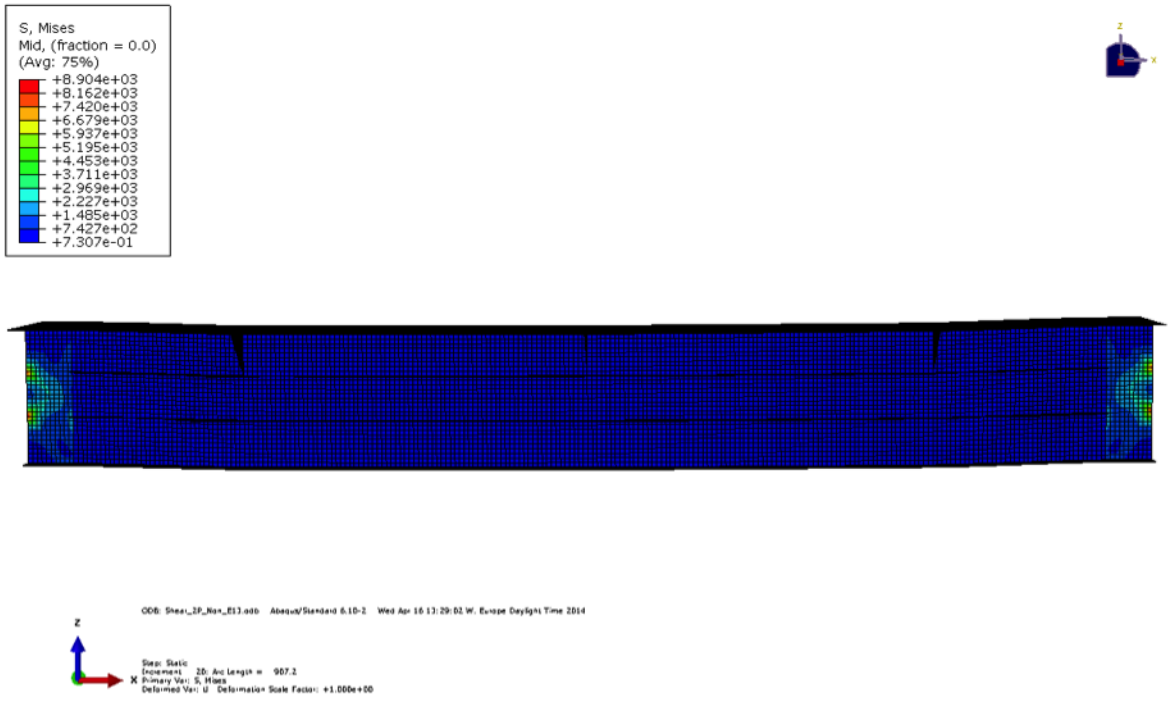

Figure B.10: Case 10

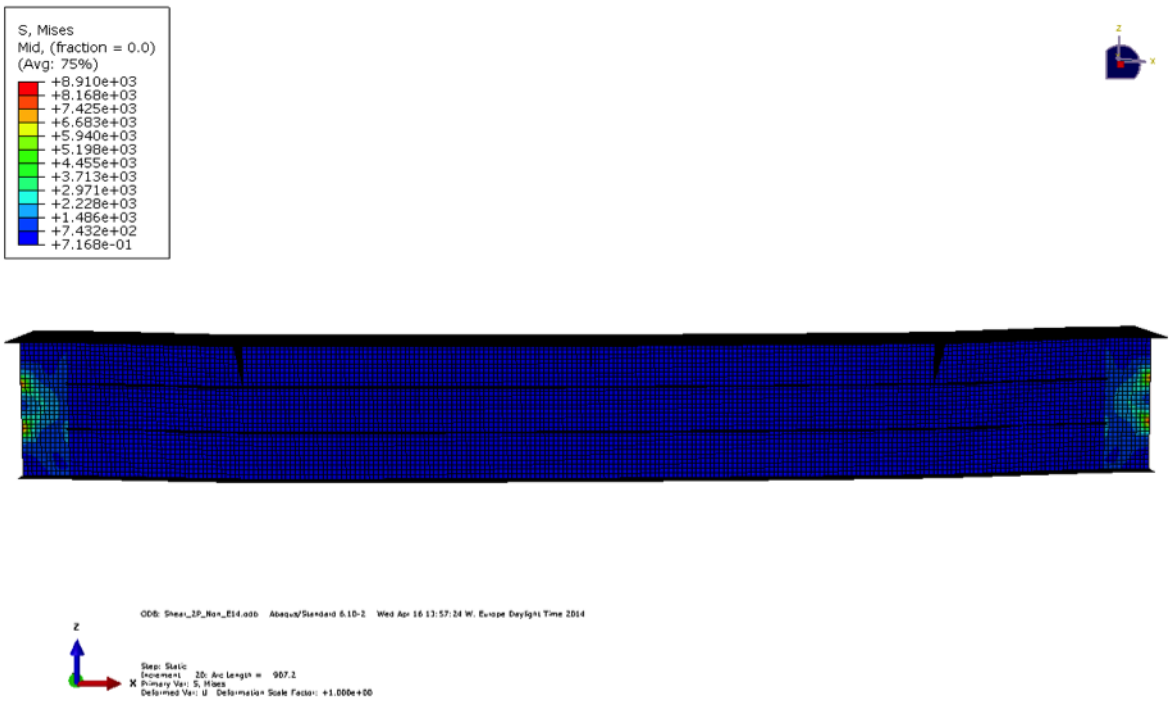

Figure B.11: Case 11

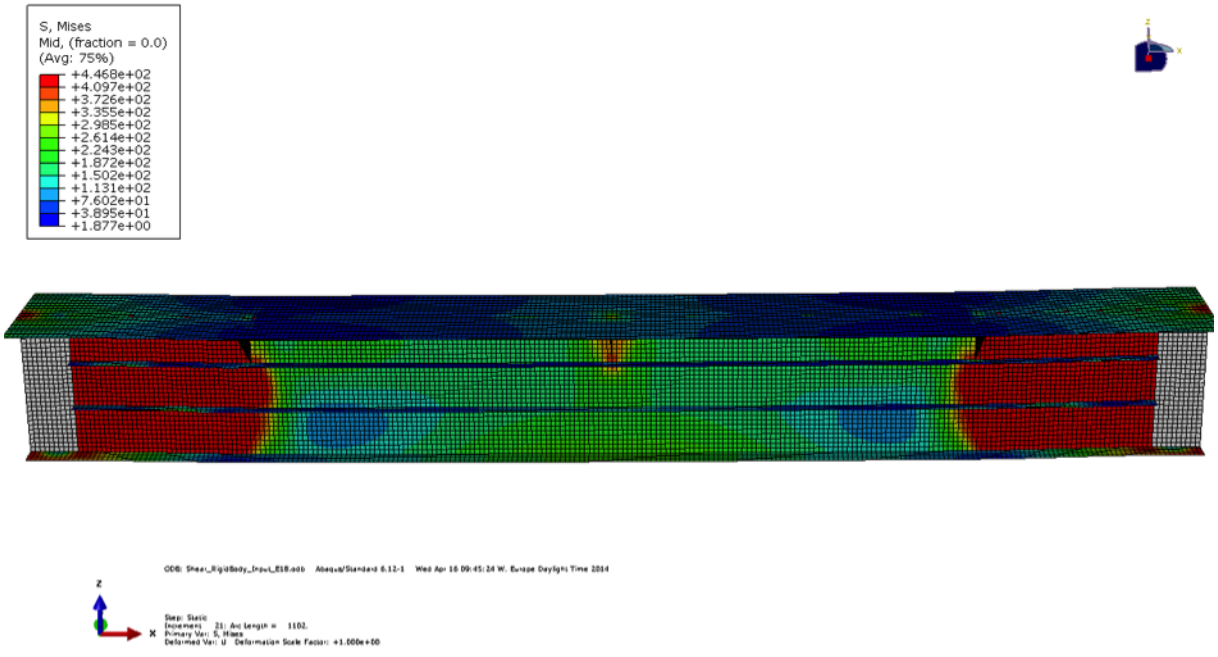

Figure B.12: Case 12

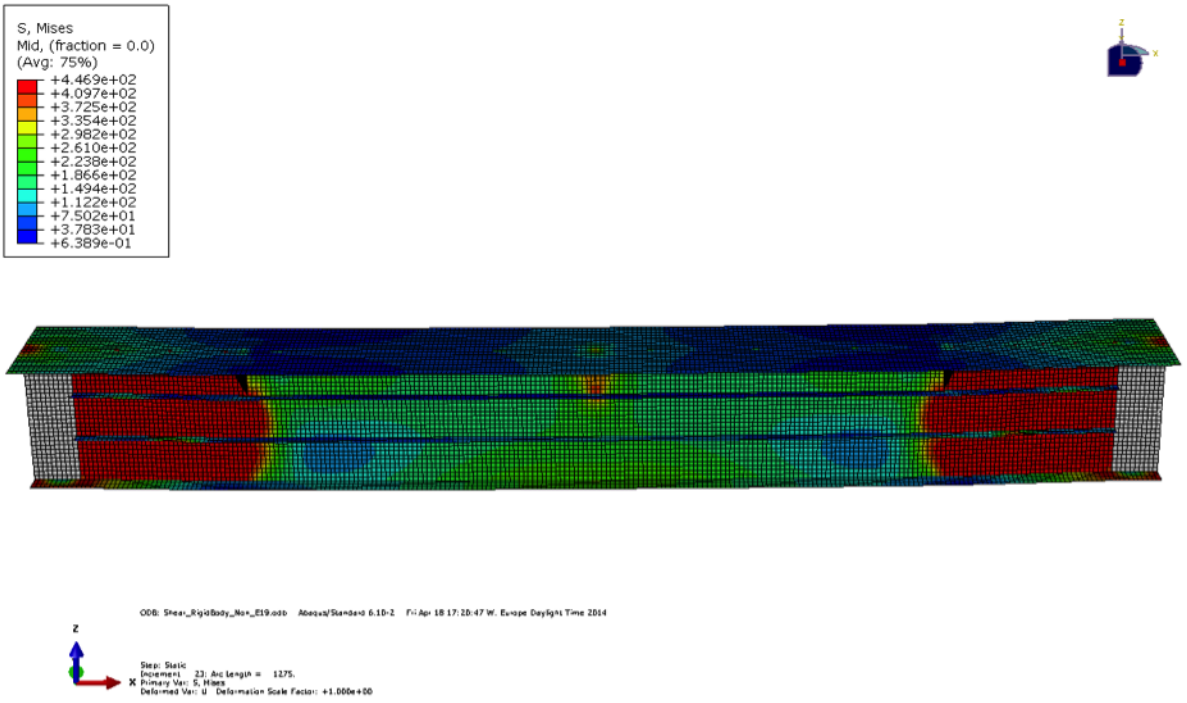

Figure B.13: Case 13

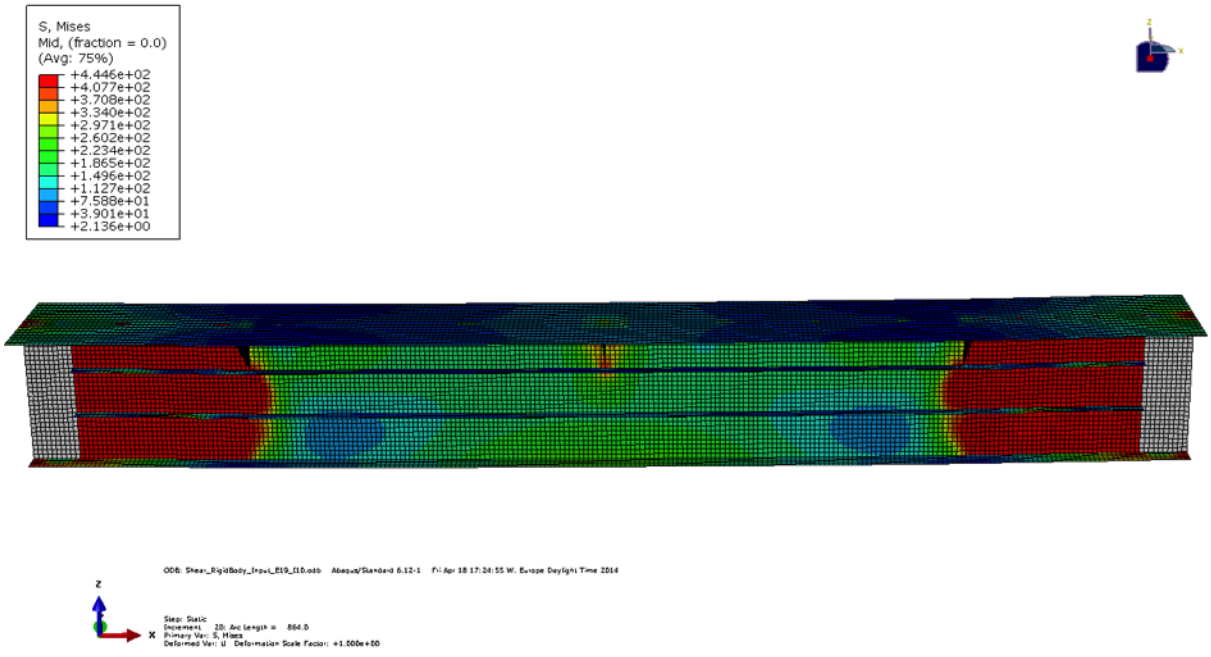

Figure B.14: Case 14

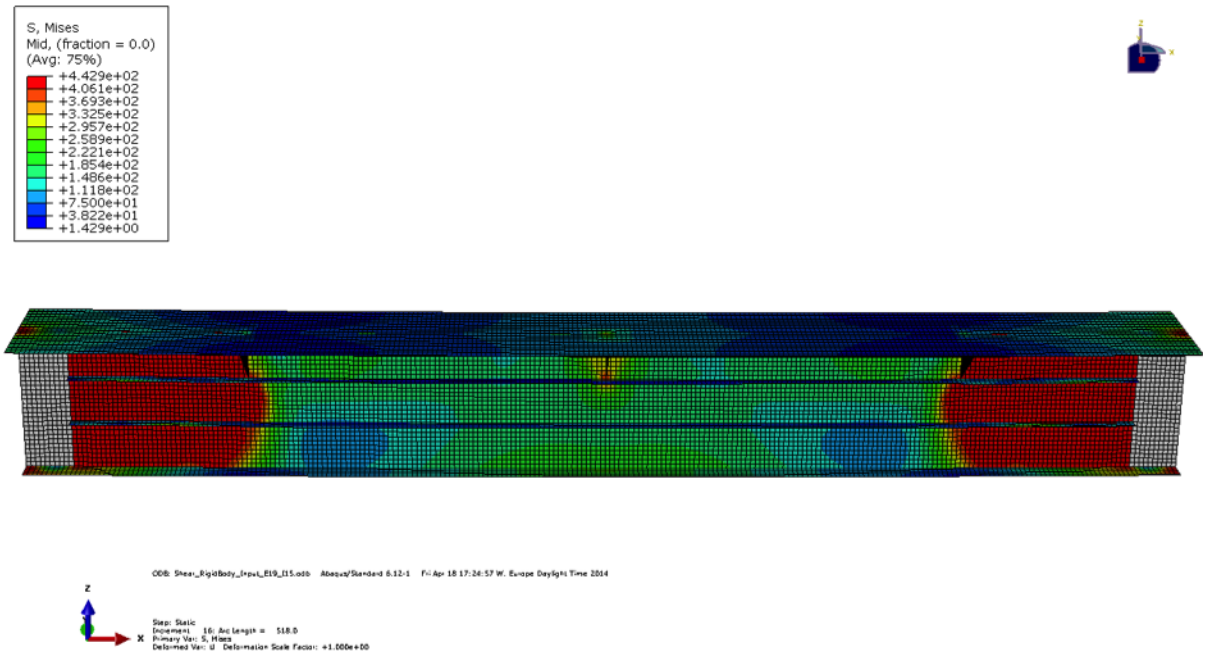

Figure B.15: Case 15

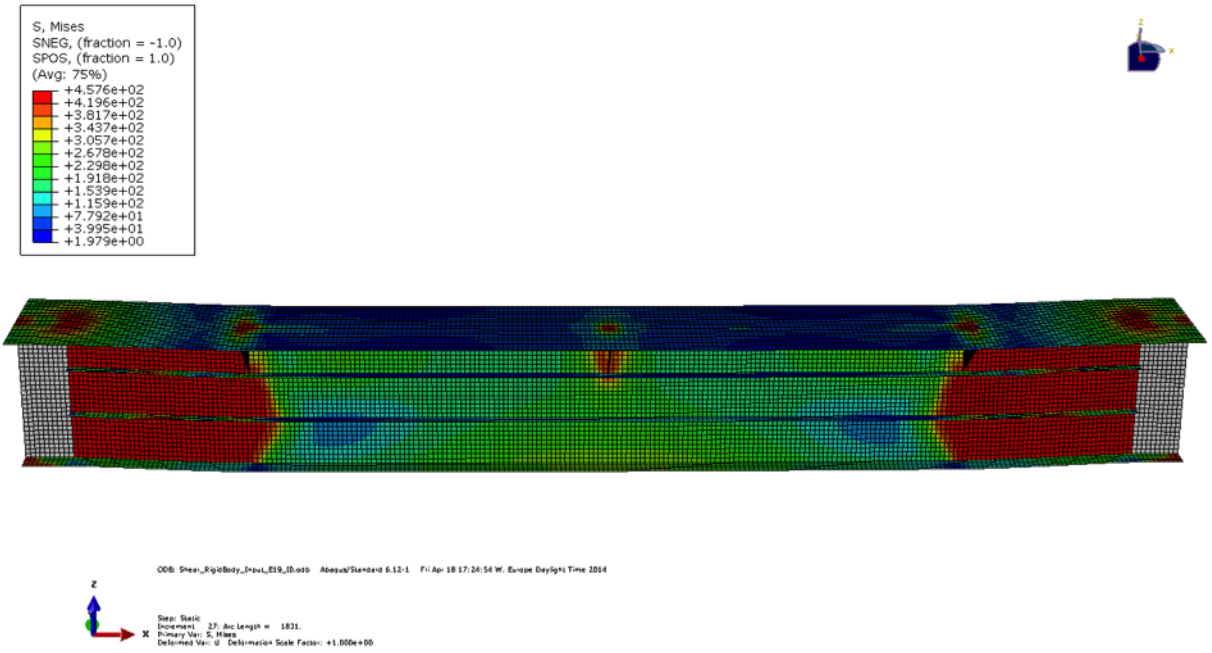

Figure B.16: Case 16

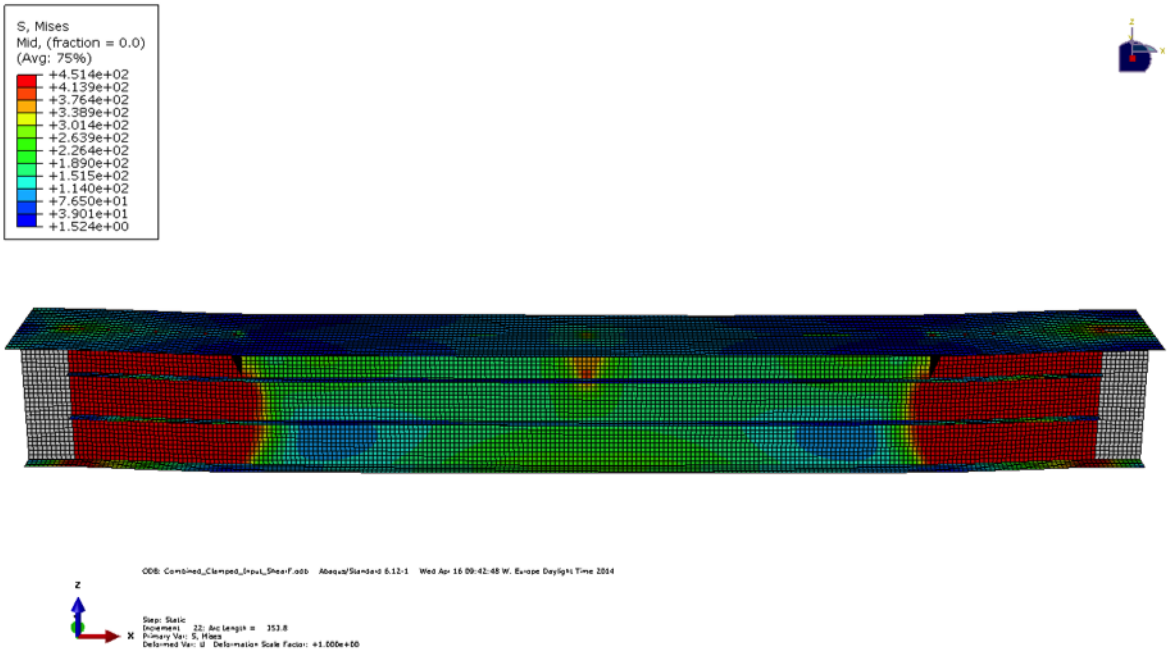

Figure B.17: Case 17

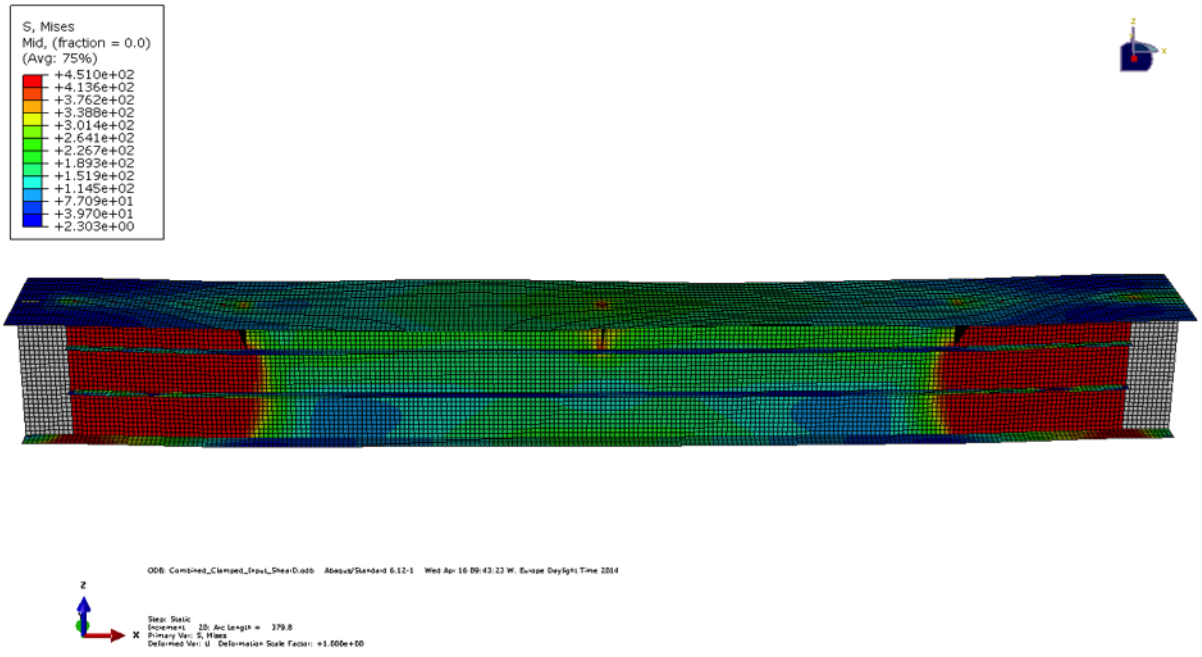

Figure B.18: Case 18

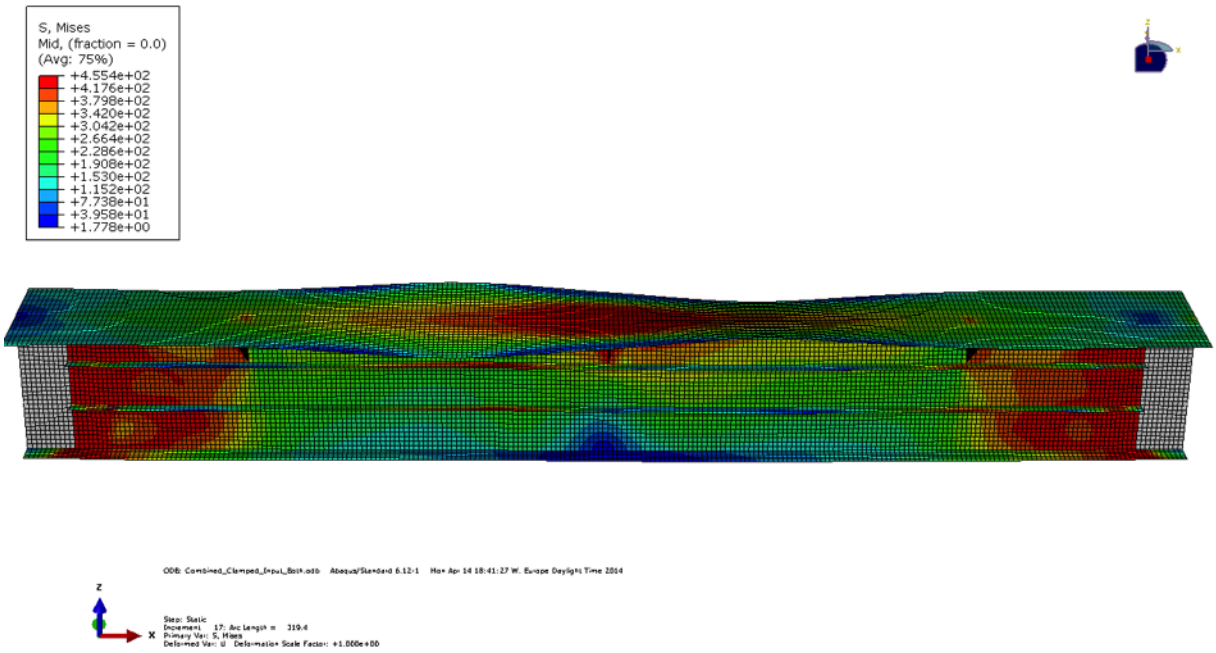

Figure B.19: Case 19

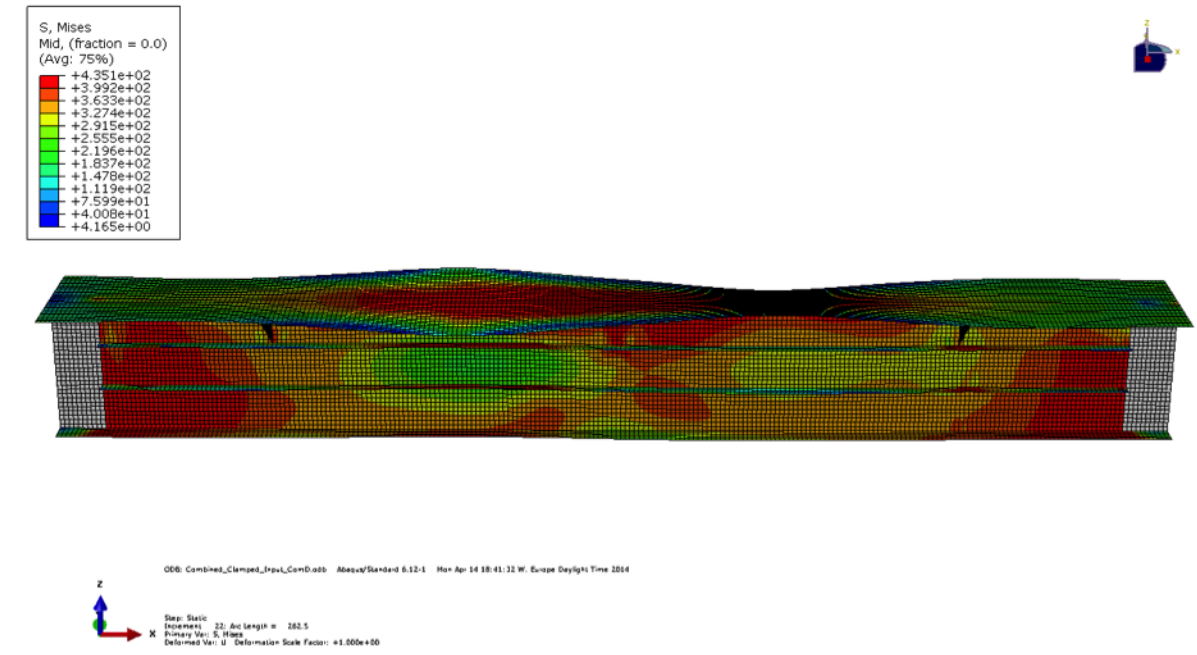

Figure B.20: Case 20

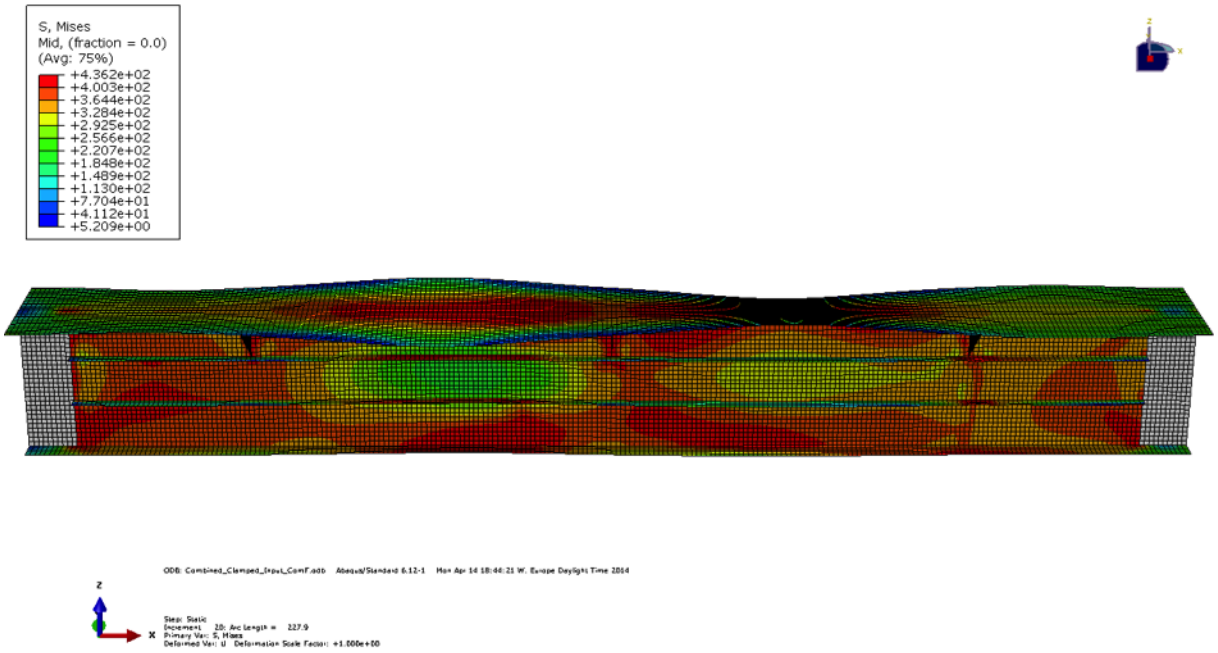

Figure B.21: Case 21

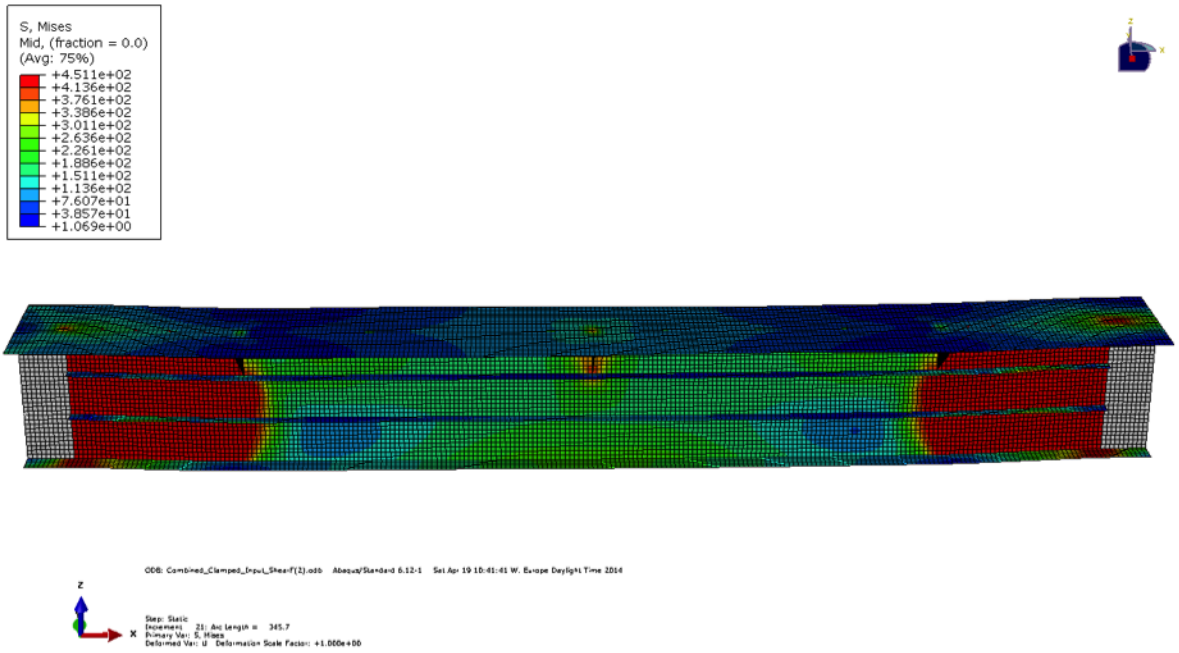

Figure B.22: Case 22

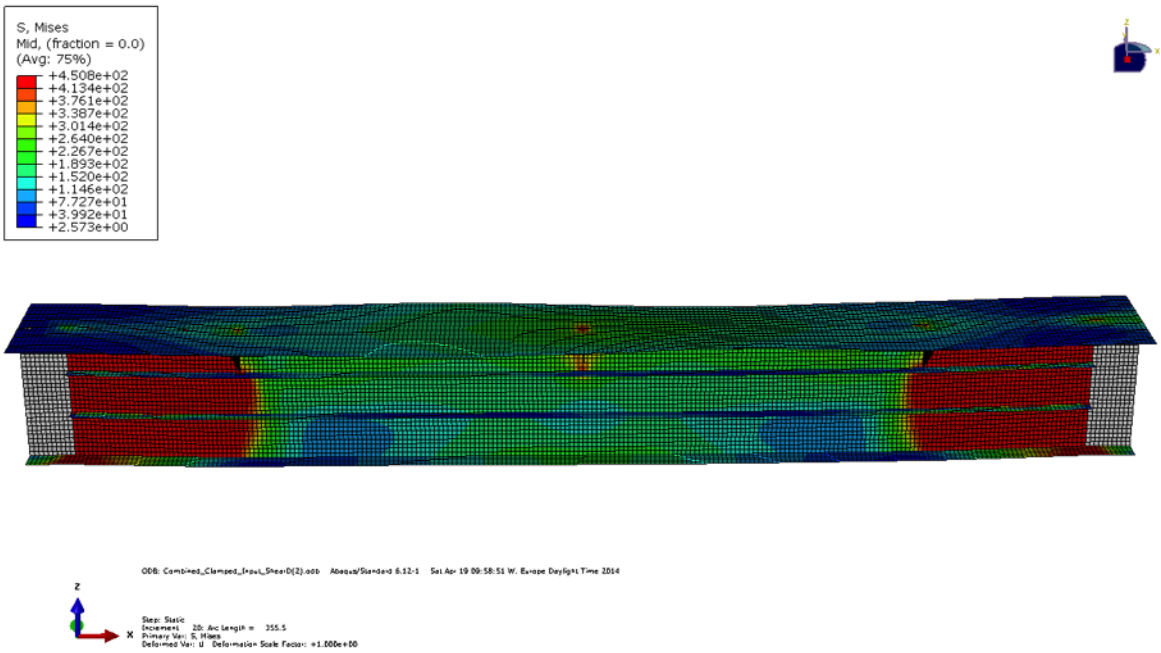

Figure B.23: Case 23

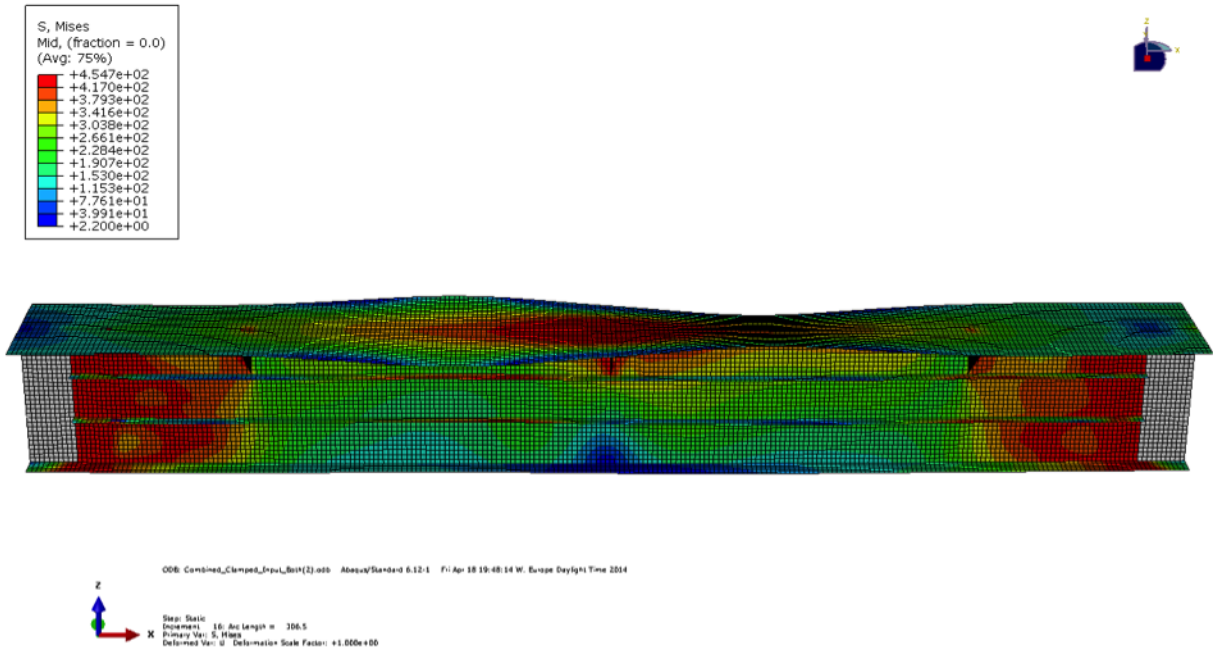

Figure B.24: Case 24

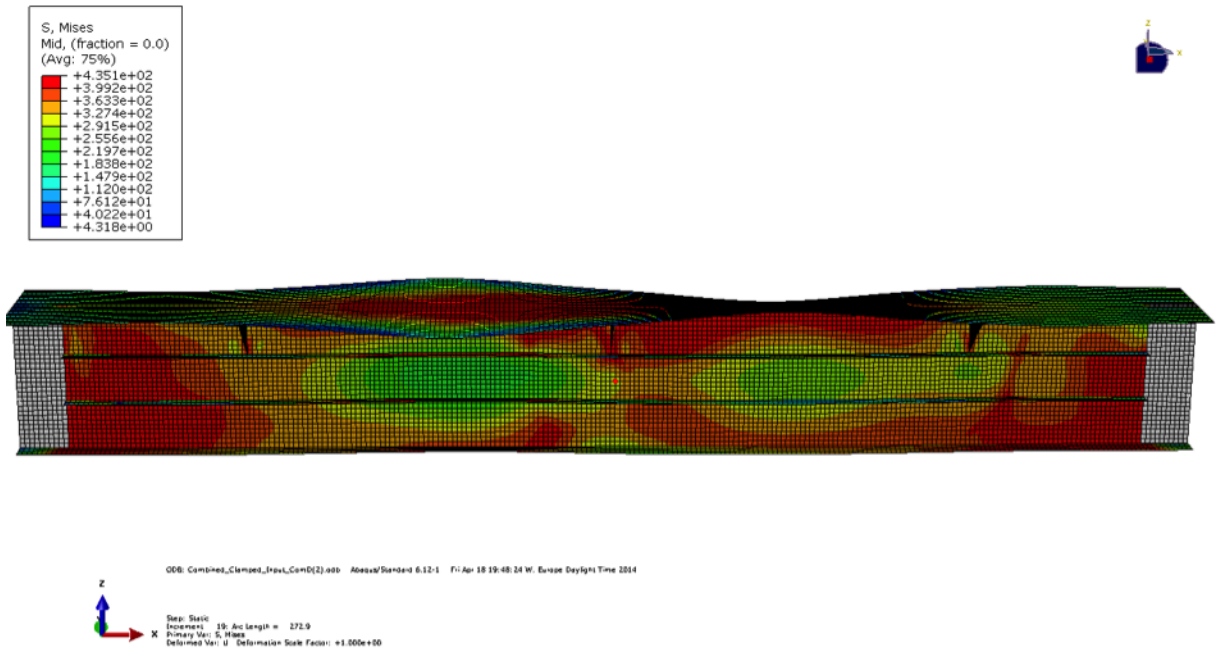

Figure B.25: Case 25

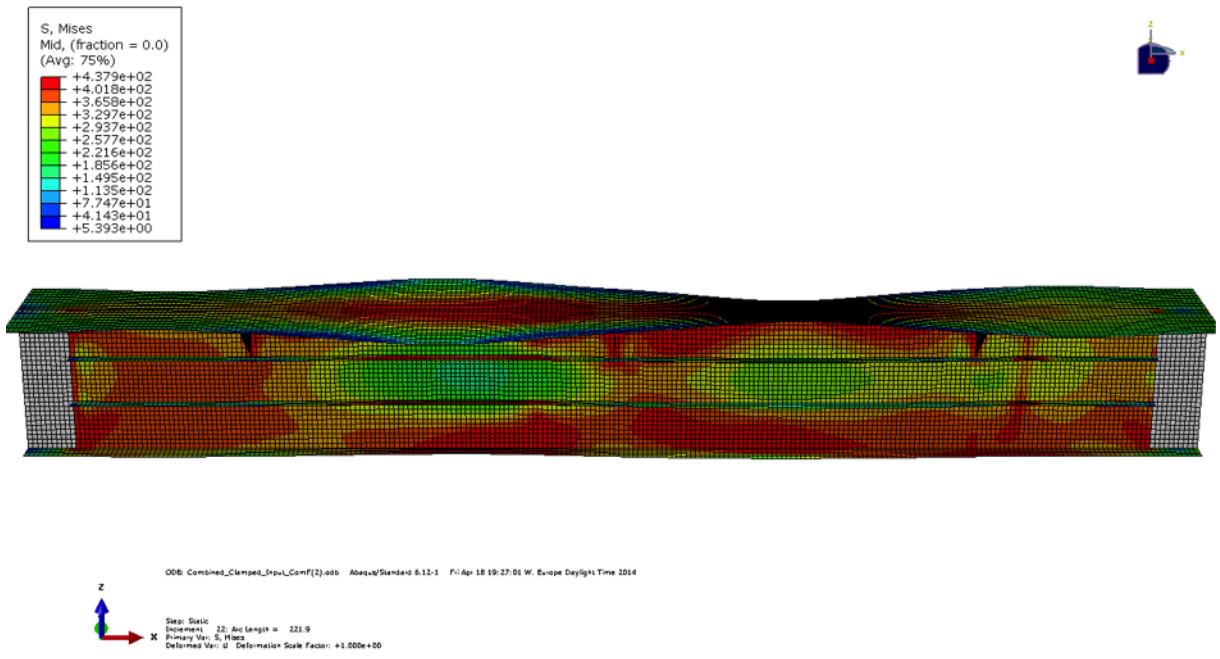

Figure B.26: Case 26

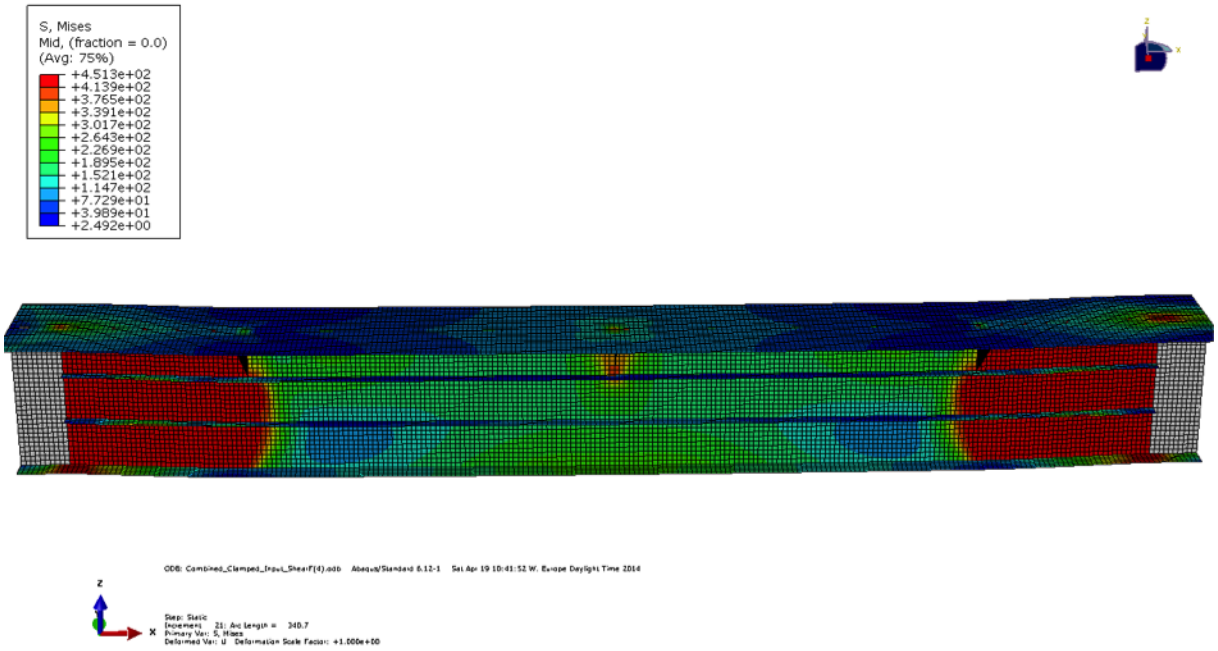

Figure B.27: Case 27

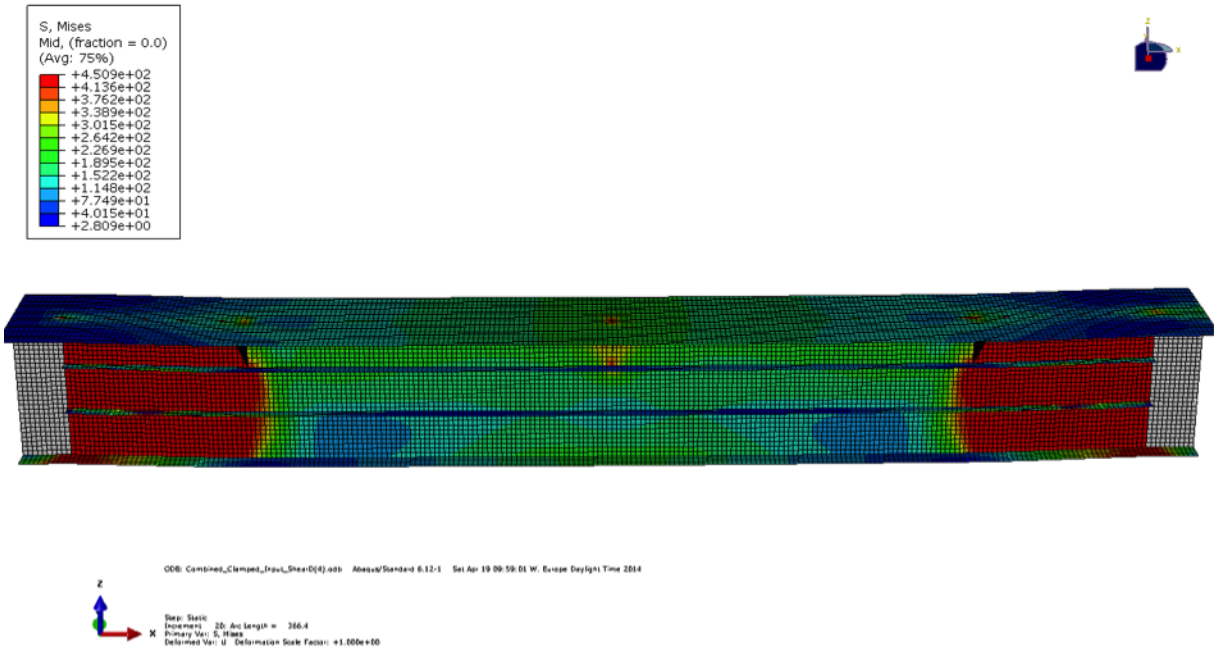

Figure B.28: Case 28

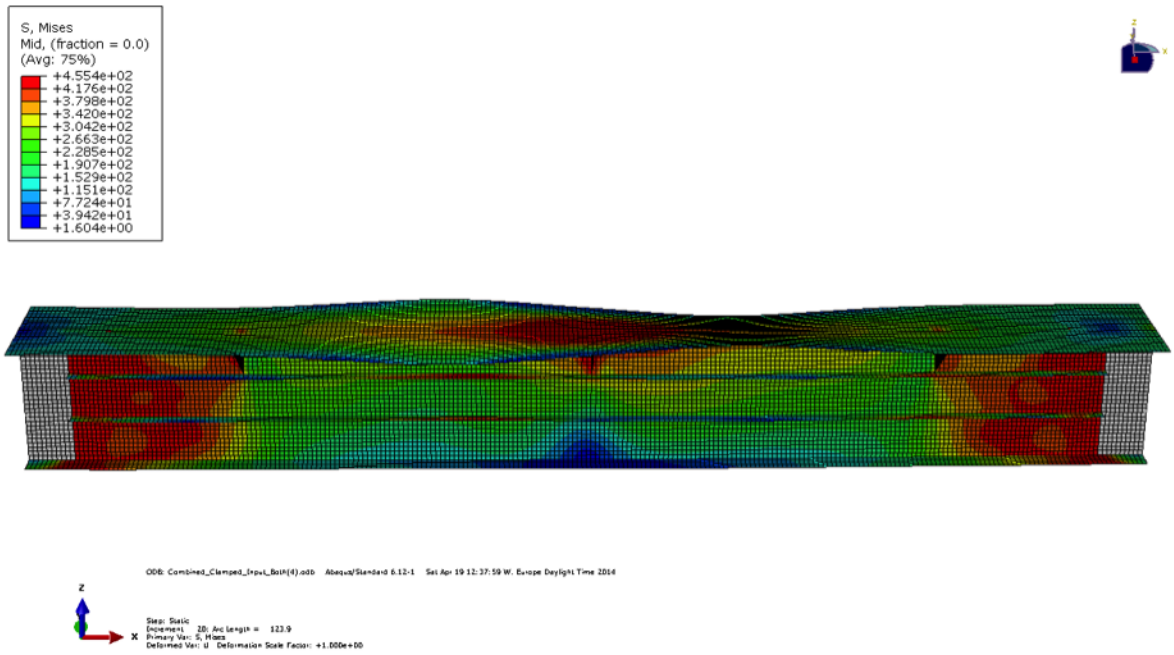

Figure B.29: Case 29

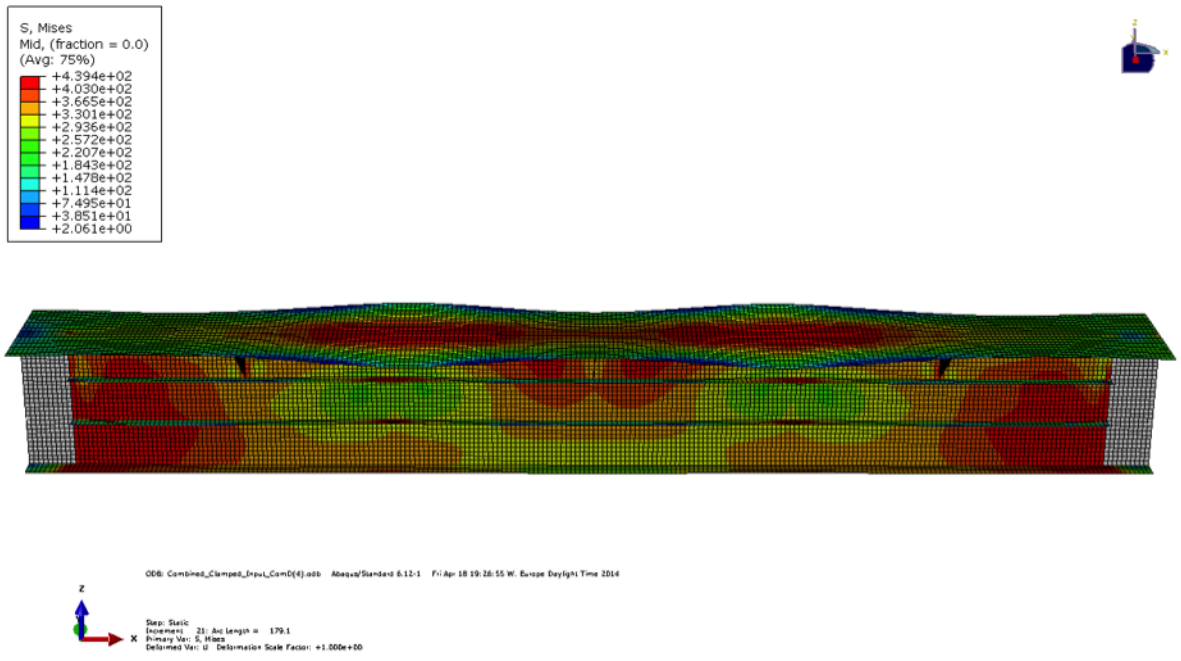

Figure B.30: Case 30

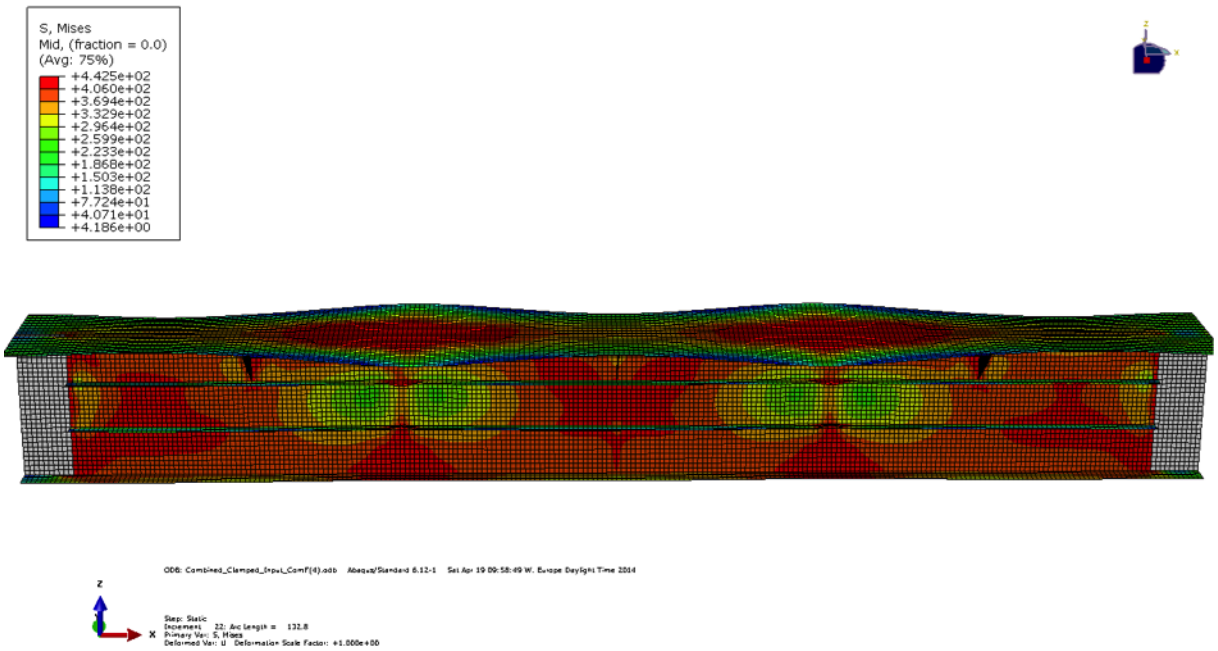

Figure B.31: Case 31

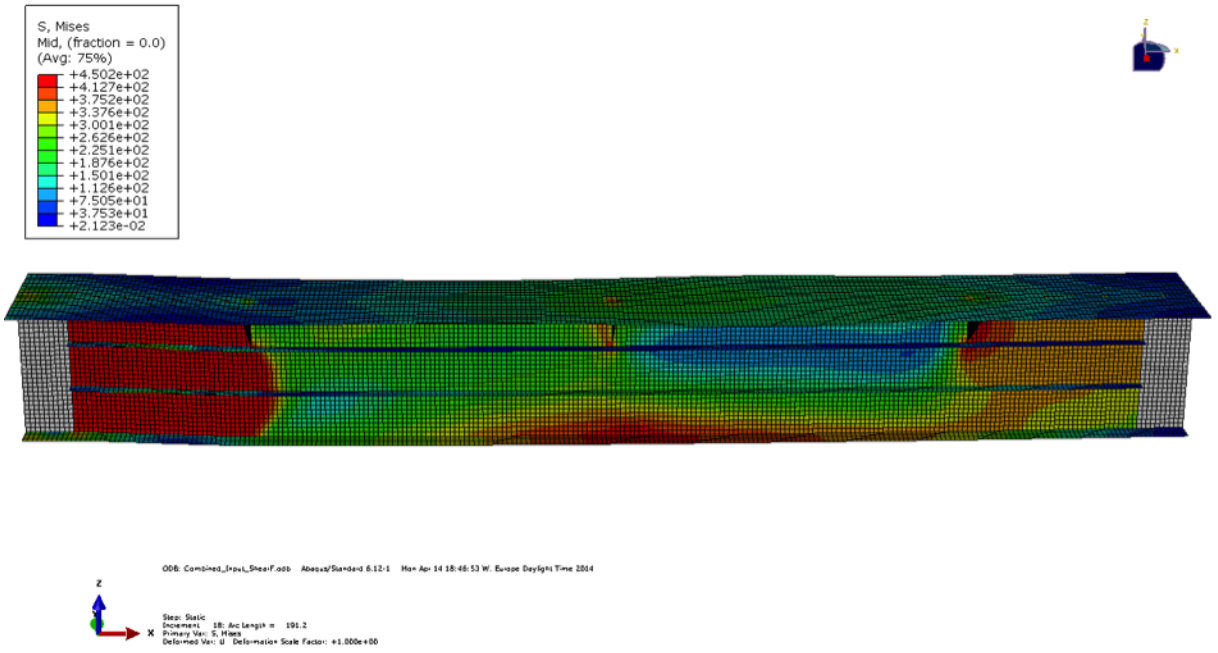

Figure B.32: Case 32

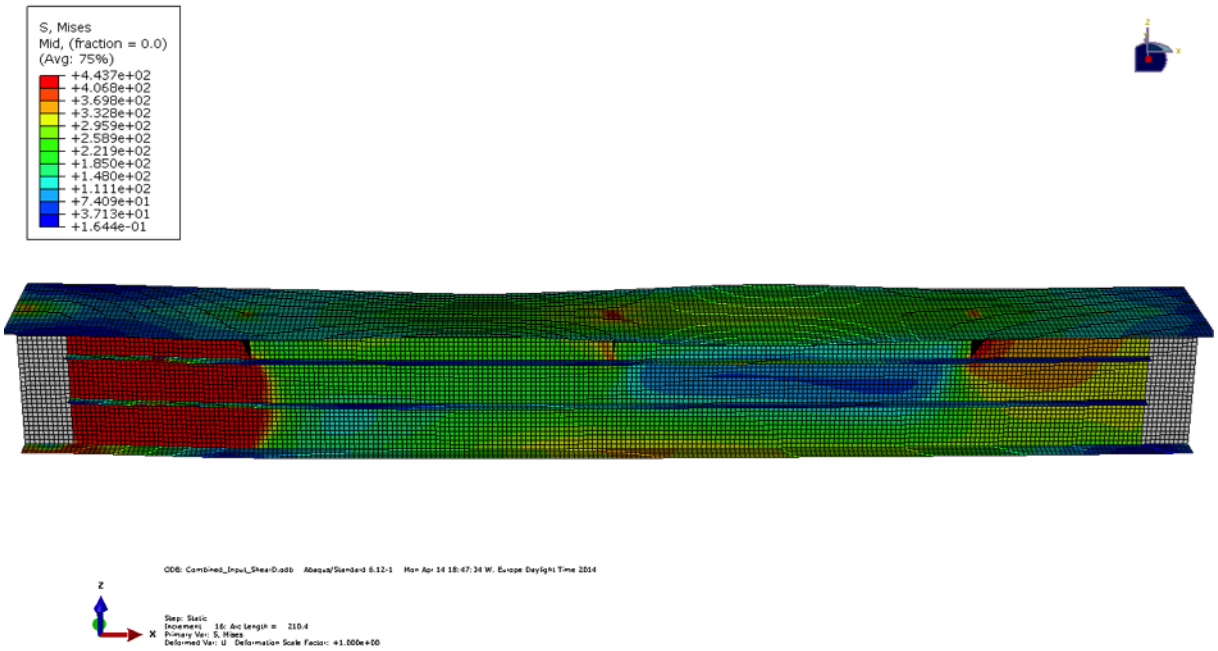

Figure B.33: Case 33

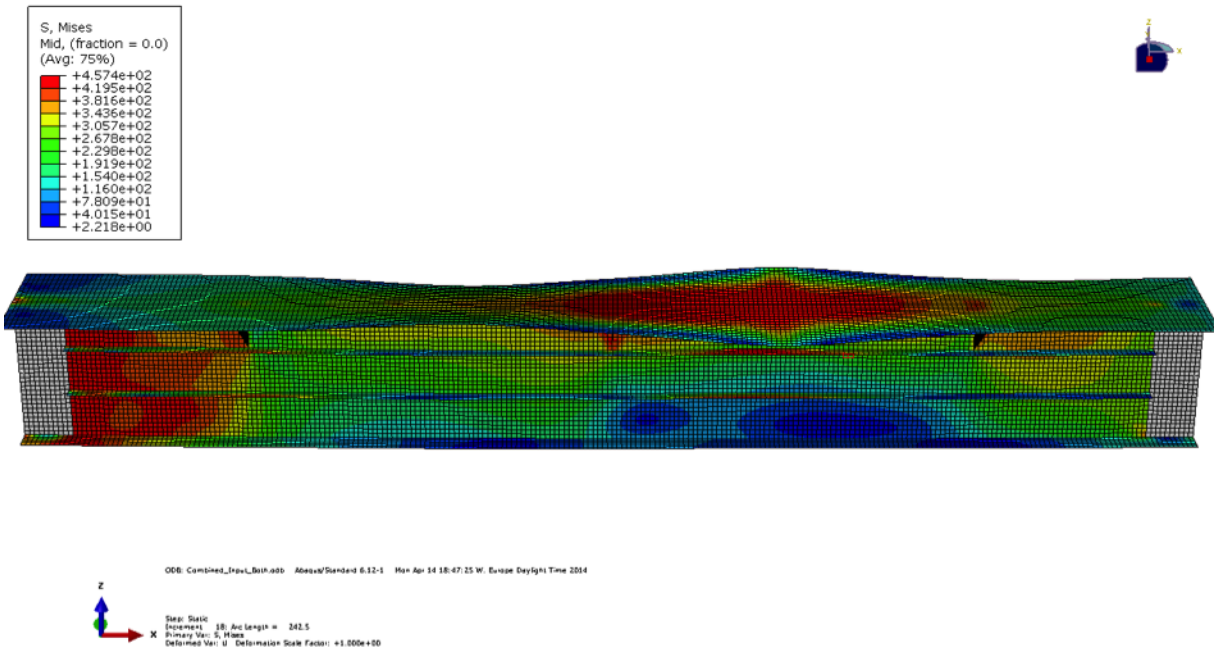

Figure B.34: Case 34

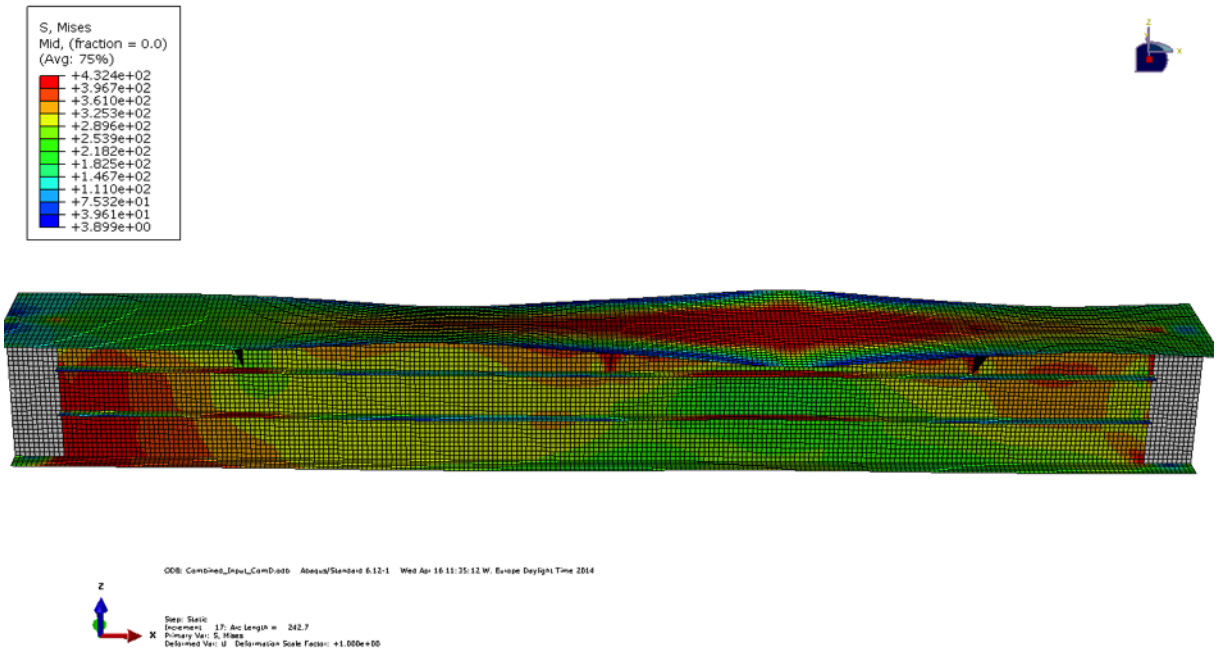

Figure B.35: Case 35

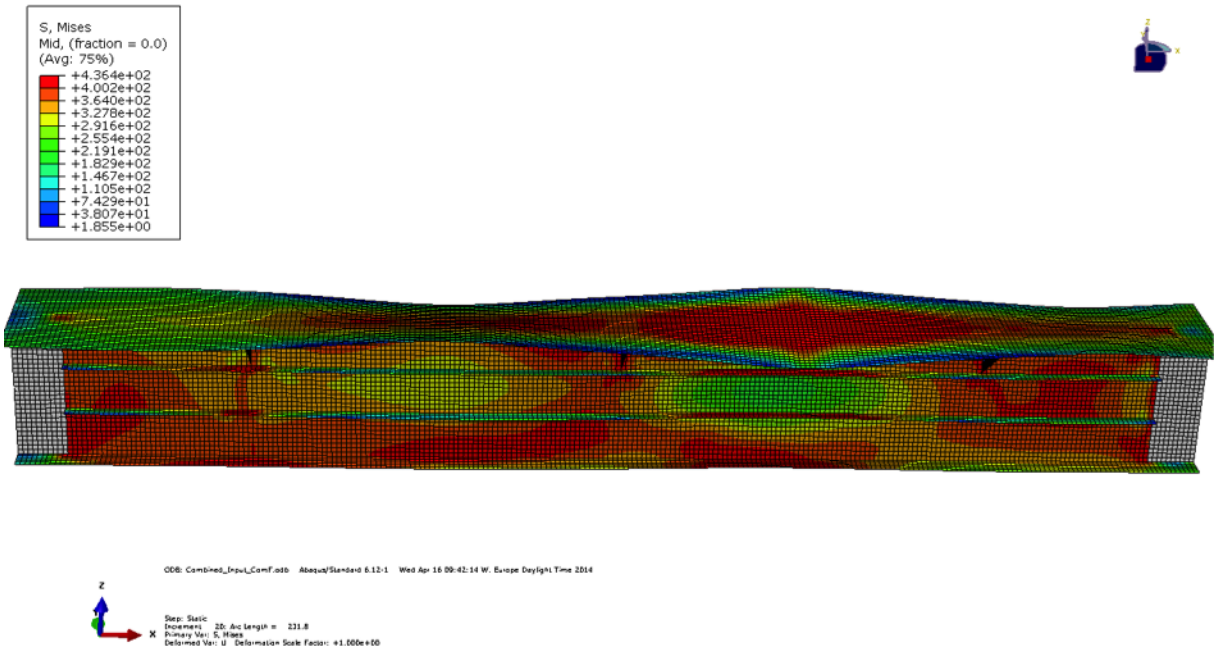

Figure B.36: Case 36

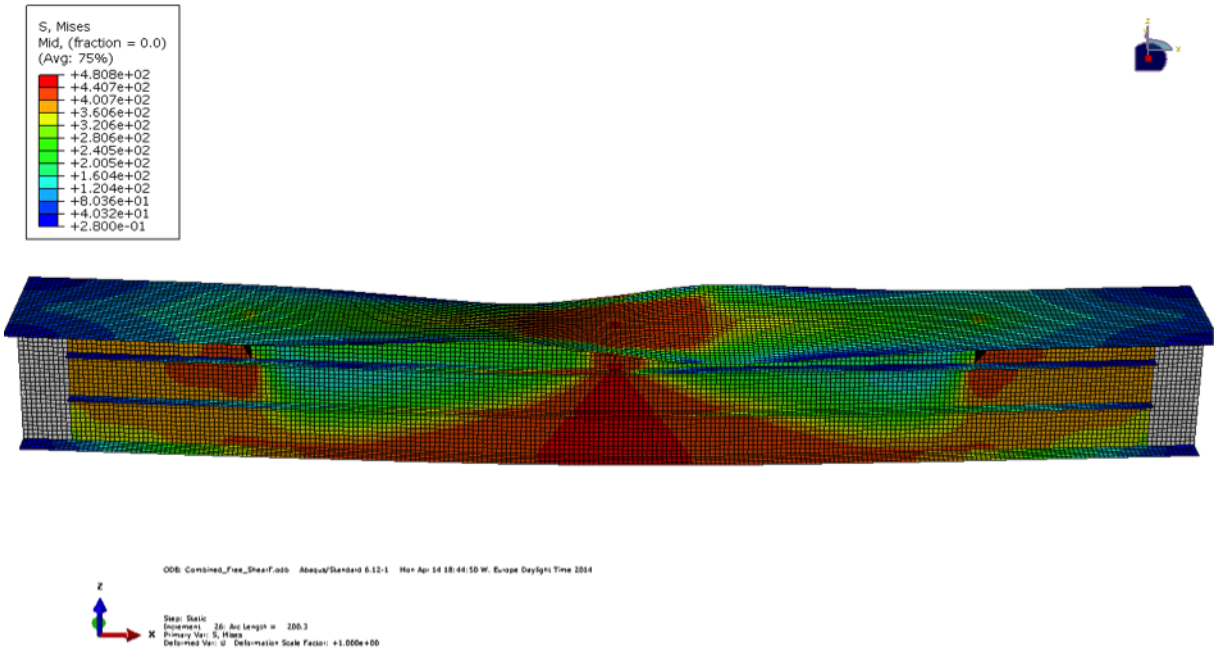

Figure B.37: Case 37

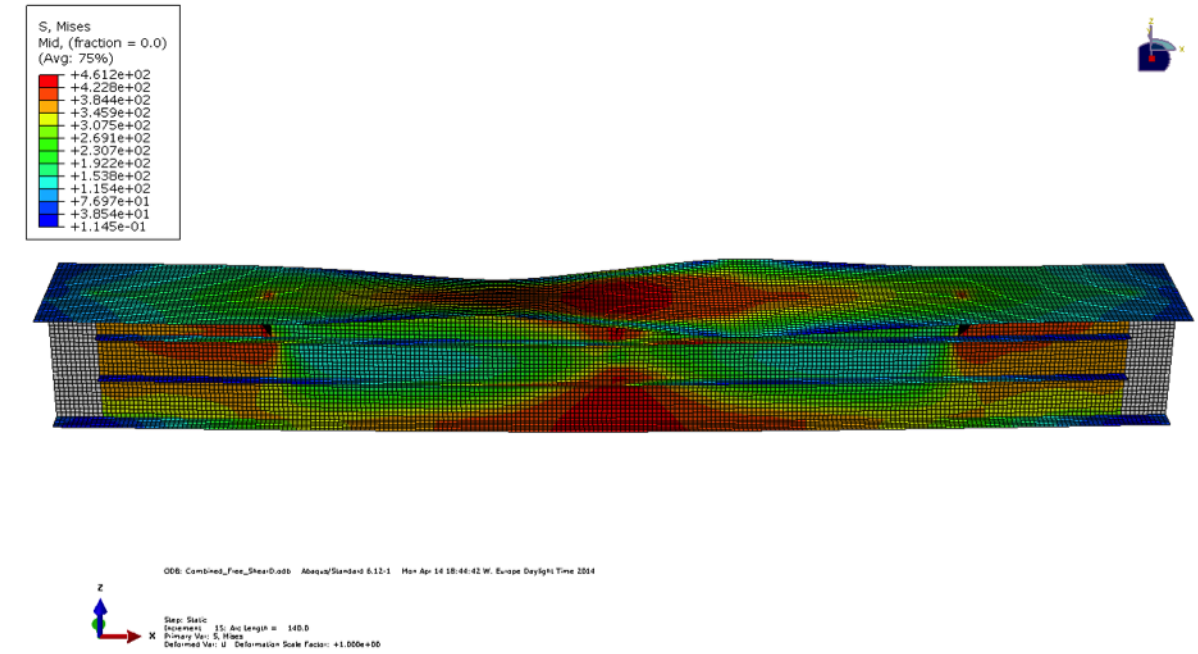

Figure B.38: Case 38

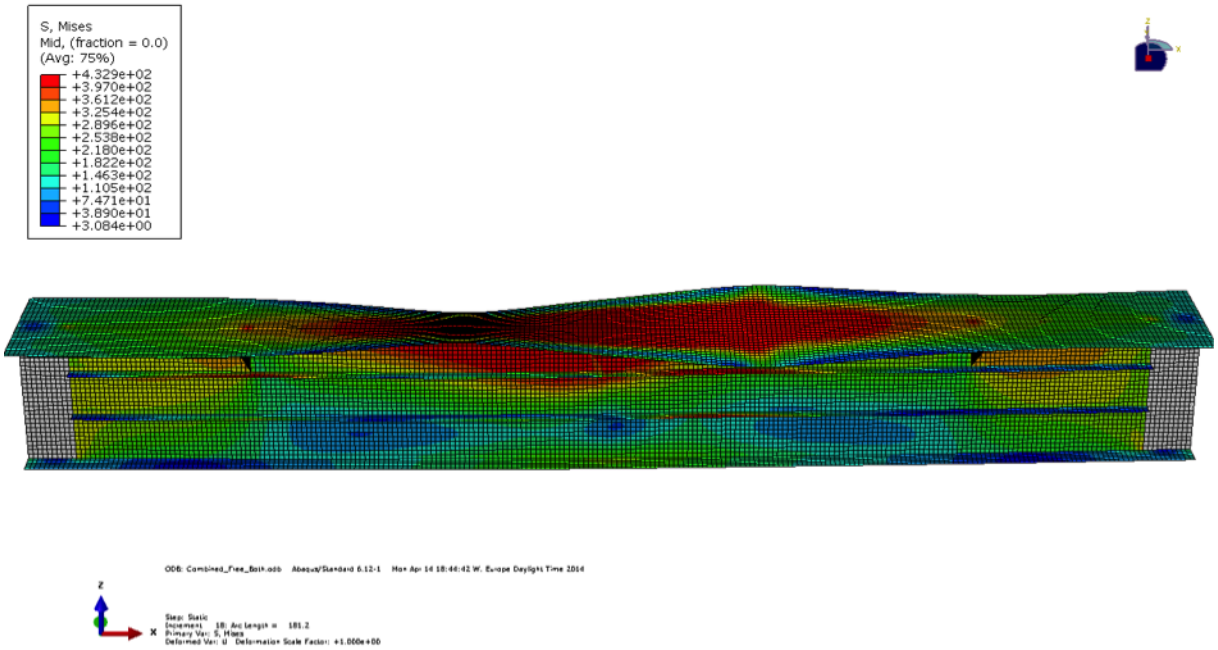

Figure B.39: Case 39

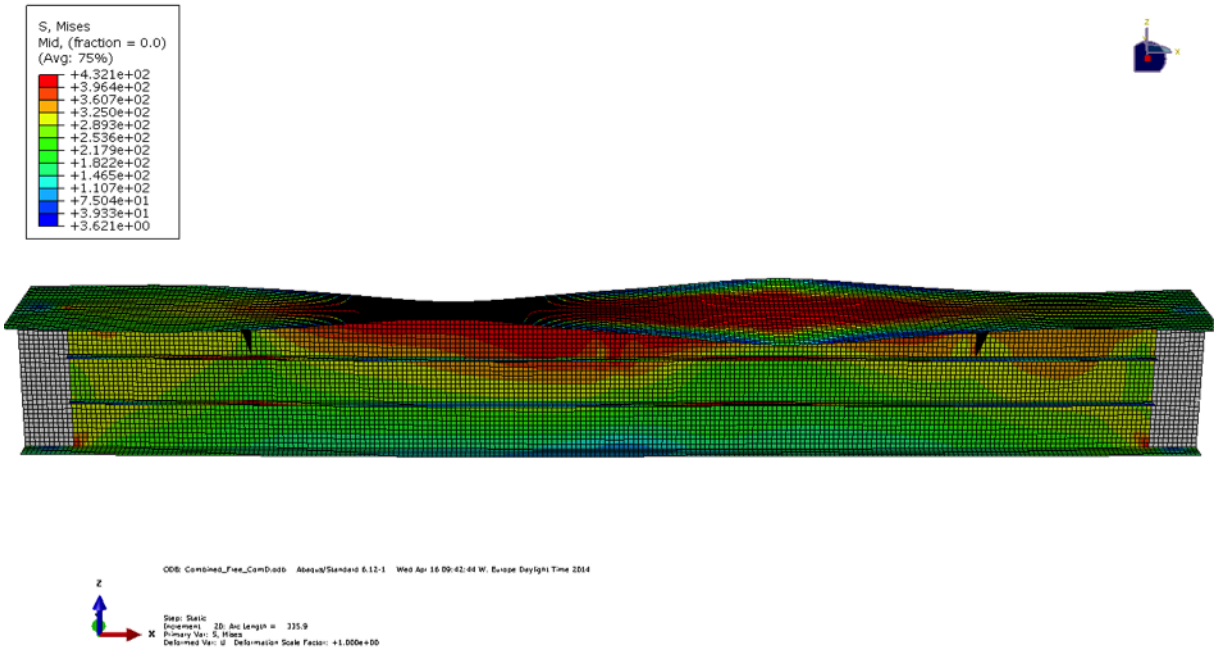

Figure B.40: Case 40

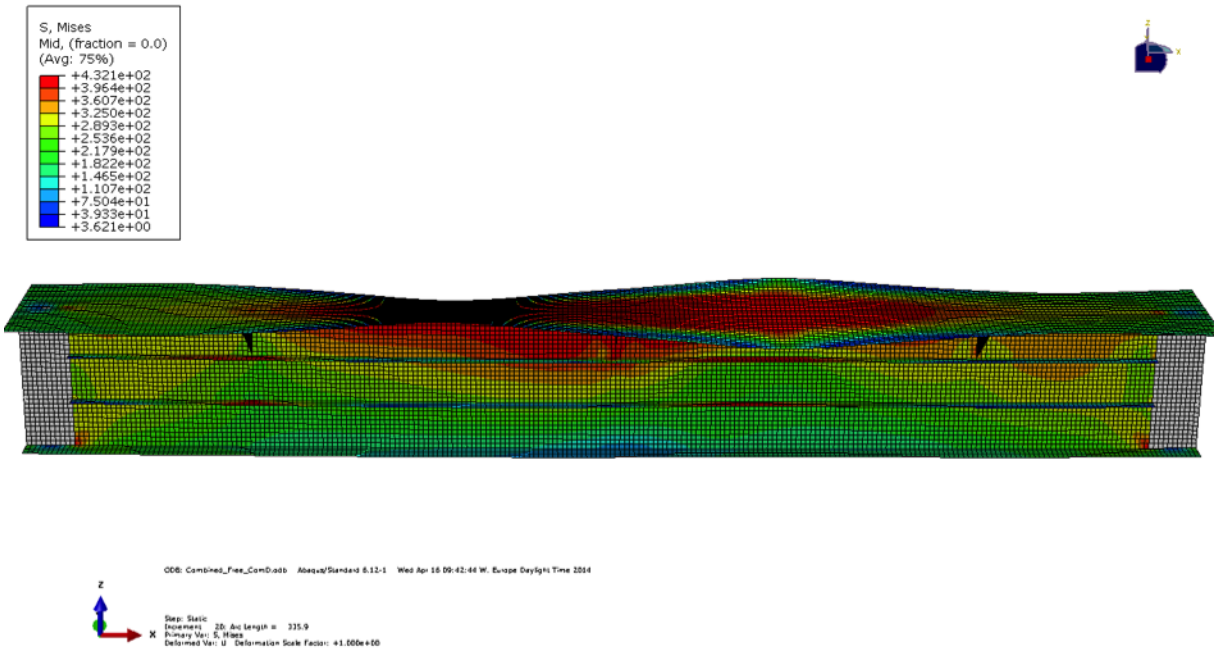

Figure B.41: Case 41

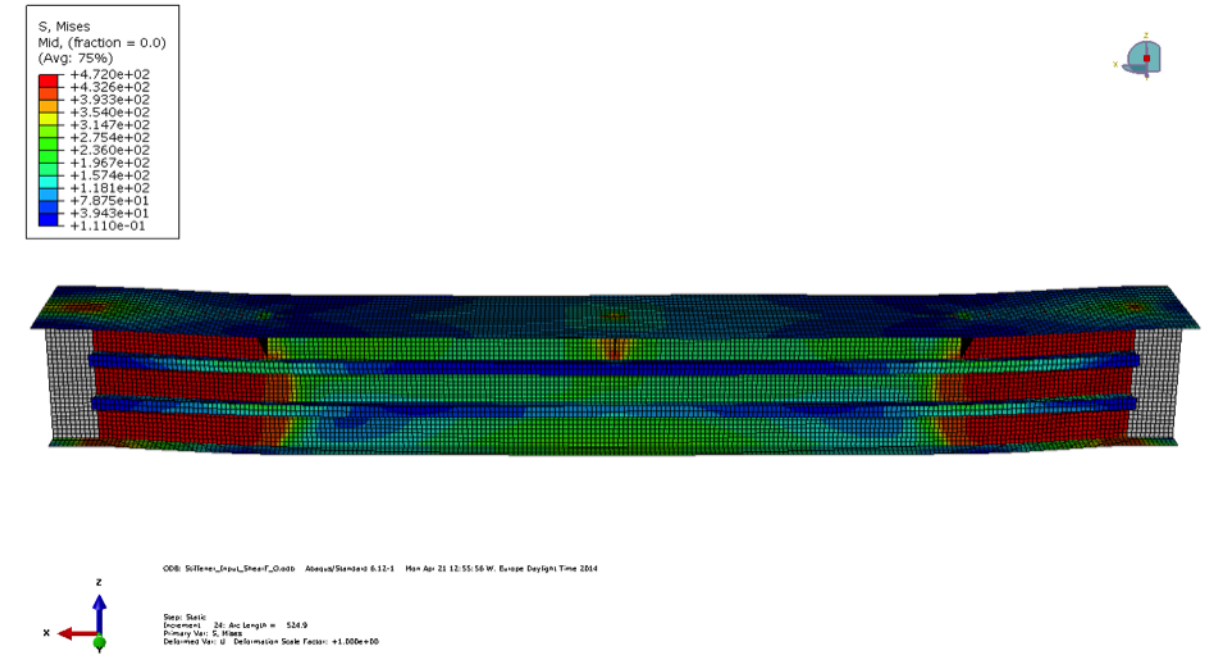

Figure B.42: Case 42

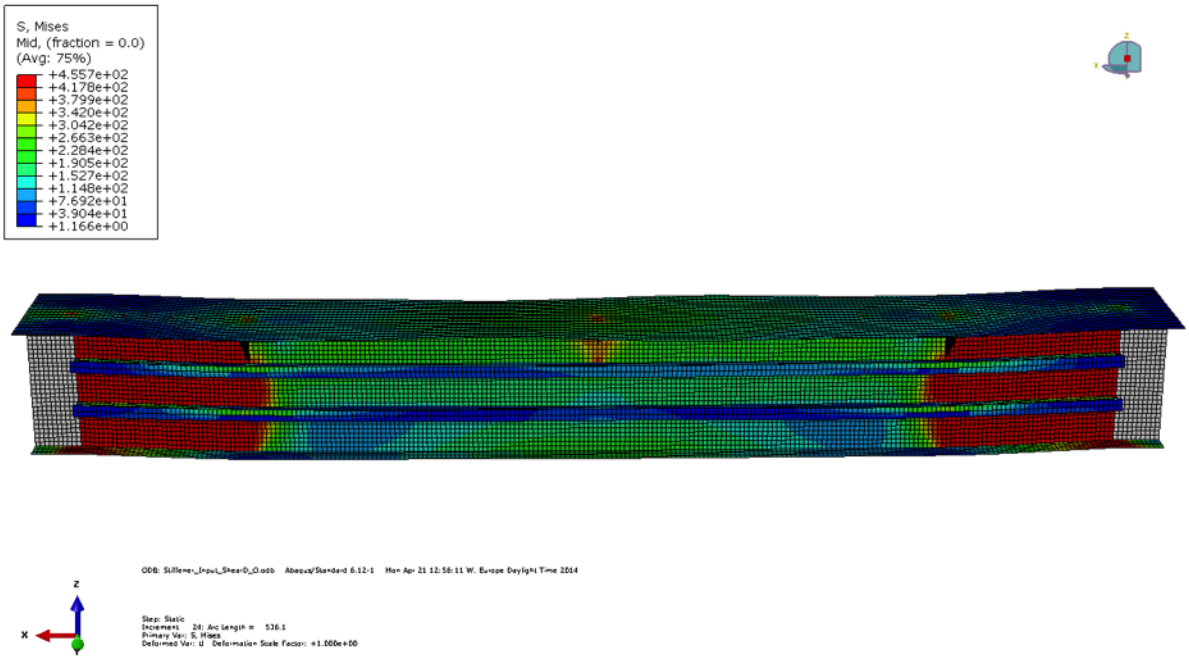

Figure B.43: Case 43

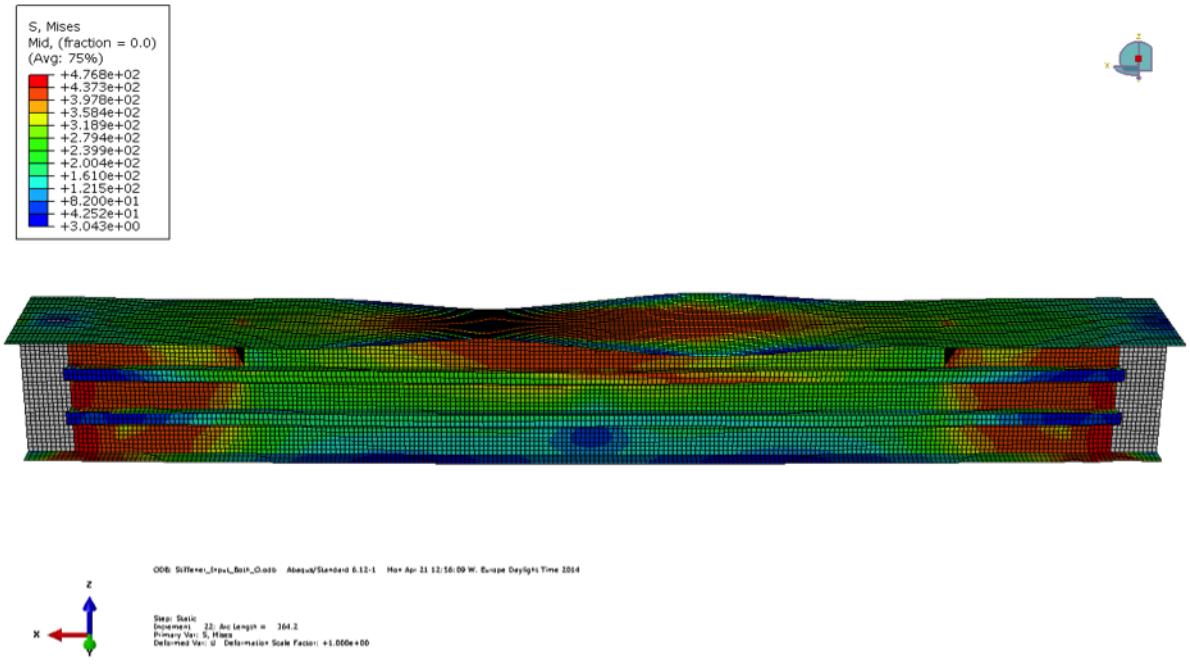

Figure B.44: Case 44

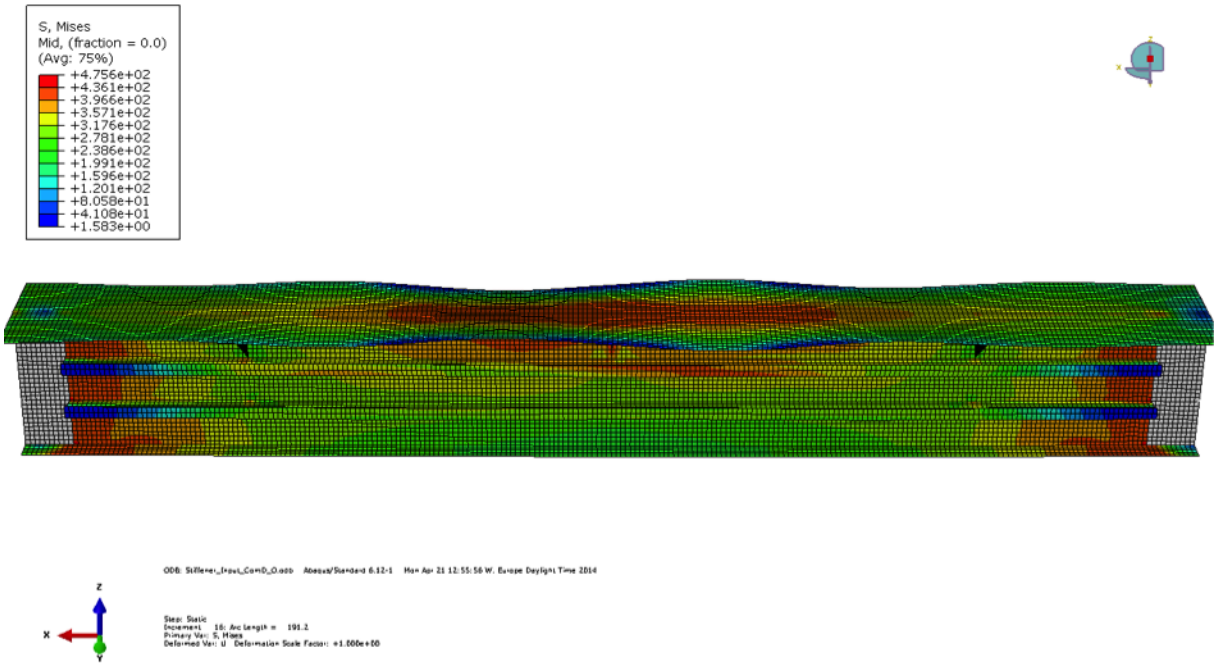

Figure B.45: Case 45

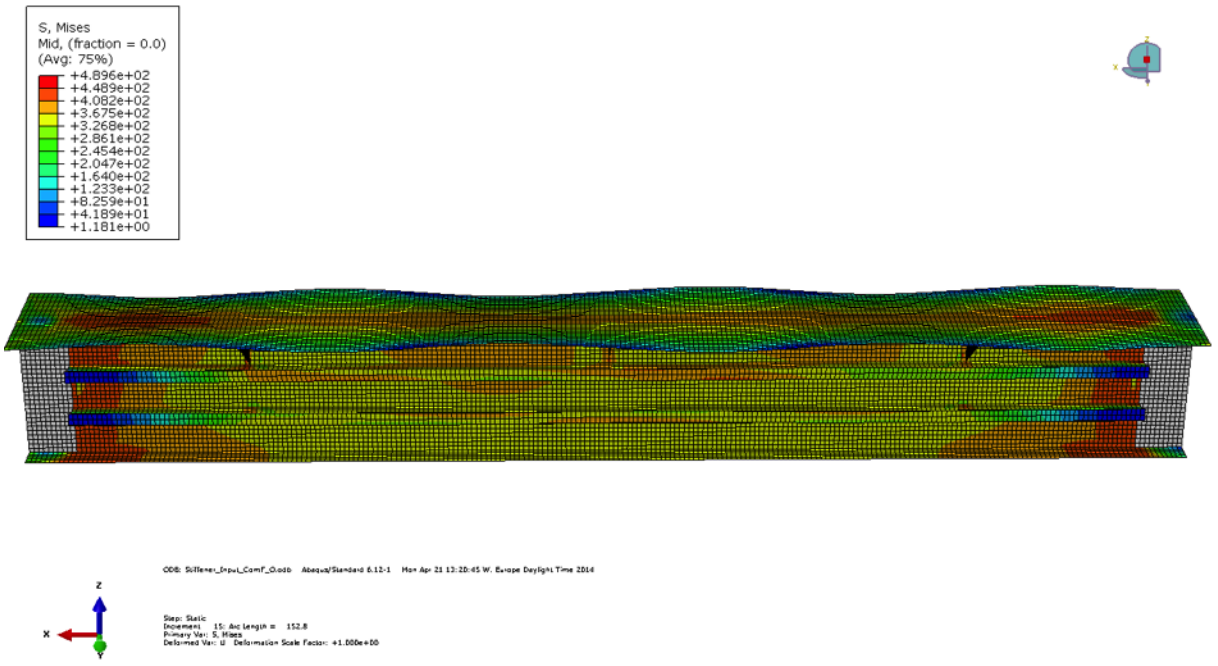

Figure B.46: Case 46

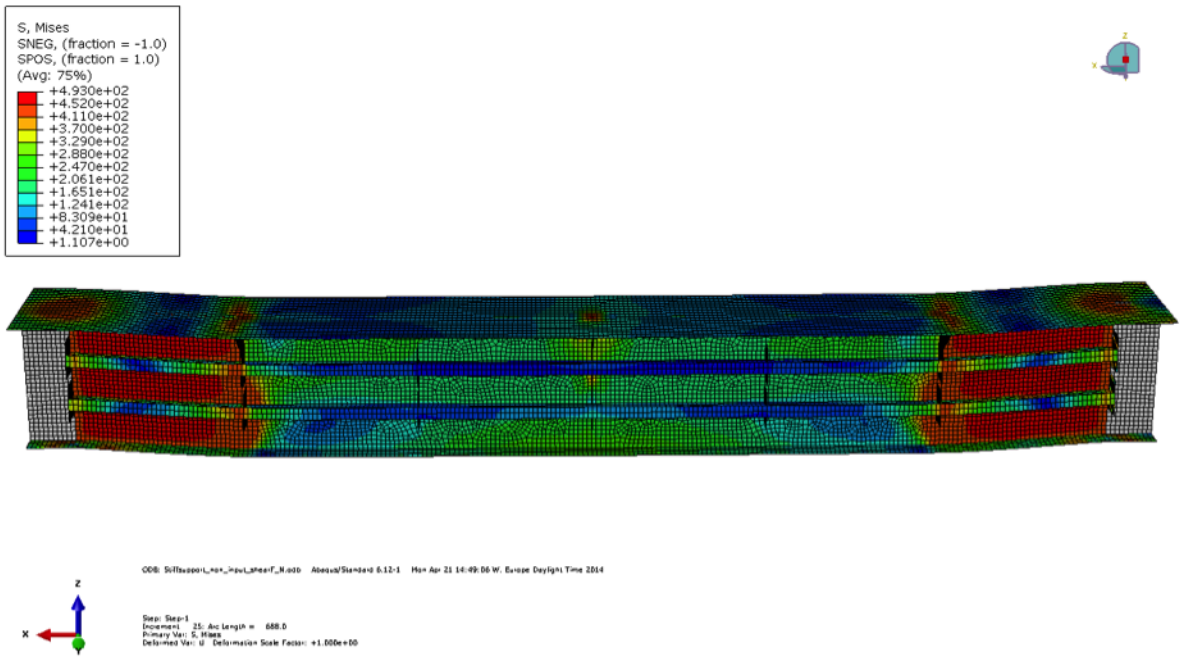

Figure B.47: Case 47

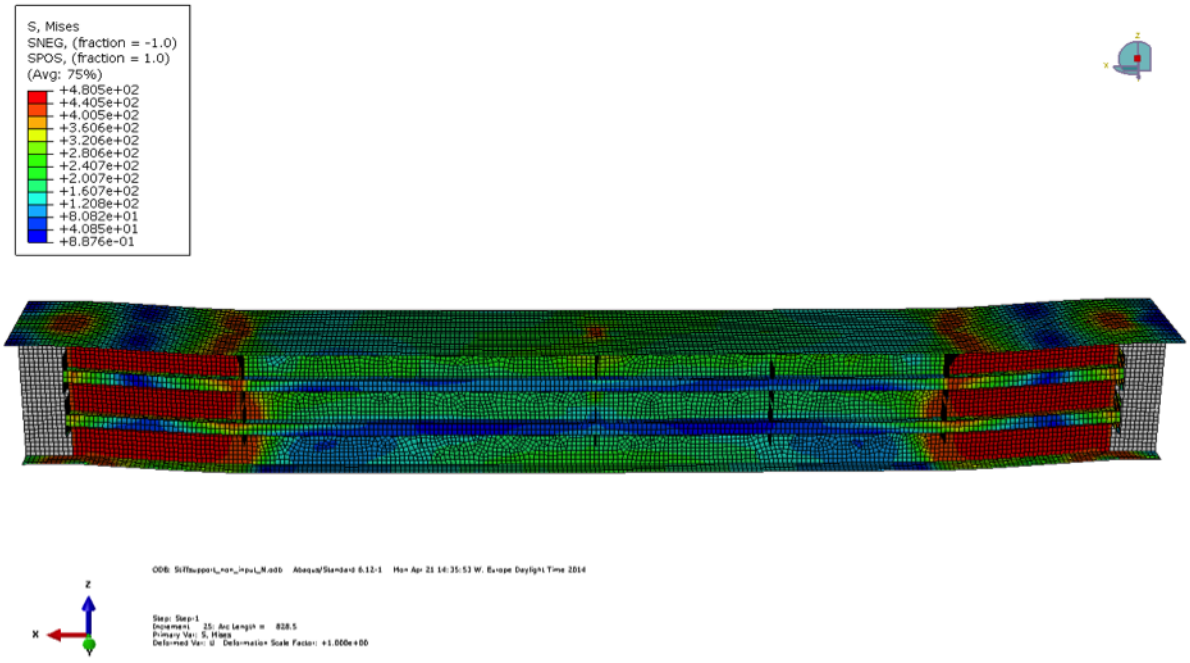

Figure B.48: Case 48

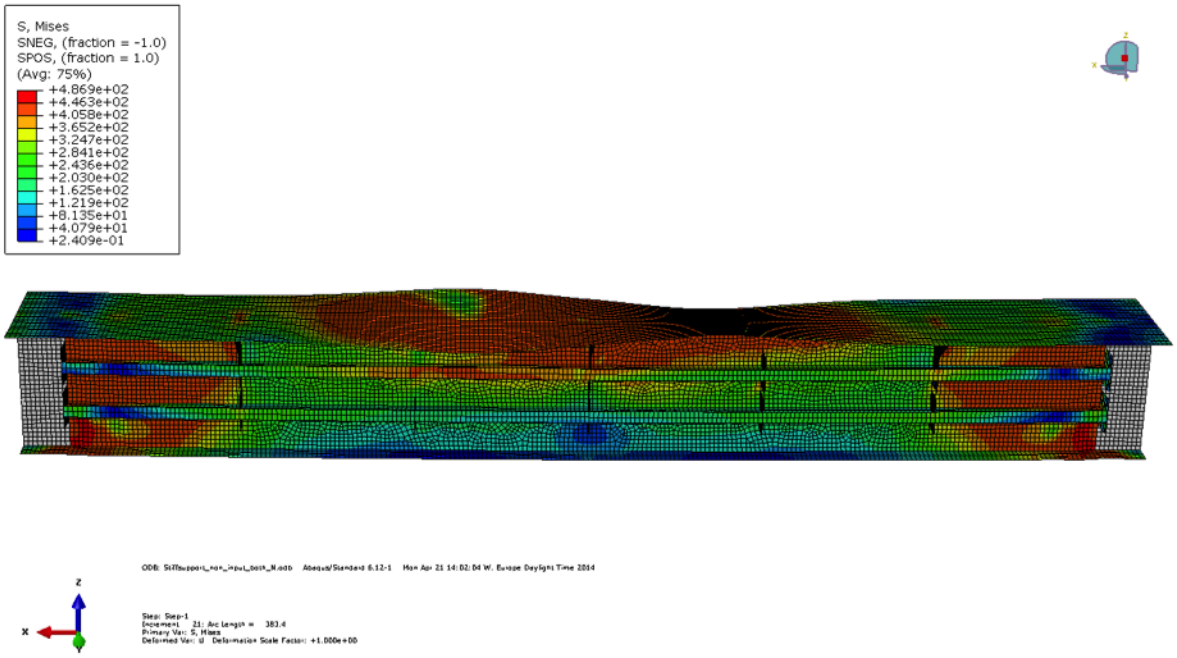

Figure B.49: Case 49

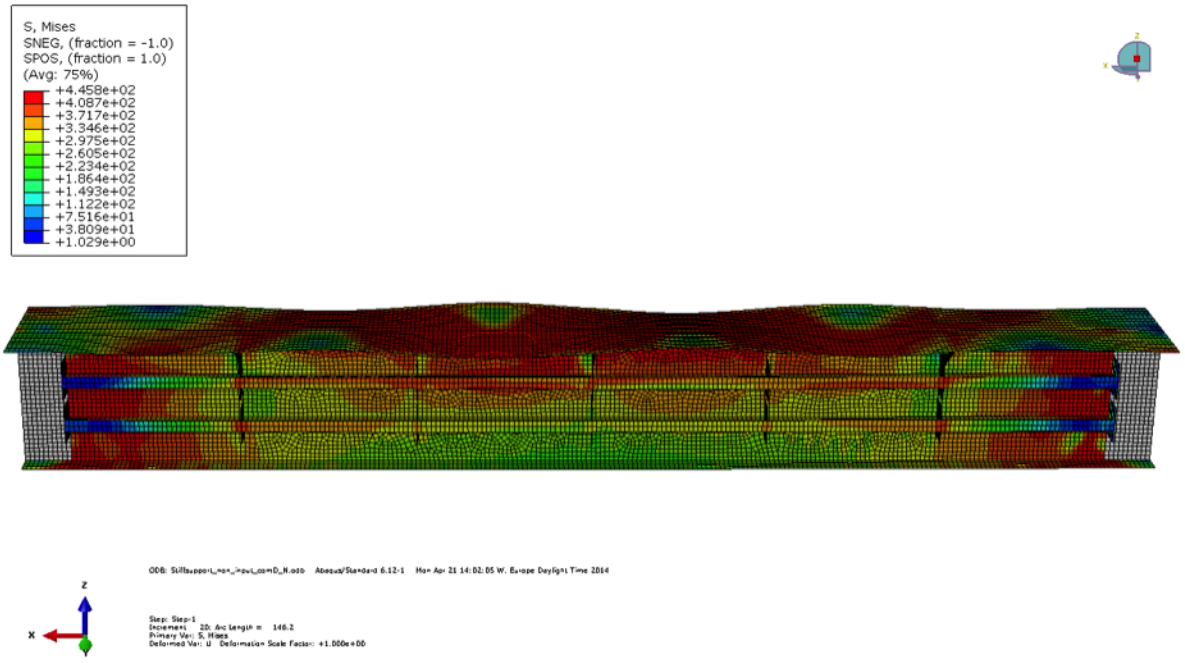

Figure B.50: Case 50

Figure B.51: Case 51

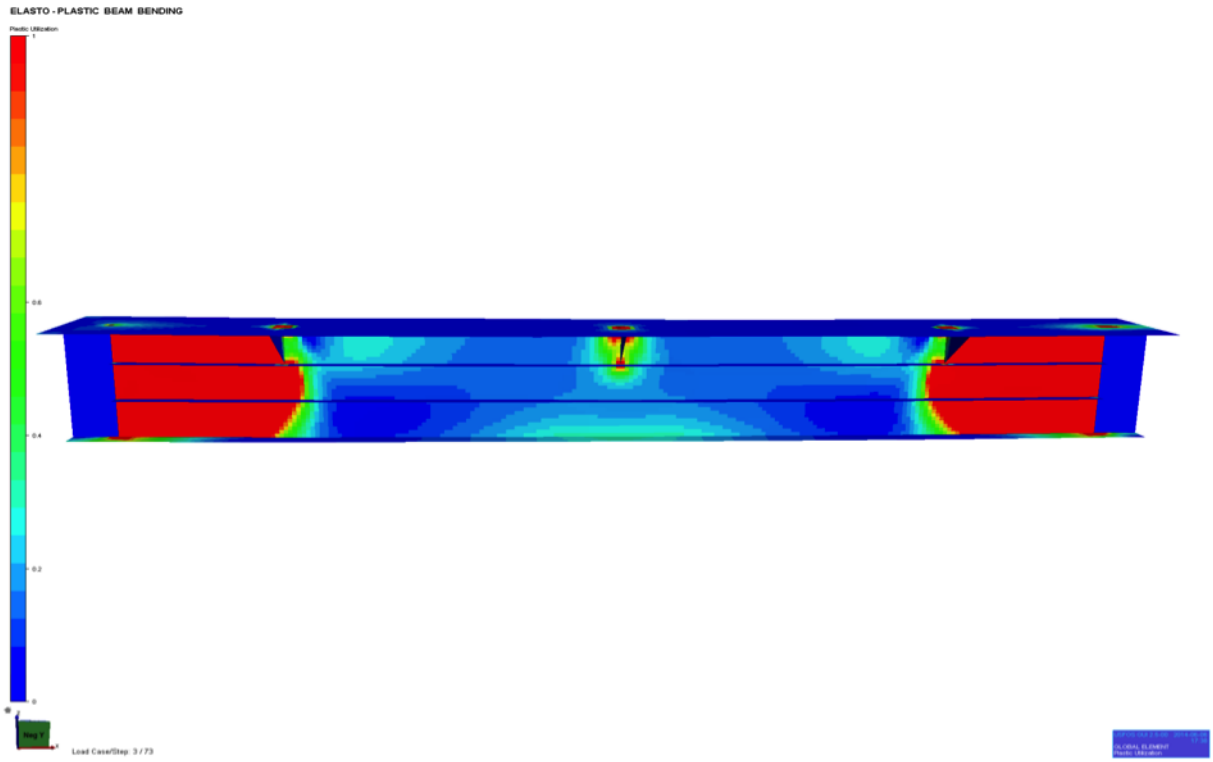

Figure B.52: Case 52

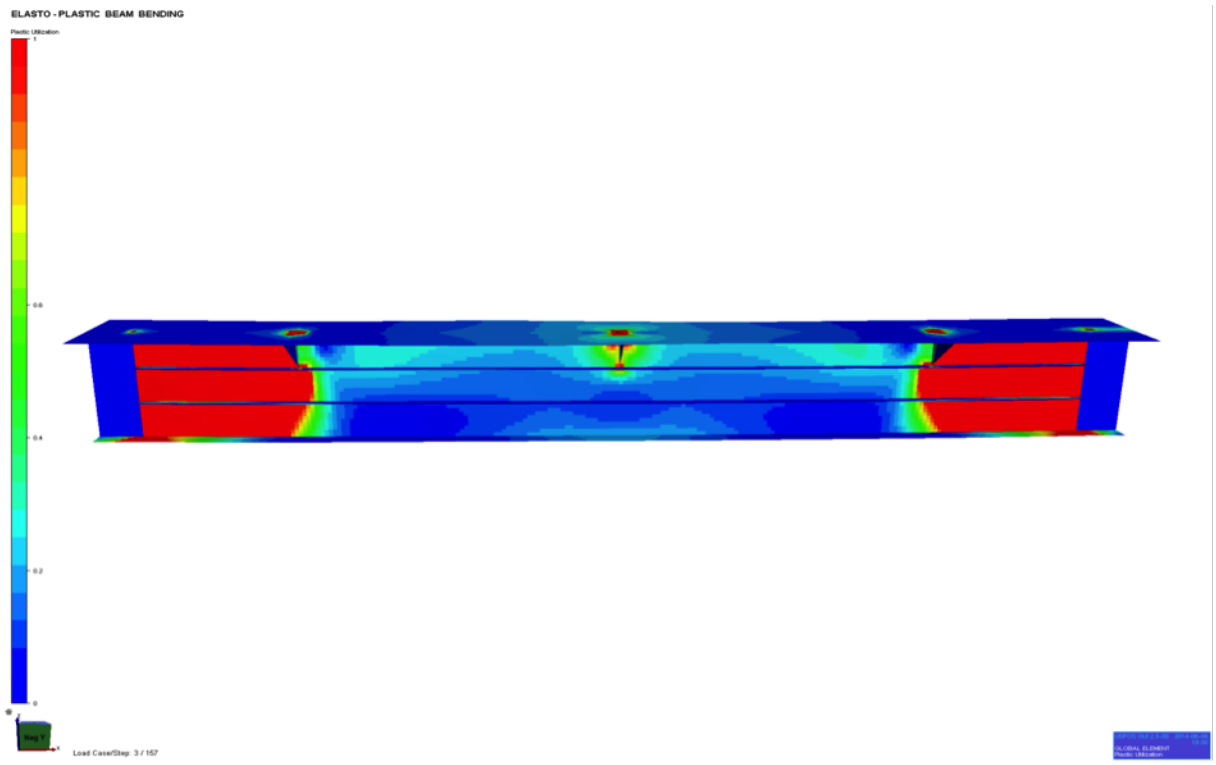

Figure B.53: Case 53

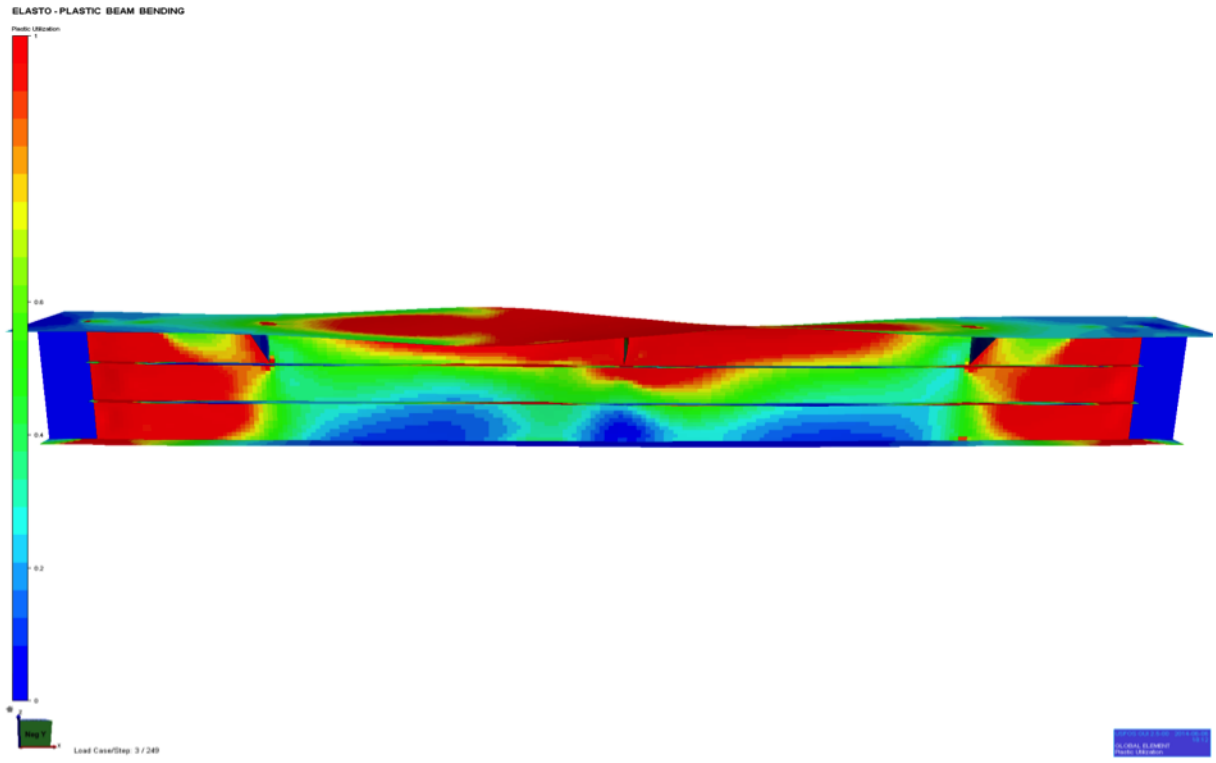

Figure B.54: Case 54

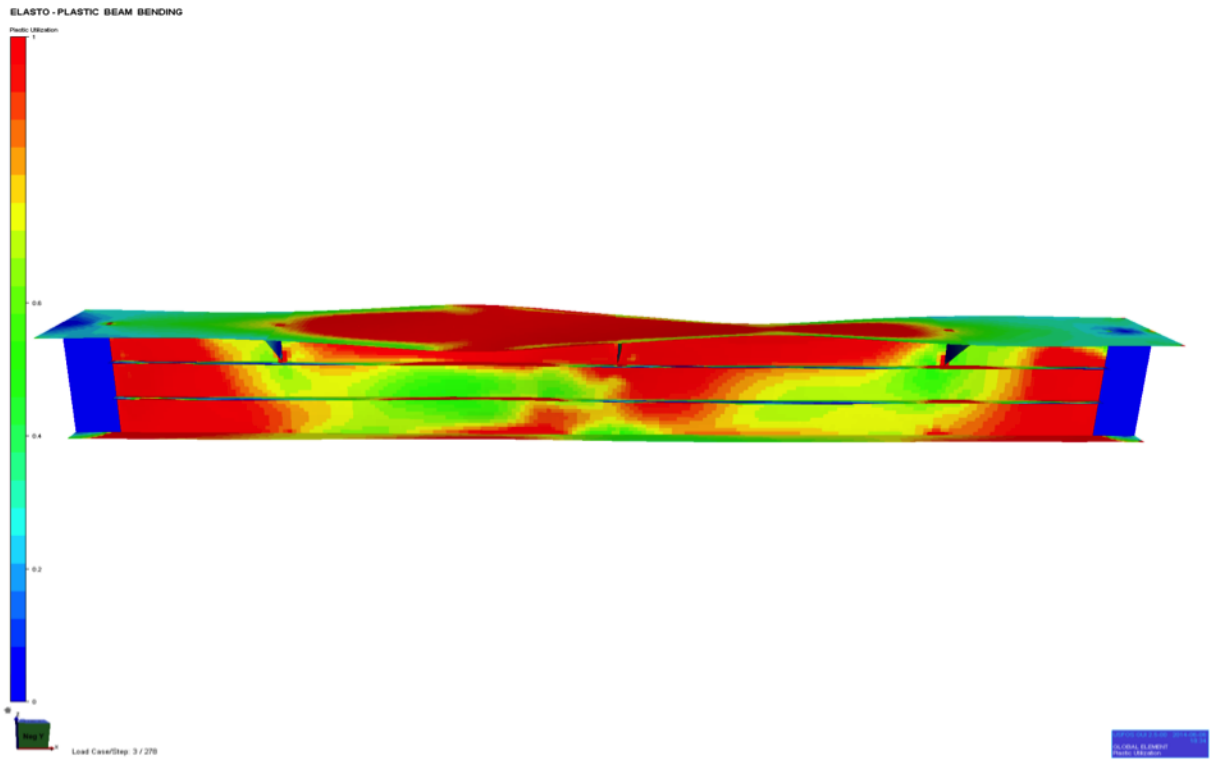

Figure B.55: Case 55

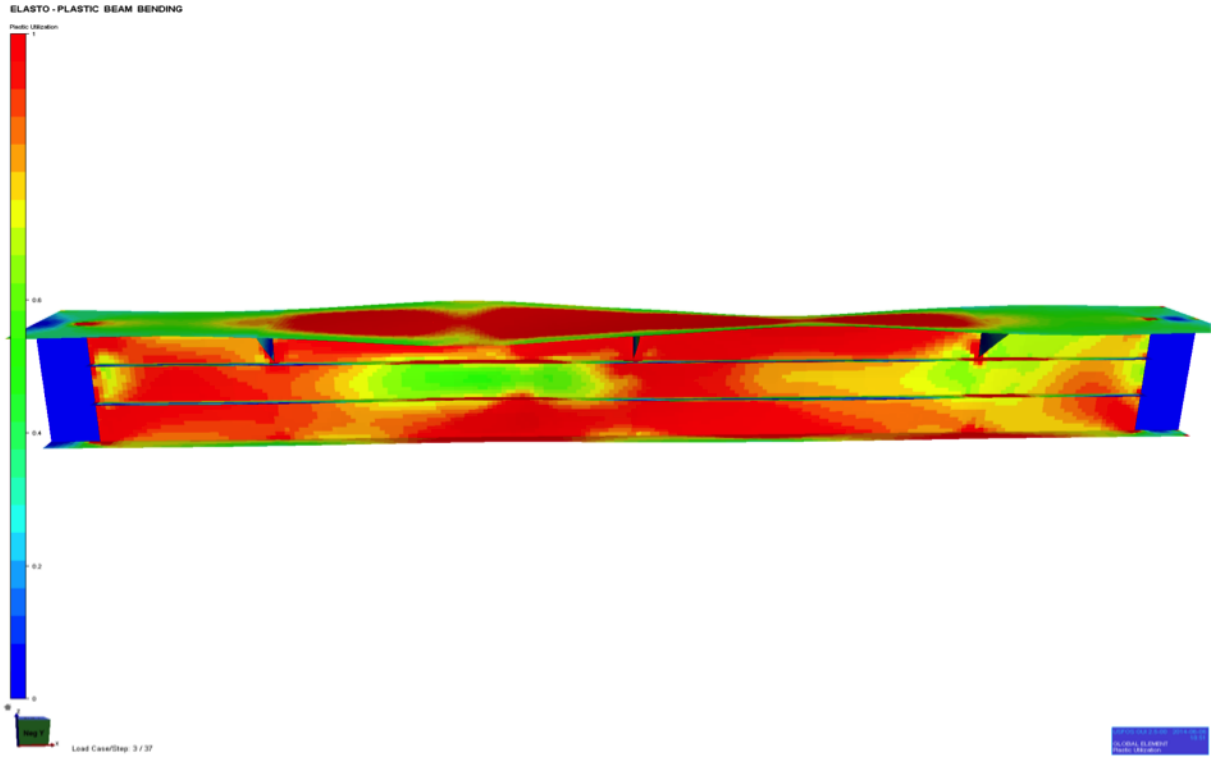

Figure B.56: Case 56

Appendix C

Nodal reaction check in Abaqus

Check reaction force at the end nodes for case No.5

Web Section	
0	341342
50	313037
100	303872
150	293597
200	286215
250	279714
300	274764
350	271068
400	268381
450	266855
500	265964
550	266155
600	266748
650	268459
700	270459
750	273634
800	277105
850	281798
900	286947
950	293533
1000	300921
1050	310287
1100	321064
1150	334540
1200	350160
1250	368654
1300	390466
1350	412700
1400	455519
sum:	8893958

Top Flange	
0	260509
50	413698
100	346488
150	344357
200	339521
250	343438
300	345765
350	350850
400	354826
450	359020
500	362377
550	364928
600	367997
650	369741
700	384296
750	588807
800	383234
850	369158
900	367515
950	364598
1000	362158
1050	359106
1100	355257
1150	351950
1200	347774
1250	346729
1300	343261
1350	349099
1400	356513
1450	426548
1500	266990
sum:	11246508

Bottom Flange	
0	293357
50	489133
100	450004
150	468596
200	494075
250	785114
300	519916
350	522749
400	542949
450	613597
500	364484
sum:	5543974

Total reaction force	25684440	=	8893958+11246508+5543974
Total applied force	25684400	=	73,384*1000*350

Appendix D

Capacity check for primary girder bases on DNV-RP-C201

NAUTICUS hull

Recommend-ed Practice DNV-RP-C201 Oct. 2010

BUCKLING OF STIFFENED PLATE PANEL

Vers. 14.0, Nauticus Hull, Jan. 2011

Sign:
Time: 22:00
Date: 02.06.2014

PRINCIPAL DATA

Identification			
Material Factor	γ_M=	1,00	-
Yield stress	f_y =	420,0	N/mm2
Modulus of Elasticity	E=	210 000	N/mm2
Poissons Ratio	ν=	0,3	-
Shear Modulus	G=	80 769	N/mm2

PLATE

Thickness	t=	15,0	mm
Stiffener Spacing	s =	500,0	mm
Stiffener Length	l =	3750,0	mm
Girder Length	L_G =	1500,0	mm
Panel length (max.no stiff spans*l)	l_P =	11250,0	mm

Plot Nothing

STIFFENER AND GIRDERS

		Stiffener:		Girder:	
Stiffener Type		Flat bar		T-profile	
Total Height of section	h_{tot} =	150,0	mm	400,0	mm
Web Thickness	t_w =	10,0	mm	15,0	mm
Flange width	b =		mm	210,0	mm
Flange thickness	t_f =		mm	35,0	mm
Buckling length factor: (optional)	k_{stiff} =	0,50		k_{girder} =	
Distance between tripping brackets:	l_T =		mm	betw.lateral supp.: L_{TG} =	mm
Fabrication method:				Welded cross section	
Stiffener end support:		Continuous Stiffeners		Continuous Girder	
Tension field action:		Tension Field Action is NOT Allowed		Stiffened plate is effective against sigma-Y	

(i.e. Method 1 is used)

LOAD DATA:

◉ Uniform Stress ○ Linear Varying Stress

Stresses on plate edge/corner				Stresses on opposite side			
Longitudinal compr.:	$\sigma_{x,sd}$ =	289,34	N/mm2	Longitudinal compr.:	$\sigma_{x2,sd}$ =	289,34	N/mm2
Transverse compress.:	$\sigma_{y,sd}$ =		N/mm2	Transverse compress.:	$\sigma_{y2,sd}$ =	0,00	N/mm2
Shear Stress:	τ_{sd} =		N/mm2	Load factor for stresses:	γ_L =	1,00	-
Lateral load / pressure:	P_{sd} =		N/mm^2				
Min. pr. in adj. spans:	P_{sdMin} =		N/mm^2	Load factor for lateral load:	γ_L=	1,00	-
Pressure distrubution:		Overpr. may occur on both sides		Support mom. factor:	k_{m3} =	12,00	0,0000E+00
Press. variation betw. spans:		Equal pressure		Midspan mom. factor:	k_{m2} =	24,00	0,0000E+00

(for stiffener with effective plate)

BUCKLING CHECK SUMMARY:

Buckling modes:	$\sigma_{j,Sd}$	$\sigma_{x,Rd}$	$\sigma_{y,Rd}$	τ_{Rd}	P_{Sd} Max	UF
Unstiffened plate buckling:	289,34	385,22	167,31	242,49	1,004	**0,689**

Stiffened plate panel:	q_{Sd}	f_k		z*	UF
Design load on plate side:	0,00	316,9		1,5	**1,000**
Design load on stiffener side:	0,00	264,4		1,5	**1,000**
Requirement to plate resistance:			$\sigma_{y,Sd}$ <= 167,3		**0,000**
Requirement to shear capacity:	V_{Sd} =	0 [kN]	V_{Rd} = 363,7 [kN]		**0,000**

Girder check:	q_{Sd}	f_k		z*	UF
Design load on plate side:	104,16	420,0		0,0	**0,016**
Design load on girder side:	104,1624	420,0		0,0	**0,016**
Requirement to shear capacity:	V_{Sd} =	0 [kN]	V_{Rd} = 1 454,9 [kN]		**0,000**

Local buckling, cross section class-type requirements:

Maximal webheight:	Stiffener:	h_w <=	314,2	Girder:	h_w <= 471,2	**OK, within Sect. Type III**
Maximal flangewidth:	Stiffener:	c <=	0,0	Girder:	c <= 366,5	**OK, within Sect. Type III**

Maximum usage factor: **1,000** OK

NAUTICUS hull

Recommend-ed Practice DNV-RP-C201 Oct. 2010

BUCKLING OF STIFFENED PLATE PANEL

Vers. 14.0, Nauticus Hull, Jan. 2011

Sign:
Time: 13:18
Date: 02.06.2014

PRINCIPAL DATA

Identification			
Material Factor	γ_M =	1,00	-
Yield stress	f_y =	420,0	N/mm2
Modulus of Elasticity	E =	210 000	N/mm2
Poissons Ratio	ν =	0,3	-
Shear Modulus	G =	80 769	N/mm2

PLATE

Thickness	t =	15,0	mm
Stiffener Spacing	s =	500,0	mm
Stiffener Length	l =	3750,0	mm
Girder Length	L_G =	1500,0	mm
Panel length (max.no stiff spans*l)	L_P =	11250,0	mm

Plot Nothing

STIFFENER AND GIRDERS

		Stiffener:		Girder:	
Stiffener Type		Flat bar		T-profile	
Total Height of section	h_{tot} =	150,0	mm	400,0	mm
Web Thickness	t_w =	10,0	mm	15,0	mm
Flange width	b =		mm	210,0	mm
Flange thickness	t_f =		mm	35,0	mm
Buckling length factor: (optional)	k_{stiff} =	0,50		k_{girder} =	
Distance between tripping brackets:	l_T =		mm	betw.lateral supp.: L_{TG} =	mm
Fabrication method:				Welded cross section	
Stiffener end support:		Continuous Stiffeners		Continuous Girder	
Tension field action:		Tension Field Action is NOT Allowed		Stiffened plate is effective against sigma-Y	

(i.e. Method 1 is used)

LOAD DATA:

◉ Uniform Stress ○ Linear Varying Stress

Stresses on plate edge/corner				Stresses on opposite side			
Longitudinal compr.:	$\sigma_{x,sd}$ =	0,00	N/mm2	Longitudinal compr.:	$\sigma_{x2,sd}$ =	0,00	N/mm2
Transverse compress.:	$\sigma_{y,sd}$ =		N/mm2	Transverse compress.:	$\sigma_{y2,sd}$ =	0,00	N/mm2
Shear Stress:	τ_{sd} =	242,42	N/mm2	Load factor for stresses:	γ_L =	1,00	-
Lateral load / pressure:	P_{sd} =		N/mm^2				
Min. pr. in adj. spans:	P_{sdMin} =		N/mm^2	Load factor for lateral load:	γ_L=	1,00	-
Pressure distrubution:		Overpr. may occur on both sides		Support mom. factor:	k_{m3} =	12,00	0,0000E+00
Press. variation betw. spans:		Equal pressure		Midspan mom. factor:	k_{m2} =	24,00	0,0000E+00

(for stiffener with effective plate)

BUCKLING CHECK SUMMARY:

Buckling modes:	$\sigma_{j,Sd}$	$\sigma_{x,Rd}$	$\sigma_{y,Rd}$	τ_{Rd}	P_{Sd} Max	UF
Unstiffened plate buckling:	419,88	385,22	167,31	242,49	0,036	**1,000**

Stiffened plate panel:	q_{Sd}	f_k		z*	UF
Design load on plate side:	0,00	316,9		-3,2	**0,999**
Design load on stiffener side:	0,00	197,2		-3,2	**0,999**
Requirement to plate resistance:			$\sigma_{y,Sd}$ <= 3,9		**1,000**
Requirement to shear capacity:	V_{Sd} =	0 [kN]	V_{Rd} = 363,7 [kN]		**0,000**

Girder check:	q_{Sd}	f_k		z*	UF
Design load on plate side:	0,00	420,0		0,0	**0,000**
Design load on girder side:	0	420,0		0,0	**0,000**
Requirement to shear capacity:	V_{Sd} =	0 [kN]	V_{Rd} = 1 454,9 [kN]		**0,000**

Local buckling, cross section class-type requirements:

Maximal webheight:	Stiffener:	h_w <=	314,2	Girder: h_w <=	471,2	**OK, within Sect. Type III**
Maximal flangewidth:	Stiffener:	c <=	0,0	Girder: c <=	366,5	**OK, within Sect. Type III**

Maximum usage factor: **1,000** OK

NAUTICUS hull

Recommend-ed Practice DNV-RP-C201 Oct. 2010

BUCKLING OF STIFFENED PLATE PANEL

Vers. 14.0, Nauticus Hull, Jan. 2011

Sign:
Time: 11:17
Date: 02.06.2014

PRINCIPAL DATA

Identification			
Material Factor	γ_M =	1,00	-
Yield stress	f_y =	420,0	N/mm2
Modulus of Elasticity	E =	210 000	N/mm2
Poissons Ratio	ν =	0,3	-
Shear Modulus	G =	80 769	N/mm2

PLATE

Thickness	t =	15,0	mm
Stiffener Spacing	s =	500,0	mm
Stiffener Length	l =	3750,0	mm
Girder Length	L_G =	1500,0	mm
Panel length (max.no stiff spans*l)	L_P =	11250,0	mm

Plot Nothing

STIFFENER AND GIRDERS

	Stiffener:			Girder:		
Stiffener Type		T-profile			T-profile	
Total Height of section	h_{tot} =	350,0	mm	h_{tot} =	400,0	mm
Web Thickness	t_w =	10,0	mm	t_w =	15,0	mm
Flange width	b =	130,0	mm	b =	210,0	mm
Flange thickness	t_f =	20,0	mm	t_f =	35,0	mm
Buckling length factor: (optional)	k_{stiff} =	0,50		k_{girder} =		
Distance between tripping brackets:	l_T =		mm	betw.lateral supp.:	L_{TG} =		mm
Fabrication method:		Welded cross section			Welded cross section	
Stiffener end support:		Continuous Stiffeners			Continuous Girder	
Tension field action:		Tension Field Action is NOT Allowed			Stiffened plate is effective against sigma-Y	

(i.e. Method I is used)

LOAD DATA:

◉ Uniform Stress ○ Linear Varying Stress

Stresses on plate edge/corner				Stresses on opposite side			
Longitudinal compr.:	$\sigma_{x,sd}$ =	335,60	N/mm2	Longitudinal compr.:	$\sigma_{x2,sd}$ =	335,60	N/mm2
Transverse compress.:	$\sigma_{y,sd}$ =		N/mm2	Transverse compress.:	$\sigma_{y2,sd}$ =	0,00	N/mm2
Shear Stress:	τ_{sd} =		N/mm2	Load factor for stresses:	γ_L =	1,00	-
Lateral load / pressure:	P_{sd} =		N/mm^2				
Min. pr. in adj. spans:	P_{sdMin} =		N/mm^2	Load factor for lateral load:	γ_L=	1,00	-
Pressure distrubution:		Overpr. may occur on both sides		Support mom. factor:	k_{m3} =	12,00	0,0000E+00
Press. variation betw. spans:		Equal pressure		Midspan mom. factor:	k_{m2} =	24,00	0,0000E+00

(for stiffener with effective plate)

BUCKLING CHECK SUMMARY:

Buckling modes:	$\sigma_{j,Sd}$	$\sigma_{x,Rd}$	$\sigma_{y,Rd}$	τ_{Rd}	P_{Sd} Max	UF
Unstiffened plate buckling:	335,60	385,22	167,31	242,49	0,767	**0,799**

Stiffened plate panel:	q_{Sd}	f_k		z^*	UF
Design load on plate side:	0,00	420,0		34,5	**1,000**
Design load on stiffener side:	0,00	262,5		27,6	**0,966**
Requirement to plate resistance:			$\sigma_{y,Sd}$ <= 167,3		**0,000**
Requirement to shear capacity:	V_{Sd} =	0 [kN]	V_{Rd} = 848,7 [kN]		**0,000**

Girder check:	q_{Sd}	f_k		z^*	UF
Design load on plate side:	179,88	420,0		0,0	**0,028**
Design load on girder side:	179,8816	420,0		0,0	**0,028**
Requirement to shear capacity:	V_{Sd} =	0 [kN]	V_{Rd} = 1 454,9 [kN]		**0,000**

Local buckling, cross section class-type requirements:

Maximal webheight:	Stiffener:	h_w <=	314,2	Girder: h_w <=	471,2	**Not OK, Local buckl. may o**
Maximal flangewidth:	Stiffener:	c <=	209,4	Girder: c <=	366,5	**OK, within Sect. Type III**

Maximum usage factor: **1,000** OK

NAUTICUS hull

Recommend-ed Practice DNV-RP-C201 Oct. 2010

BUCKLING OF STIFFENED PLATE PANEL

Vers. 14.0, Nauticus Hull, Jan. 2011

Sign:
Time: 13:13
Date: 02.06.2014

PRINCIPAL DATA

Identification			
Material Factor	γ_M=	1,00	-
Yield stress	f_y =	420,0	N/mm2
Modulus of Elasticity	E=	210 000	N/mm2
Poissons Ratio	ν =	0,3	-
Shear Modulus	G=	80 769	N/mm2

PLATE

Thickness	t=	15,0	mm
Stiffener Spacing	s =	500,0	mm
Stiffener Length	l =	3750,0	mm
Girder Length	L_G =	1500,0	mm
Panel length (max.no stiff spans*l)	L_P =	11250,0	mm

Plot Nothing

STIFFENER AND GIRDERS

	Stiffener:			Girder:		
Stiffener Type	T-profile			T-profile		
Total Height of section	h_{tot} =	350,0	mm	h_{tot} =	400,0	mm
Web Thickness	t_w =	10,0	mm	t_w =	15,0	mm
Flange width	b =	130,0	mm	b =	210,0	mm
Flange thickness	t_f =	20,0	mm	t_f =	35,0	mm
Buckling length factor: (optional)	k_{stiff} =	0,50		k_{girder} =		
Distance between tripping brackets:	l_T =		mm	betw.lateral supp.: L_{TG} =		mm
Fabrication method:	Welded cross section			Welded cross section		
Stiffener end support:	Continuous Stiffeners			Continuous Girder		
Tension field action:	Tension Field Action is NOT Allowed			Stiffened plate is effective against sigma-Y		

(i.e. Method 1 is used)

LOAD DATA:

◉ Uniform Stress ○ Linear Varying Stress

Stresses on plate edge/corner				Stresses on opposite side		
Longitudinal compr.:	$\sigma_{x,sd}$ =	0,00	N/mm2	Longitudinal compr.: $\sigma_{x2,sd}$ =	0,00	N/mm2
Transverse compress.:	$\sigma_{y,sd}$ =		N/mm2	Transverse compress.: $\sigma_{y2,sd}$ =	0,00	N/mm2
Shear Stress:	τ_{sd} =	242,42	N/mm2	Load factor for stresses: γ_L =	1,00	-
Lateral load / pressure:	P_{sd} =		N/mm^2			
Min. pr. in adj. spans:	P_{sdMin} =		N/mm^2	Load factor for lateral load: γ_L=	1,00	-
Pressure distrubution:	Overpr. may occur on both sides			Support mom. factor: k_{m3} =	12,00	0,0000E+00
Press. variation betw. spans:	Equal pressure			Midspan mom. factor: k_{m2} =	24,00	0,0000E+00

(for stiffener with effective plate)

BUCKLING CHECK SUMMARY:

Buckling modes:	$\sigma_{j,Sd}$	$\sigma_{x,Rd}$	$\sigma_{y,Rd}$	τ_{Rd}	P_{Sd} Max	UF
Unstiffened plate buckling:	419,88	385,22	167,31	242,49	0,036	**1,000**

Stiffened plate panel:	q_{Sd}	f_k		z*	UF
Design load on plate side:	0,00	420,0		-7,0	**0,999**
Design load on stiffener side:	0,00	186,7		-7,0	**0,999**
Requirement to plate resistance:			$\sigma_{y,Sd}$ <= 3,9		**1,000**
Requirement to shear capacity: V_{Sd} =		0 [kN]	V_{Rd} = 848,7 [kN]		**0,000**

Girder check:	q_{Sd}	f_k		z*	UF
Design load on plate side:	0,00	420,0		0,0	**0,000**
Design load on girder side:	0	420,0		0,0	**0,000**
Requirement to shear capacity: V_{Sd} =		0 [kN]	V_{Rd} = 1 454,9 [kN]		**0,000**

Local buckling, cross section class-type requirements:

Maximal webheight:	Stiffener:	h_w <=	314,2	Girder:	h_w <=	471,2	**Not OK, Local buckl. may o**
Maximal flangewidth:	Stiffener:	c <=	209,4	Girder:	c <=	366,5	**OK, within Sect. Type III**

Maximum usage factor: **1,000** OK

Appendix E

Capacity check for primary girder bases on DNV-RP-C201

Capacity check of primary girders according to DNV-CP-R201

Material data

Yield stress:

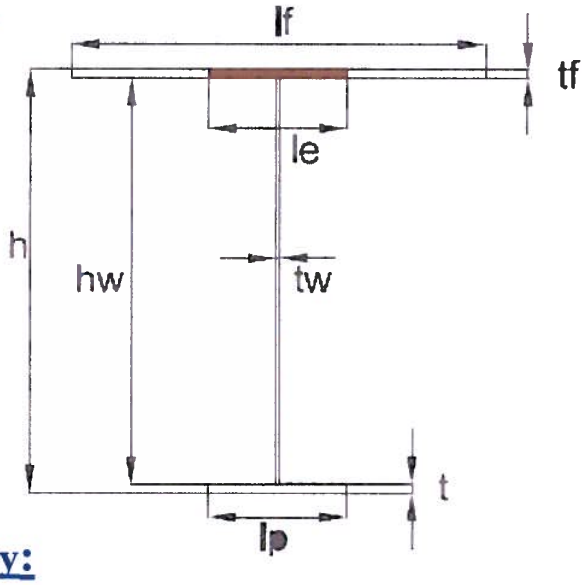

$f_y := 420 \cdot MPa$

$f_{yw} := f_y$

Elastic modulus:

$E := 2.1 \cdot 10^5 \cdot MPa$

$G := \frac{E}{2.6}$

Passion's ratio

$\nu := 0.3$

Steel density

$\rho := 7850 \cdot \frac{kg}{m^3}$

Material factors

$\gamma_m := 1.0$

Panel geometry:

Plate thickness

$t := 30 \cdot mm$

Plate width beween stiffeners

$s := 312.5 \cdot mm$

Stiffener dimensions

$h_{stiff} := 150 \cdot mm$ $t_{sf} := 20 \cdot mm$ $t_{sw} := 10 \cdot mm$

$b_{sf} := 350 \cdot mm$ $h_s := h_{stiff} + t$

Girder geometry T profile

Plot of the girder section

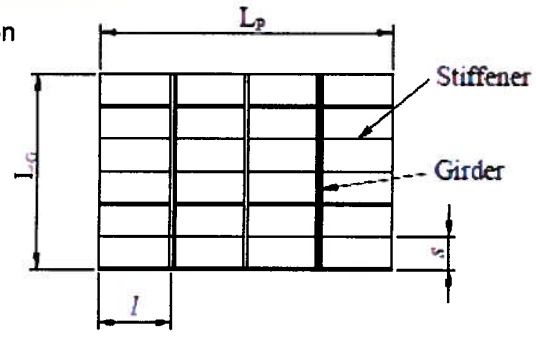

Girder span

$L_G := 15.0 \cdot m$

Buckling length factor

$\beta := 0.8$

Buckling length $L_k := \beta \cdot L_G$

Distance between vertical stiffeners/tripping brackets on girder $L_{GT} := 3.75 \cdot m$

Span of stiffeners (distance between secondary girders) $l_w := 3.75 \cdot m$

Primary girder dimensions $h_G := 1500 \cdot mm$ $l_p := 500 \cdot mm$ $t_w := 15 \cdot mm$

$t_f := 30mm$ $h_w := h_G - t_f$ $h_w = 1.47\,m$

$h := h_G + t$

Length of panel: $L_P := 12.5 \cdot m$

Analysis method

Method 1 assuming that the stiffened plate is effective against transverse compression stresses.

Method 2 assuming that the stiffened plate is not effective against transverse compression stresses.

Method := 2

Design forces (The maximum collapse load at the collapse step)

Stresses in the top flange of girder, mid filed (from FEM analysis) $\sigma_{Top} := 239.84 \cdot MPa$

Stresses in the bottom flange of girder, mid filed (from FEM analysis) $\sigma_{Bot} := 364.89 \cdot MPa$

Stresses in the top flange of girder, support (from FEM analysis) $\sigma_{Tops} := 169.89 \cdot MPa$

Stresses in the bottom flange of girder, support (from FEM analysis) $\sigma_{Bots} := 334.87 \cdot MPa$

f-factor for variable action on the deck $f := \left(\frac{235}{420}\right)^{0.5}$

Design variable function load (include load factor) $PSd := f \cdot 0 \cdot 1.3 \cdot g \cdot \frac{kg}{m^2}$

Effective flange

Assumptions

- Postive bending moment gives compression in top flange
- Positive stresses are in compression
- One cross section is checked
- The web satisfies section class 3

Total length of top flange

$l_f := 1500 \cdot mm$

Choose to use the same width in top and bottom flange

$l_e := 500 \cdot mm$

Elastic section properties (based on gross area of web and effective area of flange

$A_p := l_p \cdot t$ $\quad A_p = 0.015\,m^2$

$A_f := l_e \cdot t_f$ $\quad A_f = 0.015\,m^2$

$A_w := h_w \cdot t_w$ $\quad A_w = 0.022\,m^2$

$A_g := A_p + A_f + A_w$ $\quad A_g = 0.052\,m^2$

$A_{eff} := A_g$

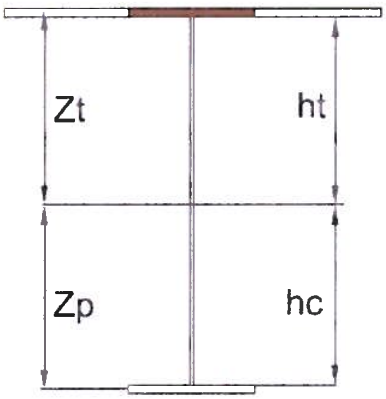

$$z_0 := \frac{A_f \cdot \frac{t_f}{2} + A_w \cdot \left(\frac{h_w}{2} + t_f\right) + A_p \cdot \left(h - \frac{t}{2}\right)}{A_g} \qquad z_0 = 0.765\,m$$

$$I_0 := \frac{1}{12} \cdot l_e \cdot t_f^{\,3} + \left(z_0 - \frac{t_f}{2}\right)^2 \cdot A_p + \frac{t^3 \cdot l_p}{12} + A_f \left(h - z_0 - \frac{t}{2}\right)^2 + A_w \left(z_0 - t_f - \frac{h_w}{2}\right)^2 + \frac{t_w \cdot h_w^{\,3}}{12}$$

$I_0 = 0.021\,m^4$

$h_t := z_0 - t$ $\quad h_t = 0.735\,m$

$h_c := h_w - h_t$ $\quad h_c = 0.735\,m$

$z_t := \frac{h_w}{2} + t_f$ $\quad z_t = 0.765\,m$

$z_p := \frac{h_w + t}{2}$ $\quad z_p = 0.75\,m$

Effective elastic section modulus on plate side

$W_p := \frac{I_0}{z_p}$ $\quad W_p = 27.797\,L$

Effective elastic section modulus on stiffener side

$W_s := \frac{I_0}{z_t}$ $\quad W_s = 27.252\,L$

$M_y := \min(W_p, W_s) \cdot f_y$ $\quad M_y = 1.145 \times 10^7\,J$

Equivalent load

$P_0 := 0 \cdot MPa$

For simply calculation, the equivalent stress is assumed to be zero. Assessement of P0 can be obtained in Nauticus Hull for secondary girders

Dimensioning forces for girder

Calculate the bending momend and axial force in the middle field

$M := \frac{(\sigma_{Top} - \sigma_{Bot})}{2} \cdot W_p$

$N := \frac{(\sigma_{Top} - \sigma_{Bot})}{2} \cdot A_g$

Calculate the bending momend and axial force in the supports

$M_S := \frac{(\sigma_{Tops} - \sigma_{Bots})}{2} \cdot W_p$

$$N_S := \frac{(\sigma_{Tops} - \sigma_{Bots})}{2} \cdot A_g$$

Bending moment at the middle section $M_{FEM} := M$

Bending moment at the supports $M_{supFEM} := M_S$

For the case under pure compression $V_{FEM} := 0 \cdot kN$

Shear force

$$q_{Sd1} := (PSd + P_0) \cdot L_P$$

$$q_{Sd} := PSd + P_0 \qquad q_{Sd1} = 0$$

For simpicity calculation, the shear is not considered for this case, but it can be introduced to compare the shear combination cases.

Based on the buckling check of the maximum axial force at the middle of the girder span:

$$N_{Sd} := 13.9194 \cdot MN$$

Support Moment, p on the plate side

$$M_{1Sd} := \left| \frac{q_{Sd} \cdot L_P \cdot L_G^{\,2}}{12} \right| + \left| M_{supFEM} \right| \qquad M_{1Sd} = 2.293 \times 10^6 J$$

Field Moment, p on the plate side

$$M_{2Sd} := \left| \frac{q_{Sd} \cdot L_P \cdot L_G^{\,2}}{12} \right| + \left| M_{FEM} \right| \qquad M_{2Sd} = 1.738 \times 10^6 J$$

Torsional buckling

Moment of inertia (exclusive of plate flange)

$$I_Z := \frac{1}{12}\cdot\left(h_w\cdot {t_w}^3 + t_f\cdot {l_e}^3\right)$$

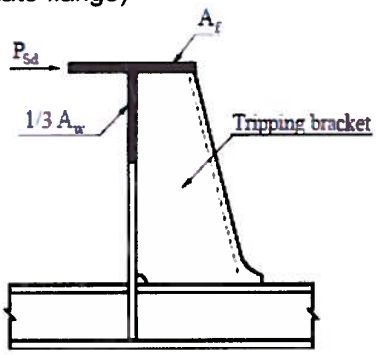

$$I_Z = 3.129\times 10^{-4}\,m^4$$

$$A_Z := h_w\cdot t_w + t_f\cdot l_e$$

$$f_{EGT} := \frac{\pi^2\cdot E\cdot I_Z}{\left(A_f + \frac{A_w}{3}\right)\cdot {L_{GT}}^2}$$

$$f_{EGT} = 2.063\times 10^{9}\,Pa$$

$$\lambda_{GT} := \sqrt{\frac{f_y}{f_{EGT}}}$$

$$\lambda_{GT} = 0.451$$

$$\mu_T := 0.35\cdot\left(\lambda_{GT} - 0.6\right)$$

$$\mu_T = -0.052$$

Torsional buckling strength of girders

$$f_{TG} := \begin{cases} f_y & \text{if } \lambda_{GT} \le 0.6 \\ f_y\cdot\left[\dfrac{1 + \mu_T + {\lambda_{GT}}^2 - \sqrt{\left(1 + \mu_T + {\lambda_{GT}}^2\right)^2 - 4\cdot {\lambda_{GT}}^2}}{2\cdot {\lambda_{GT}}^2}\right] & \text{otherwise} \end{cases}$$

$$f_{TG} = 4.2\times 10^{8}\,Pa$$

Characteristic buckling strength of girder

Radius of gyration

$$i_e := \sqrt{\frac{I_0}{A_g}}$$

cross area =section class 3 in this section

$$i_e = 0.633\,m$$

Buckling slenderness $\lambda := \frac{L_k}{i_e}$ $\lambda = 18.961$

Euler stress $f_E := \pi^2 \cdot E \cdot \left(\frac{i_e}{L_k}\right)^2$ $f_E = 5.765 \times 10^9\,\text{Pa}$

Check at stiffener side

$\lambda_G := \sqrt{\frac{f_{TG}}{f_E}}$ $\lambda_G = 0.27$

$\mu_s := \left(0.34 + 0.08 \cdot \frac{z_t}{i_e}\right) \cdot \left(\lambda_G - 0.2\right)$ $\mu_s = 0.031$

$f_r := f_{TG}$

$$f_{Gs} := \begin{cases} f_r & \text{if } \lambda_G \le 0.2 \\ \left[f_r \cdot \left[\frac{1 + \mu_s + \lambda_G^2 - \sqrt{\left(1 + \mu_s + \lambda_G^2\right)^2 - 4 \cdot \lambda_G^2}}{2 \cdot \lambda_G^2} \right] \right] & \text{otherwise} \end{cases}$$

$f_{Gs} = 4.066 \times 10^8\,\text{Pa}$

Check at plate side

$\lambda_{Gp} := \sqrt{\frac{f_y}{f_E}}$ $\lambda_{Gp} = 0.27$

$\mu_p := \left(0.34 + 0.08 \cdot \frac{z_p}{i_e}\right) \cdot \left(\lambda_{Gp} - 0.2\right)$ $\mu_p = 0.03$

$f_{rp} := f_{TG}$

$$f_{Gp} := \begin{cases} f_{rp} & \text{if } \lambda_G \le 0.2 \\ \left[f_{rp} \cdot \left[\frac{1 + \mu_p + \lambda_G^2 - \sqrt{\left(1 + \mu_p + \lambda_G^2\right)^2 - 4 \cdot \lambda_G^2}}{2 \cdot \lambda_G^2} \right] \right] & \text{otherwise} \end{cases}$$

$f_{Gp} = 4.067 \times 10^8\,\text{Pa}$

Resistance parameters

Design axial force resistance

$$N_{Rd} := A_g \cdot \frac{f_y}{\gamma_m} \qquad N_{Rd} = 2.186 \times 10^7\,\text{N}$$

Design stiffener induced axial buckling resistance

$$N_{ksRd} := A_g \cdot \frac{f_{Gs}}{\gamma_m} \qquad N_{ksRd} = 2.117 \times 10^7\,\text{N}$$

Design plate induced axial buckling resistance

$$N_{kpRd} := A_g \cdot \frac{f_{Gp}}{\gamma_m} \qquad N_{kpRd} = 2.117 \times 10^7\,\text{N}$$

Design bending moment resistance on stiffener side in tension

$$M_{stRd} := W_s \cdot \frac{f_y}{\gamma_m} \qquad M_{stRd} = 1.145 \times 10^7\,\text{J}$$

Design bending moment resistance on plate side in tension

$$M_{pRd} := W_p \cdot \frac{f_y}{\gamma_m} \qquad M_{pRd} = 1.167 \times 10^7\,\text{J}$$

Assuming

$$l_{tl} := 0.4 \cdot L_G$$

$$\lambda_{GT04} := \sqrt{\frac{f_y}{\frac{\pi^2 \cdot E \cdot I_Z}{\left(A_f + \frac{A_w}{3}\right) \cdot \left(\min\left(0.4 L_G, L_{GT}\right)\right)^2}}} \qquad \lambda_{GT04} = 0.451$$

$$\mu_{T04} := 0.35 \cdot \left(\lambda_{GT04} - 0.6\right) \qquad \mu_{T04} = -0.052$$

$$f_{TG04} := \begin{cases} f_y & \text{if } \lambda_{GT04} \le 0.6 \\ \left[f_y \cdot \left[\frac{1 + \mu_{T04} + \lambda_{GT04}^2 - \sqrt{\left(1 + \mu_{T04} + \lambda_{GT04}^2\right)^2 - 4 \cdot \lambda_{GT04}^2}}{2 \cdot \lambda_{GT04}^2} \right] \right] & \text{otherwise} \end{cases}$$

$$f_{TG04} = 4.2 \times 10^8\,\text{Pa}$$

Assuming

$$l_{t2} := 0.8 \cdot L_G$$

$$\lambda_{GT08} := \sqrt{\frac{f_y}{\frac{\pi^2 \cdot E \cdot I_Z}{\left(A_f + \frac{A_w}{3}\right) \cdot \left(\min\left(0.8 L_G, L_{GT}\right)\right)^2}}} \qquad \lambda_{GT08} = 0.451$$

$$\mu_{T08} := 0.35 \cdot \left(\lambda_{GT08} - 0.6\right) \qquad \mu_{T08} = -0.052$$

$$f_{TG08} := \begin{cases} f_y & \text{if } \lambda_{GT08} \le 0.6 \\ f_y \cdot \left[\frac{1 + \mu_{T08} + \lambda_{GT08}^2 - \sqrt{\left(1 + \mu_{T08} + \lambda_{GT08}^2\right)^2 - 4 \cdot \lambda_{GT08}^2}}{2 \cdot \lambda_{GT08}^2}\right] & \text{otherwise} \end{cases}$$

$$f_{TG08} = 4.2 \times 10^8 \text{ Pa}$$

Design bending moment resistance on stiffener side

$$M_{s1Rd} := W_s \cdot \frac{f_{TG04}}{\gamma_m} \qquad M_{s1Rd} = 1.145 \times 10^7 \text{ J}$$

Design bending moment resistance on stiffener side

$$M_{s2Rd} := W_s \cdot \frac{f_{TG08}}{\gamma_m} \qquad M_{s2Rd} = 1.145 \times 10^7 \text{ J}$$

Design bending moment resistance on stiffener side in tension

$$M_{sRd} := W_s \cdot \frac{f_{TG}}{\gamma_m} \qquad M_{sRd} = 1.145 \times 10^7 \text{ .}$$

Euler buckling strength

$$N_{Ey} := f_E \cdot A_{eff} \qquad N_{Ey} = 3.001 \times 10^8 \text{ N}$$

Check of continuous girders

Buckling check:

z* is the distance from the neutral axis of the effective section to the working point of axial force. z* may be varied in order to optimise the resistance. The value of z* is positive towards the plate and the simplification z*=0 is always allowed to calculate the problem conservatively.

$z_{star} := -150 \cdot mm$

Lateral pressure on plate side

At support

$$\frac{N_{Sd}}{N_{ksRd}} + \frac{M_{1Sd} - N_{Sd} \cdot z_{star}}{M_{s1Rd} \cdot \left(1 - \frac{N_{Sd}}{N_{Ey}}\right)} = 1.059$$

$$\frac{N_{Sd}}{N_{kpRd}} + \frac{M_{1Sd} - N_{Sd} \cdot z_{star}}{M_{pRd} \cdot \left(1 - \frac{N_{Sd}}{N_{Ey}}\right)} - 2 \cdot \frac{N_{Sd}}{N_{Rd}} = -0.222$$

In the middle of the section

$$\frac{N_{Sd}}{N_{ksRd}} + \frac{M_{2Sd} - N_{Sd} \cdot z_{star}}{M_{stRd} \cdot \left(1 - \frac{N_{Sd}}{N_{Ey}}\right)} - 2 \cdot \frac{N_{Sd}}{N_{Rd}} = -0.265$$

$$\frac{N_{Sd}}{N_{kpRd}} + \frac{M_{2Sd} - N_{Sd} \cdot z_{star}}{M_{pRd} \cdot \left(1 - \frac{N_{Sd}}{N_{Ey}}\right)} = 1.001$$

Section check

Support $$\left(\frac{N_S}{A_g} + \frac{M_{1Sd}}{W_p}\right) \cdot \frac{1}{f_y} = 0$$

Middle $$\left(\frac{N}{A_g} + \frac{M_{2Sd}}{W_p}\right) \cdot \frac{1}{f_y} = 0$$

Bibliography

[1] H. Wagner. Flat sheet metal girder with very thin metal web. *Zeitschrift fur Flugtechnik Motorlurftschiffahrt*, 20:200–207, 1929.

[2] K.H. Tang and H.R. Evans. Transverse stiffeners for plate girder webs-an experimental study. *Journal of constructional steel research*, 4:253–280, 1984.

[3] D.M. Porter H.R. Evans and K.C. Rockey. The collapse behaviour of plate girders subjected to shear and bending. *1ABSE proceedings*, pages P–18/78, 1978.

[4] D.M. Porter H.R. Evans and K.C. Rockey. A parametric study of the collapse behaviour of plate girders. *University College, Cardiff, Report*, 1976.

[5] A. Kendrick and C.G. Daley. Framing design in the unified requirement for polar class ships.

[6] C. Graciano and A. Ayestaran. Steel plate girder webs under combined patch loading, bending and shear. *Journal of Constructional Steel Research*, 80:202–212, 2013.

[7] IACS. I2 structure requirements for polar class ships. *IACS requirements*, 2010.

[8] ECCS. Design of steel structures – general rules and rules for buildings. *EUROCODE 3 , PART 1-1*, 1993.

[9] E. Casanova C. Graciano and E. Martinez. Imperfection sensitivity of plate girder webs subjected to patch loading. *Journal of Constructional Steel Research*, 67:1128–1133, 2011.

[10] Det Norske Veritas. Buckling strength of plated structures. *DNV recommended practise*, 2010.

[11] J. Amdahl. Ultimate strength of plate- and box- girders. *TMR4205 compendium, Faculty of engineering science and technology, NTNU*, 2005.

[12] H.R. Evans and K.H. Tang. The influence of longitudinal web stiffeners upon the collapse behaviour of plate girders. *Journal of Constructional Steel Research*, 4:201–234, 1984.

[13] H.R. Evans K.C. Rockey and D.M. Porter. A design method for predicting the collapse behavior of plate girders. *ICE proceedings*, 65, 1987.

[14] H.R. Evans. Longitudinally and transversely reinforced plate girders. *University College, Cardiff, UK*, pages 7–11.

[15] K. Balser. Strength of plate girders in shear. *Fritz Engnineering Laboratory Report*, 1960.

[16] C. Massonnet. Experimental reseaches on the buckling strength of the webs of solid girders. *4th congress IABSE*, (539-555), 1952.

[17] M. Skaloud and M. Zornerova. Linear buckling theory optimum rigidity of the longitudinal stiffeners of the compression flanges of steel box-girder bridegs. *Acta technica*, 1:33–51, 1977.

[18] M. Skaloud. Optimum rigidity of stiffeners of webs and flanges. *Plated structures: Stability and strength. London: Applied Science Publishers*, pages 103–34, 1983.

[19] T. Moan. Finite element modelling and analysis of marine structure. *TMR4190 compendium, Faculty of engineering science and technology, NTNU*, chapter 12:1–58, 2003.

[20] I. Fried. Orthogonal trajectory accession on the nonlinear equilibrium curve. *J. comp. methods appl. mech. engng.*, 47:283–297, 1984.

[21] M.A. Crisfield. Non-linear finite element analysis of solids and structures. *J. Wiley and Sons, Chichester*, 1, 1991.

[22] A. Abraham. Plastic response of ship structure subjected to ice loading. *Master thesis, Memorial University of Newfoundland*, 2008.

[23] Abaqus user manual.

[24] Yao Ma. Duktilitetsgrenser for rørkutepunkt. *Master thesis, Norwegian University of Science and Technology*, 2013.

[25] T.H. Soreide and J. Amdahl et al. Usfos theory manual. *Division of structural engineering*, 1993.

[26] USFOS. Usfos user's manual.